Titre: Title:	Development of a Production Process for a Virus Like Particle Based Vaccine in Cell Culture
Auteur: Author:	Christine Marie Thompson
Date:	2013
Type:	Mémoire ou thèse / Dissertation or Thesis
Référence: Citation:	Thompson, C. M. (2013). Development of a Production Process for a Virus Like Particle Based Vaccine in Cell Culture [Mémoire de maîtrise, École Polytechnique de Montréal]. PolyPublie. https://publications.polymtl.ca/1252/

UNIVERSITÉ DE MONTRÉAL

DEVELOPMENT OF A PRODUCTION PROCESS FOR A VIRUS LIKE PARTICLE BASED VACCINE IN CELL CULTURE

CHRISTINE MARIE THOMPSON

DÉPARTEMENT DE GÉNIE CHIMIQUE

ÉCOLE POLYTECHNIQUE DE MONTRÉAL

MÉMOIRE PRÉSENTÉ EN VUE DE L'OBTENTION

DU DIPLÔME DE MAÎTRISE ÈS SCIENCES APPLIQUÉES

(GÉNIE CHIMIQUE)

OCTOBRE 2013

UNIVERSITÉ DE MONTRÉAL

ÉCOLE POLYTECHNIQUE DE MONTRÉAL

Ce mémoire intitulé :

DEVELOPMENT OF A PRODUCTION PROCESS FOR A VIRUS LIKE PARTICLE BASED VACCINE IN CELL CULTURE

présenté par : THOMPSON Christine Marie

en vue de l'obtention du diplôme de : Maîtrise ès sciences appliquées

a été dûment accepté par le jury d'examen constitué de :

M. DE CRESCENZO Gregory, Ph.D., président

M. HENRY Olivier, Ph.D, membre et directeur de recherche

M. KAMEN Amine, Ph.D, membre et codirecteur de recherche

Mme HOEMANN Caroline, Ph.D., membre

DEDICATION

To my family and Julien, for your never ending support, encouragement, patience and love

ACKNOWLEDGMENTS

Firstly, I'd like to thank my supervisors, Olivier Henry and Amine Kamen for supporting me during this project and providing guidance, constructive advice and interesting discussions. Additionally, I'd like to thanks Marc Aucoin, who not only introduced me to this project but also continued to provide support and guidance on a regular basis.

Secondly, I'd like to thank Emma Petiot, who was working at NRC during this project. Emma became a mentor to me and was very involved in the project, even when she didn't have to be. I am very thankful to have had the opportunity to work and learn from her and also happy that I have made such a great friend.

I'd also like to thank the employees at NRC that also helped me; Johnny Montes, for training me to work with insect cell culture and bioreactor operation. Julia Transfiguracion, for passing on her knowledge on virus purification and HPLC analysis. Alice Bernier, Parminder Chalal, Danielle Jacob, Stéphane Lanthier, Alaka Mullick and Aziza Manceur, thank you for your help at different times.

Thank you to Micheline Letarte at INRS-Institut Armand Frappier for helping me with the NSEM images and quantification.

To all the other students at NRC that overlapped with my stay, specifically, Céline Raymond, Alina Venereo-Sanchez, Alexandre Lennaertz, Igor Slivac, and Charles Fortier, thank you for the lively atmosphere in the office, lab and lunchtime and great discussions on all things research related or not. Good luck with your current projects, jobs and future endeavours, I hope our paths will cross again one day.

I'd like to acknowledge Dr. Ted Ross from the University of Pittsburg for kindly donating to us the bacmam plasmids and bacmids.

Finally, I'd like to thank the Natural Sciences and Engineering Research Council for providing funding for this research.

ABSTRACT

Each year, influenza is the cause for many cases of illness and deaths worldwide. Due to the virus' fast mutation rate, the World Health Organization (WHO) is constantly on alert to be able to respond rapidly in the case of the emergence of a pandemic strain. Although anti-viral therapies exist, the most proficient way to stop the spread of disease is through vaccination. The majority of influenza vaccines on the market are produced in embryonic hen's eggs and are composed of purified viral antigens split from inactivated whole virus. This manufacturing system, however, is limited in its production capacity, especially in the case of a pandemic, producing approximately one vaccine dose per egg. Additionally, the process from strain identification to vaccine release is about 6 months, which is relatively long especially if a vaccine is urgently needed.

For this reason, cell culture processes for vaccine production are a topic of interest amongst the vaccine industry to better respond to the threat of a potential influenza pandemic. Recently, the FDA, supporting the basis for this research, has approved two cell culture based vaccines, the first produced in mammalian cells and the second in insect cells using recombinant technology.

Virus-like particle (VLP) vaccines are one of the most promising approaches to respond to the constant threat of the emergence of pandemic strains. VLPs are particles produced in cell culture utilizing recombinant protein technology composed of viral antigens that can elicit immune response but lack viral genetic material. Most of the work done on influenza VLPs have focused on the immunological aspects of VLPs with little attention paid to bioprocessing, in particular the scalability of the production methods. Another challenge stems from the fact that researchers have used standard influenza virus quantification techniques up to this point to characterize VLP vaccine candidates, as they are suitable methods to use for purified samples. These methods, however, are not suitable for in-process analysis of samples, which is generally the case for process development. As a result, process development is quite challenging without an appropriate quantification method, which is one reason this avenue has not been fully explored.

Past influenza VLP studies have been mainly performed in the baculovirus expression vector system (BEVS) in insect cells and report contamination with recombinant baculovirus. However, baculovirus with mammalian promoters (Bacmam) have been shown to efficiently transduce

mammalian cells and further express genes under mammalian promoter control but are unable to replicate, efficiently repressing contaminating baculovirus production.

In order to address the issue of baculovirus contamination, VLP production was performed in HEK 293 suspension cells using the Bacmam gene delivery system. The proposed system was assessed for its ability to produce influenza VLPs composed of Hemagglutinin (HA), Neuraminidase (NA) and Matrix Protein (M1) and compared to VLPs produced in Sf9 cells through the lens of bioprocessing. VLPs from both systems were characterized using currently available influenza quantification techniques such as single radial immunodiffusion assay (SRID), HA assay, negative staining electron microscopy (NSEM) and western blot. VLPs were found to be associated with the cell pellet in HEK 293 production in addition to in the supernatant. It was found that VLP production in Sf9 cells produced 1.5 logs more VLPs than in HEK 293. Sf9-VLPs had higher total HA activity and were generally more homogeneous in morphology and size. However, Sf9 VLP samples contained 20 times more baculovirus than VLPs. Baculovirus can contribute to HA activity in both the HA assay and SRID, which should be acknowledged during process development stages. This study shows the strength of the insect-cell baculovirus system for VLP production when compared to proposed alternatives in HEK 293 cells from the bioprocessing point of view but also highlights that there is a major need for baculovirus removal to properly characterize and consider them as vaccine candidates.

RÉSUMÉ

Chaque année, le virus de l'influenza est responsable d'un grand nombre de maladies et décès. Aux vues de la fréquence élevée de mutation du virus, l'Organisation Mondiale de la Santé (OMS) est en alerte permanente afin de répondre rapidement à toute émergence d'une souche pandémique. Bien que des thérapies anti-virales existent, la méthode la plus efficace contre toute propagation de la maladie est la vaccination. La majorité des vaccins disponibles sur le marché sont produits dans des oeufs et sont composés d'antigènes viraux purifiés séparés des virus entiers inactifs. Le système de production n'est cependant pas adapté à une situation de pandémie, la capacité étant limitée à une dose de vaccin par oeuf. Aussi, l'intervalle de 6 mois entre l'identification de la souche virale et la production du vaccin est trop longue pour envisager répondre de manière adéquate à la case l'émergence d'une pandémie.

Pour ces raisons, les procédés de production de virus par culture cellulaire peuvent permettre de répondre de manière adéquate à une pandémie potentielle. Récemment, la Food and Drug Administration (FDA) a approuvé deux vaccins produits par culture cellulaire, le premier étant produit dans des cellules de mammifère tandis que le second est produit de manière recombinante dans des cellules d'insecte.

Les vaccins à base de particules pseudo-virales (PPVs) représentent une des approches les plus prometteuses afin de répondre à la menace constante de l'apparition de souches pandémiques. Les PPVs sont des particules produites en culture cellulaire de manière recombinante et qui sont composées d'antigènes viraux capables d'induire une réponse immunitaire, bien que ces particules soient dénuées de matériel génétique viral. Alors que la plupart des travaux effectués sur les PPVs de l'influenza se sont concentrés sur les aspects immunologiques, peu d'études se sont attachées au procédé de production lui-même, et en particulier à son adaptation à une production industrielle. Une autre difficulté résulte du fait que les chercheurs ont jusqu'à présent utilisé des méthodes standards de quantification du virus de l'influenza afin de caractériser les vaccins potentiels, ces méthodes étant compatibles pour la quantification d'échantillons purifiés. Elles ne sont pas compatibles, cependant, avec l'analyse d'échantillons durant le procédé de production. C'est une des raisons pour lesquelles l'étude du procédé de production lui-même reste à accomplir.

Les études précédentes sur les PPVs de l'influenza ont été principalement effectuées dans des cellules d'insecte en utilisant le système d'expression du baculovirus (BEVS). Ces études ont également démontré une contamination par le baculovirus recombinant. Cependant, il a été également démontré que le baculovirus comprenant des promoteurs de mammifères (Bacmam) est capable de transduire de manière efficace des cellules de mammifères et d'exprimer ultérieurement des gènes sous le contrôle de promoteurs de mammifères. Un tel baculovirus est ainsi incapable de se répliquer, ce qui réprime de manière efficace la production contaminante de baculovirus.

Afin de remédier à une possible contamination par le baculovirus, la production de PPVs a été effectuée dans des cellules HEK 293 cultivées en suspension en utilisant le système Bacmam. Le système fut évalué pour sa capacité de production PPVs de l'influenza composées d'hémaglutinine (HA), de neuraminidase (NA) ainsi que de protéines matricielles (M1). Ces PPVs ont ensuite été comparées à des PPVs produites dans ces cellules Sf9. Les PPVs des deux systèmes ont été caractérisées avec les méthodes de quantification présentement disponibles : test SRID (single radial immunodiffusion assay), test d'hémagglutination, microscopie électronique en coloration négative et western blot. Les PPVs étaient présents dans le culot ainsi que dans le surnageant dans la production pour les cellules HEK 293. Dans les cellules Sf9, la production de PPVs était 1.5 log plus importante que dans les cellules HEK 293. Les PPVs produites dans les cellules Sf9 avaient une activité totale HA plus importante et étaient de manière générale plus homogènes en termes de morphologie et taille. Cependant, les PPVs produites dans les cellules Sf9 contiennent 20 fois plus de baculovirus que de PPVs, ce qui peut contribuer à l'activité détectée dans les tests HA et SRID. Cette conclusion doit être prise en compte au cours du développement du procédé de production.

Cette étude démontre les avantages du système de baculovirus pour la production de PPVs dans les cellules d'insecte par rapport à de la production dans les cellules HEK 293. Cette étude démontre également qu'une purification du baculovirus contaminant est également nécessaire avant de pouvoir considérer ces PPVs comme des vaccins potentiels.

TABLE OF CONTENTS

LIST OF TABLES

LIST OF FIGURES

LIST OF ABBREVIATIONS

BEVS	Baculovirus Expression Vector System
BV	Baculovirus
CMV	cytomegalovirus
FC	flow cytometry
GP64	major envelope glycoprotein
HA	Hemagglutinin
HEK 293SF	human embryonic kidney cells serum free
HPLC	high performance liquid chromatography
HPI	hours post infection
HPT	hours post transduction
IVLP	influenza virus like particle
IVP	infectious viral particles
kDa	kilodalton
MCDK	madin-darby canine kidney
MOI	multiplicity of infection
M1, M2	Matrix protein
NA	Neuraminidase
NSEM	negative staining electron microscopy
Per.C6	human fetal retinoblast cells
polh	polyhedron
PR	Puerto Rico
SC	sucrose cushion
SCC	sucrose cushion concentrated
SDS-PAGE	sodium dodecyl sulfate polyacrylamide gel electrophoresis
Sf9	*Spodoptera frugiperda*

SN	supernatant
SRID	Single Radial Immunodiffusion Assay
TCA	Trichloroacetic acid
TCID50	50% tissue culture infective dose
TPCK	1-tosylamido-2-phenylethyl chloromethyl ketone
Vero	African green monkey epithelial
VLP	virus like particle
WT	wild type

LIST OF APPENDICES

INTRODUCTION

Context

Each year, influenza is responsible for approximately 500 million cases of infection and between 250,000 to 500,000 deaths due to seasonal epidemics (WHO, 2009), as reported by the World Health Organization (WHO). Currently, vaccination remains the most proficient strategy to prevent infection and to battle the persistent threat of influenza epidemics. Egg-based production has remained the standard method to produce seasonal influenza vaccines since the 1950s; however, the influenza H1N1 pandemic of 2009 has highlighted the limitations associated with this manufacturing method in the case of the emergence of a pandemic strain (Cohen, 2009; Michaelis, Doerr, & Cinatl, 2009). The main problem is the long 6-month period from strain isolation to final dose formulation and validation (Gerdil, 2003). Strategies to shorten the response time and expand production capacity are currently being investigated. Seasonal influenza vaccines derived from cell culture are gaining attention and in November 2012, the first seasonal vaccine produced in cell culture (Flucelvax, Novartis) was approved by the FDA (FDA, 2012) for adults 18 years of age and older. Additionally, in January 2013, the first trivalent influenza vaccine, Flublok (Protein Science Corporation), made in insect cells using a virus expression system (baculovirus) and recombinant DNA technology was approved for the prevention of seasonal influenza in people aged 18 through 49 (FDA, 2013). These recent advances reflect an important trend of adopting modern cell culture manufacturing in the vaccine industry and is supported by public health and regulatory agencies that currently promote strategies to improve responses to emerging infectious diseases.

Other strategies, such as subunit or DNA vaccines (Chua & Chen, 2010), are potential methods to overcome the limitations of egg-based production, but one of the most promising approaches is the recombinant protein based virus-like particle (VLP) vaccine (Haynes, 2009; Kang, Song, Quan, & Compans, 2009)

Influenza VLPs are non-infectious and non-replicating particles, displaying intact and biochemically active antigens. They do not contain genetic material, but are empty particles composed of one or both of the two viral immunogenic antigens of influenza: HA and/or NA (Haynes, 2009). Additionally, influenza VLPs can be constructed with one or both of the two

matrix proteins, M1 and M2 (Kang et al., 2009; Pushko et al., 2005; Wu et al., 2010). Although NA is not a quantified antigen in final vaccine formulations, the presence of NA in influenza VLP constructions is advantageous, as it has been demonstrated to help in protection against influenza infection (Gravel et al., 2010; Marcelin et al., 2011).

Thus far, immunizations with influenza VLPs to protect against either seasonal or pandemic influenza strains have shown promising results (Latham & Galarza, 2001; Pushko et al., 2005, 2011). A general description of the different immunization trials performed thus far is presented in Kang *et al.* (2009). Now that more clinical trials are underway for VLP vaccines (Landry et al., 2010; López-Macías et al., 2011), it is important for the scientific and engineering community to tackle the challenges still associated the bioprocessing aspects of VLP production. Moreover, in order to develop robust manufacturing processes, production values (number of particles/ml, µg HA/ml), limiting factors (quantification methods, contamination), and product stability studies need to be communicated and completed.

Thesis Organization

Chapters 1-3 will give the reader background on the influenza virus, vaccines and the methods currently used to produce and purify influenza VLPs. Chapter 4 outlines the objectives of this work, and Chapter 5 describes all the methods used for experimentation. Chapters 6 and 7 present the results from VLP production in both Sf9 and HEK 293 platforms, and Chapters 8 and 9 are discussion and conclusions, respectively. The appendices provide extra material, calculations, raw data and a section with preliminary results for the application of VLPs on a total influenza HPLC detection method developed in-house.

Chapter 1: Influenza Virus

1.1 Virus Characteristics

The influenza virus is a single stranded RNA virus belonging to the Orthomyxoviridae family. Orthomyxoviruses are enveloped viruses that have the ability to bind sialic acid residues in mucoproteins. Influenza is made up of three different types of virus; A, B and C. Influenza type A, which infects avian and mammalian hosts, is the most widely studied and the cause of most influenza epidemics. Type B is limited to human hosts and type C infects both porcine and humans. Within each type of influenza, different subtypes exist based on the two surface glycoproteins, hemagglutinin (HA) and neuraminidase (NA). The virus' genome is composed of seven or eight individually wrapped gene segments in helical nucleocapsids that are packaged within the virion's envelope. Six of the gene segments code for influenza proteins (PB_2, PB_1, PA, HA, NP, NA) and 2 of the gene segments are spliced to produce another four viral proteins (M1, M2, NS1 and NS2 (or NEP)) (Acheson, 2007). Influenza virus undergoes the phenomena of antigenic shift and drift, resulting in the emergence of mutated and new strains. Antigenic drift is the gradual mutation of specific strains, occurring every 2-8 years from subtle point mutations within the HA and NA antibody binding sites (Carrat & Flahault, 2007). Due to annual antigenic drift, updated vaccines are required each flu season in the northern and southern hemispheres. The other phenomenon is antigenic shift, which occurs only with influenza type A viruses when HA (and sometimes NA) is replaced with novel types. This causes the emergence of new viral strains that have the potential to cause worldwide pandemics due to the population's lack of immunity. It is estimated that antigenic shift occurs three times every 100 years and was the cause for the three major pandemics in the 20^{th} century (1918, 1957 and 1968) (Carrat & Flahault, 2007). Currently there are 16 HA and 9 NA subtypes (Noda, 2011).

1.2 Structure

All viruses are composed of genetic material and viral proteins and can be classified as either enveloped or non-enveloped. Enveloped viruses acquire a lipid bilayer when they bud from a cell membrane that coats the nucleocapsids with membrane containing nucleocapsids. Most viruses bud from the cell plasma membrane, however some viruses bud from internal cellular membranes such as the endoplasmic reticulum or the Golgi membrane to acquire their envelope (Welsch,

Müller, & Kräusslich, 2007). Non-enveloped viruses do not bud from cellular membranes, but are released from the cell through lysis and therefore do not have envelopes (Acheson, 2007). Influenza is classified as an enveloped virus that buds from the plasma membrane. The influenza genome replicates in the nucleus and when HA, NA and M2 glycoproteins have been synthesized, they are trafficked to the plasma membrane via the Golgi network where the assembly and budding process begins. Currently, the main driving force for influenza virus assembly and budding is not exactly known but it is believed that multiple proteins possess the ability to initiate budding, resulting in a redundant system capable of survival even if certain proteins have lost their functionality (Rossman & Lamb, 2011). Each gene segment is assembled in a helical nucleocapsid where RNA is wrapped around the NP protein and bound at the 5' and 3' ends to a trimer of PB2, PB1, and PA. The virion is said to contain one copy of each genetic segment that are packaged inside. The matrix protein (M1) interacts with both the nucleocapsids and the plasma membrane by binding to the cytoplasmic tails of either HA, NA or M2. Additionally, it serves as the structural backbone of the virion and helps to maintain its morphology (Noda, 2011). Figure 1.1 shows the structure of an influenza virus particle. Influenza virions can be spherical, elliptical, filamentous or irregular in shape and range from 80-120 nm in diameter, with a length of up to 20 μm in the case of filamentous particles. Cell culture and egg produced influenza particles are usually spherical or elliptical in shape, while clinical isolates tend to be filamentous (Noda, 2011).

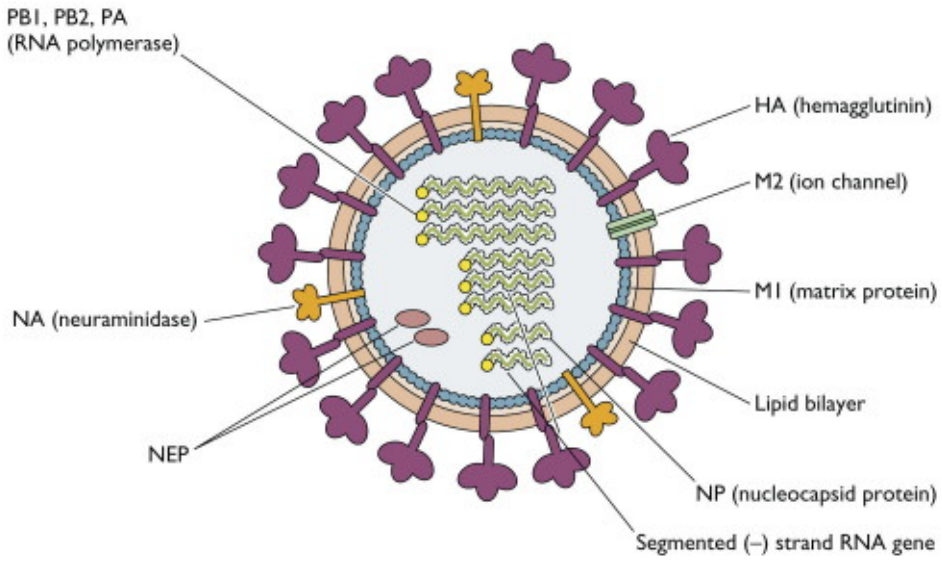

Figure 1.1: Diagram of the structure of influenza virus (Racaniello, 2009)

1.3 Infection Cycle

The influenza life cycle can be divided into several stages, as shown in Figure 1.2; entry to the host cell, entry of viral genome into the nucleus, transcription and replication; export of the genome from the nucleus, and assembly and budding of the viral particle at the host plasma membrane (Samji, 2009).

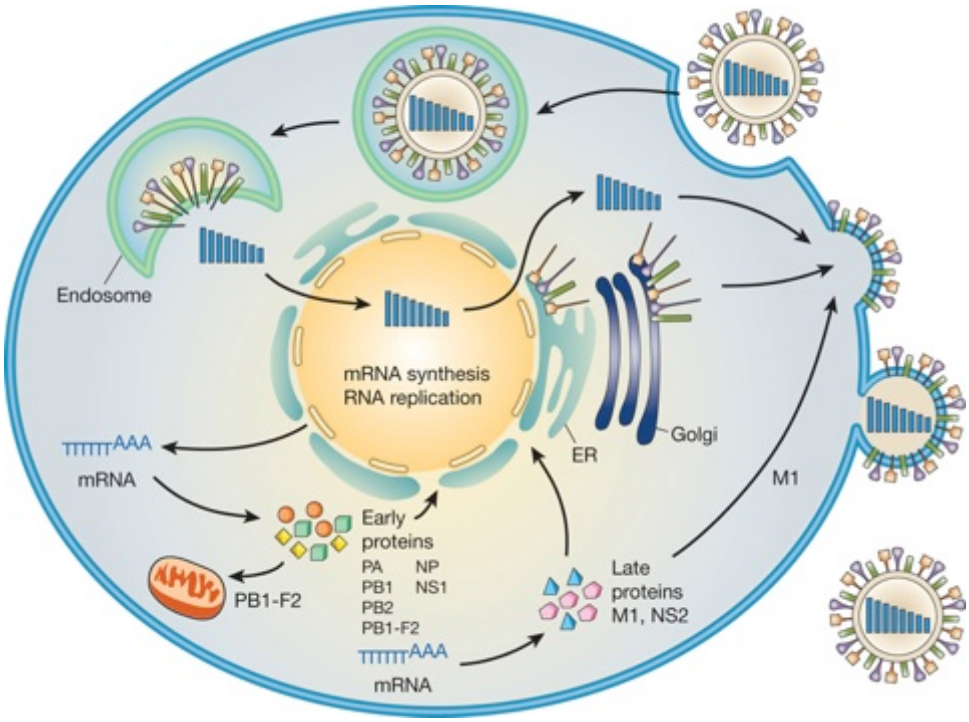

Figure 1.2: Influenza life cycle (Neumann, Noda, & Kawaoka, 2009)

Influenza virus enters host cells via the attachment of HA to sialic acid receptors located on the cells' surface. HA forms as a trimer and each individual HA molecule consists of 2 subunits, HA1 and HA2, which exist in the precursor form HA0. Subunits HA1 and HA2 are linked by disulfide bonds that are cleaved by different serine proteases depending on the strain (trypsin cleaves H1 and futin cleaves H5, for example). To initiate infection, HA1 binds to sialic acid receptors on the host cell membrane followed by entry via receptor-mediated endocytosis in an endosome. Upon entry into the cell, the virus must shed its envelope to release its genome to begin producing new virions. Once inside the endosome, the acidic environment works by triggering a conformational change in HA0 that exposes the fusion peptide of HA2, which fuses the viral envelope with the endosomal membrane. Additionally, the acidic environment opens the M2 ion channel that acidifies the viral core and helps to release viral RNA. Once the viral genomic material is free it is able to enter the nucleus to begin transcription of viral proteins and the replication cycle using both its own and the host's cell machinery (Samji, 2009). After replication the nucelocapsids are exported out of the nucleus by binding to M1 and NP (Acheson, 2007) where they are incorporated into the viral particle. Mature virions then bud out of the cell via the plasma membrane. At this point, the particles may bind back to the cell via sialic acid

receptors and HA1, however NA prevents this by cleaving sialic acid from the host cell leaving the virion free to move on and further infect susceptible cells.

1.4 Immune Response

Influenza is a respiratory disease characterized by the onset of high fever, cough, head and muscle aches and in rare cases can cause viral pneumonia (Taubenberger, Jeffery K., Morens, 2008). The virus is transmitted person to person by either direct contact or through aerosols spread by coughing or sneezing and replicates in both the upper and lower respiratory tract. Once infected with influenza the immune system responds in two ways; the first line of defense is the innate immune response, which secrets interferon molecules that interact with healthy cells to turn them into an infection resistant state. This helps slow the spread of infection and give the immune system a chance to destroy the virus. The innate immune system also induces cytotoxic T-cells that destroy infected cells before they have the chance to release mature virions (Hancioglu, Swigon, & Clermont, 2007). The second line of defense is an adaptive immune response where specific antibodies produced work by attacking the virus itself. Anti-HA antibodies prevent infection by either targeting HA1, which blocks the virus from attaching to the cell or HA2, which stops membrane fusion once taken up by an endosome. Anti-NA antibodies prevent NA from cleaving sialic acid thereby preventing further infection by arresting viral release (Chun, Li, Van Domselaar, & Al., 2008).

Recovery from acute symptoms occurs after 7-10 days, however the infected person can be fatigued for up to weeks after infection, especially older people (65+). Due to the fact that symptoms occur 2 or 3 days after infection, the acquired immunity that occurs after the first week cannot prevent respiratory problems that could develop during this time, requiring advanced immunity from vaccines to prevent the complications and spread of the disease (Hancioglu et al., 2007).

Chapter 2: Influenza Vaccines

2.1 Current Influenza Vaccine

Due to the fast mutation rate of influenza, the WHO has put an epidemiological surveillance system in place to try to predict the emerging strains for each upcoming flu season in both the northern and southern hemispheres. Once the strains that are predicted to be the most common for each flu season have been identified, vaccine manufacturers take approximately 6 months to produce their vaccines and supply them to health care providers (Gerdil, 2003). Currently, two influenza A (H1N1 and H3N2) and one B strains are included in each vaccine dose. Before production, a seed stock for each emerging influenza A strain is made by genetic re-assortment with a backbone strain such as A/H1N1/Puerto Rico/8/1934 (A/PR8/34) or an A/PR8/34-like strain. This is done because A/PR8/34 is a well characterized strain that grows to high titers in embryonated hen's eggs, increasing the yield from potentially low titer wild type strains (Gerdil, 2003). Once the seed stocks are produced, bulk vaccine production can begin. Whole virus is grown in the allantoic cavity of embryonated hen's eggs, harvested and chemically deactivated (with formalin or β-propiolactone), purified by ultracentrifugation and finally split chemically. Prior to 2001, both inactivated whole and split vaccines were on the market, but due to increased side effects from the inactivated whole vaccine, such as fever and reaction at the injection site, it was discontinued (National Network For Immunization Information, 2010). There is also a cold-temperature attenuated nasal spray vaccine (FluMist, Medimmune) available. The drawbacks of the egg based production system include the relatively long 6-month period from strain identification to validation and the lack of scalability, where approximately one egg produces one vaccine dose. Additionally, avian influenza strains, such as the H5N1, cannot be produced in eggs due to its pathogenicity, which is a significant problem considering the potential emergence of a pandemic avian strain (Gerdil, 2003). Moreover, vaccines produced in eggs cannot be given to persons allergic to eggs, limiting their use.

2.2 Cell Culture Based Vaccines

To overcome the challenges associated with egg based production of influenza vaccines, cell culture alternatives have been proposed. Cell culture processes have several advantages over egg

based production such as a superior potential for scale-up, higher initial purity and the absence of potential allergens that exist in the egg-based system (Feng, Jiao, Qi, Fan, & Liao, 2010). However, anticipated bottlenecks of these systems are purification schemes, especially for recombinant VLP systems where it is difficult to purify contaminants that are of similar shape and size (i.e baculovirus, system vesicles). Many steps may be involved in order to assure the VLPs are free of any contaminants, making this step slower than actual cell culture production. The major limitation with this system is higher associated costs, however, their potential still remains and both whole virus split and recombinant subunits vaccines have been produced in cell culture and will be discussed in the following section.

2.2.1 Whole Virus

Many mammalian cell lines have been used as a production platform for influenza vaccines. They include Madin Darby Canine Kidney (MDCK) cells (Voeten et al., 1999), African Green Monkey Kidney Cells (Vero) (Kistner et al., 1998), Human Embryonic Retinal Cells (Per.C6) (Pau et al., 2001), Human Embryonic Kidney (HEK 293) cells (Le Ru et al., 2010), Human Amniocyte CAP (Genzel et al., 2013), Duck AGE1.CR (Jordan et al., 2009; Lohr et al., 2009) and Duck EB66 (Mehtali, Champion-Arnaud, & Arnaud, 2006). Generally, the MDCK cells are favored for influenza virus production because they can produce influenza titers similar to those of eggs, however they grow in adherence and require serum-containing media, which limits the scalability of this system and requires the use of undesirable and unspecified amounts of animal products (Le Ru et al., 2010). In 2012, the first seasonal trivalent inactivated split influenza vaccine made in cell culture from MDCK suspension cells, Flucelvax by Novartis, was approved by the FDA (FDA, 2012), showing the promise of cell culture based productions. The advantage of cell culture derived influenza vaccines over egg-based production is their fast response time and scalability, which is important if a pandemic strain was to emerge. However, there are some drawbacks, such as high cost, potential of lower yields with some cell types and the possibility of producing adventitious agents (Patriarca, 2007). Recombinant strategies to produce subunit vaccines which contain no dangerous infectious material, are another potential solution to these underlying problems of influenza vaccine production (Cox & Hollister, 2009; Haynes, 2009).

2.2.2 Recombinant Subunit Vaccines

Subunit vaccines consist of the purified influenza viral antigen HA. One method to produce subunit vaccines is by production of the target antigens with recombinant technology. The different kinds of recombinant influenza vaccines have been outlined in a review by Sedova *et al* (2012). Recently, an insect cell produced season subunit influenza vaccine, Flublok by Protein Sciences Corporation has been approved by the FDA (FDA, 2013). Influenza virus-like particles can be considered as recombinant subunit vaccine candidates. They are non-infectious and non-replicating particles displaying intact and biochemically active antigens, HA and/or NA that do not contain genetic material (Haynes, 2009). Additionally, influenza VLPs can be constructed with one or both of the two matrix proteins, M1 and M2 (Kang et al., 2009; Pushko et al., 2005; Wu et al., 2010).

Thus far, different production platforms have been studied for influenza VLPs. They vary according to the viral strain produced, the type of gene delivery used and the host-cell expression system. Currently, influenza VLPs have been produced in mammalian, insect and plant cell platforms using a variety of vectors and gene delivery techniques (D'Aoust et al., 2010; Krammer, Nakowitsch, et al., 2010; Tang, Lu, & Ross, 2011). The most extensive amount of VLP studies thus far have been done in insect cells with the baculovirus expression vector system (BEVS) (Bright et al., 2007; Krammer, Nakowitsch, et al., 2010; Pushko et al., 2005; Quan, Huang, Compans, & Kang, 2007). Mammalian cells have also been used to produce VLPs with transfection/transduction (B. J. Chen, Leser, Morita, & Lamb, 2007; Tang et al., 2011), vaccinia virus (Schmeisser et al., 2012) and murine leukemia virus (MLV) (Szécsi et al., 2006) based systems in HEK 293T, HeLa and COS-1 cells. Finally, H5 and H1 VLPs containing HA have been successfully produced in plant cells using the *Agrobacterium* infiltration-based transient expression in the tobacco plant, *Nicotiana benthamiana* (D'Aoust et al., 2008). This system is currently in clinical trials (Landry et al., 2010) and has shown to be very promising in terms of speed and manufacturing costs (D'Aoust et al., 2010).

Considering that recombinant vaccines are biosafety level 1 (BSL-1), and whole virus production is BSL2, recombinant methods are more attractive from a safety point of view. If recombinant vaccines can produce equivalent material (i.e highly efficacious antigens), compared to those produced from whole virus production at similar costs, then they the most promising platform for future vaccines.

Chapter 3: VLP Production in Cell Culture

3.1 General VLP Production and Purification Scheme

Shown below in Figure 3.1 is the general procedure for influenza VLP production and purification that will be described in this section. Generally, clarification by centrifugation is has been the gold standard for this step. However, a more scalable method using membrane filtration in either dead-end or tangential flow modes are also an option (Vicente, Roldão, Peixoto, Carrondo, & Alves, 2011). To concentrate and purify VLPs, ultracentrifugation schemes have been generally used, however chromatography methods have been explored, as they are generally more scalable than ultracentrifugation and easier to use in a manufacturing environment. Bind and elute mode is good because is has the ability to purify and concentrate the product, however purification in flow-through mode has also been used for influenza VLP purification (GE Healthcare, 2012; Vicente et al., 2011).

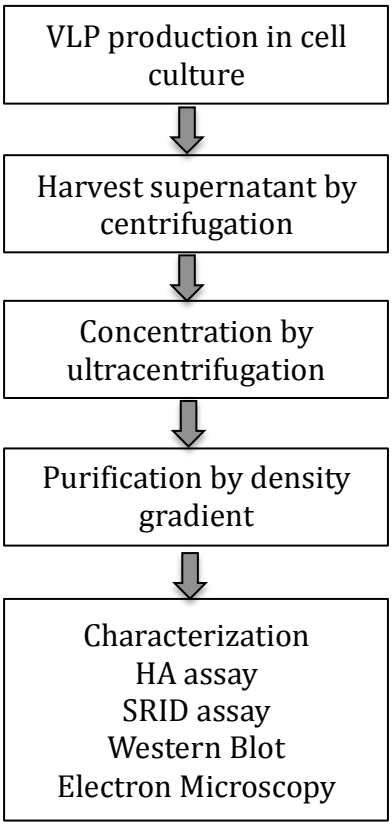

Figure 3.1: General steps for influenza VLP production and purification

3.2 Upstream

3.2.1 Baculovirus Expression Vector System (BEVS)

The BEVS is a well-established system for recombinant protein expression and has been used in industry for over 20 years (Jarvis, 2009). *Autographa californica* nuclear polyhedrosis virus (AcNPV) is the most well-known and used baculovirus (BV) in the biotechnology industry. It infects the alfalfa looper (*A.californica)*, the fall armyworm (*Spodoptera frugiperda)* and also the American cabbage looper (*Trichoplusia ni)*. BV is a double-stranded DNA based enveloped virus that buds from the cell's plasma membrane to produce rod shaped particles 40-50 nm in diameter and 200-400 nm in length (Gerster et al., 2013). The two cell lines most widely used are Sf9 (*S. frugiperda)* and BTI-TN5B1-4 (*T.ni,* commercially known as High Five™) and have been used extensively for the production of both intracellular and secreted proteins (Krammer & Grabherr, 2010). The most commonly used promoter is the strong polyhedron (polh) promoter, which produces the polyhedron protein that coats the occlusion derived (OD) particle that is produced during insect infection. In biotechnology applications, only the budded virion (BV) is used, leaving the polyhedron promoter open to express a gene of interest (Jarvis, 2009). The BEVS has the ability to operate at high cell densities up to 14.0 x 10^6 cells/ml and uses less expensive media compared to mammalian cell culture, allowing for higher yields at lower cost (Bernal, Carinhas, Yokomizo, Carrondo, & Alves, 2009; Elias, Zeiser, Bédard, & Kamen, 2000). Insect cell glycosylation differs from mammalian glycosylation in the N-glycans, producing paucimannosidic and oligomannosidic acid instead of sialic/galactose acids (Krammer & Grabherr, 2010). Many commercial by suppliers such as BD Biosciences and Invitrogen produce kits to construct baculovirus vectors yielding a gene of interest and a working viral stock can be created as fast as one month. The BEVS system has been the most widely used production platform explored thus far for influenza VLP production. However, this system suffers from contamination with BV particles as they also bud from the cell into the supernatant. During the budding process, BV has the ability to take up influenza glycoproteins into its membrane, complicating VLP quantification, characterization and purification (Tang, Lu, & Ross, 2010).

Baculovirus also has the ability to transduce a variety of cell types such as human, rodent, porcine, rabbit, bovine, fish and avian (C.-Y. Chen, Lin, Chen, & Hu, 2011). Once inside the cell,

genes of interest can be expressed as long as they are under control of an appropriate promoter (i.e cytomegalovirus intermediate-early CMV or *hsp70*) (Kost, Condreay, & Jarvis, 2005). Baculovirus is unable to replicate or integrate its DNA into host human cells, making it an ideal system for gene delivery (C.-Y. Chen et al., 2011). The addition of butyric acid, which causes hyperacetylation of histones, leads to enhanced transcription, and an increased amount of protein production (Kruh & Saint, 1982). Another additive that performs the same function as butyric acid is valproic acid (Backliwal et al., 2008). The baculovirus-mammalian cell transduction system (Bacmam) has been applied for influenza VLP production by Tang *et al* (2011) in adherent HEK 293T cells to try and avoid the recurring problem of baculovirus contamination in VLP production with Sf9 cells (Margine, Martinez-Gil, Chou, & Krammer, 2012). Tang *et al* showed that transduction produced equivalent amounts of influenza VLPs compared to liposome transfection with analysis with western blot and fluorescence. Advantages of producing influenza VLPs in mammalian cells include obtaining human-like glycosylation that cannot be obtained in insect cells. De Vries *et al* showed that recombinant HA with complex mammalian glycan structures were able to elicit higher HI antibody titers in chicken and mice compared to recombinant HA produced in insect cells with less complex glycans (2012). However due to the contamination and purification problems encountered for VLP production in insect cells, a direct comparison on the immune response between purified influenza VLPs with insect or human-like glycosylation patterns have not yet been studied.

3.2.2 Cell Culture Processes

VLP production in insect and mammalian cells has been relatively simple, at small scales (i.e – up to 200 ml) usually in shake or T flasks. Generally, DNA is introduced to insect cells through infection with baculovirus, or to mammalian cells by plasmid transfection or transduction with baculovirus. They are then left to incubate for 48-72 hours after which the supernatant is harvested on the assumption that VLPs bud out of the cell. For VLP production in HEK 293 cells the addition of butyric acid and valproic acid at concentrations in the media ranging from 0.25-5 mM were explored. Studies on scale up from shake flask to bioreactor have not been reported for influenza VLP production. In the literature, the methods focus on how VLPs were produced, but most of the time quantitative aspects deal with characterizing final purified products and immunological challenge responses. One of the major limiting factors for the development of

production processes for influenza VLPs is the lack of quantification methods suitable during all stages of process development.

3.3 Downstream Processing

3.3.1 Purification

After the culture supernatant has been harvested, influenza VLPs are purified in downstream processing steps (DSP). The first step involves slow centrifugation (300 x g) to remove cells and any other large debris. Next, the clarified supernatant needs to be concentrated, which is usually done with ultracentrifugation with or without a sucrose cushion of 25-30%. In a protein purification scheme, proteins are usually concentrated with affinity chromatography (i.e - with the use of a histidine tag). Due to their large size, VLPs are usually concentrated by ultracentrifugation, however in an affinity-based scheme specific to VLP proteins (HA), concentration could also be achieved. For ultracentrifugation concentration, larger particles (such as VLPs) are able to pass through the sucrose cushion and pellet at the bottom of the bottle based on their density. Free proteins will pellet at a slower rate, therefore this step also partially purifies the VLPs from smaller contaminants such as free cellular proteins that were not removed during slow centrifugation. Further purification is usually done with ultracentrifugation steps, but can also be accomplished using chromatography based methods, outlined in the next sections.

3.3.1.1 Density Gradient Ultracentrifugation

Currently, most researchers use ultracentrifugation steps to purify influenza VLPs (Bright et al., 2007; Latham & Galarza, 2001; Margine et al., 2012; Tang et al., 2011). This is done either with the use of a sucrose or iodixanol gradient ultracentrifugation. This step works by layering different concentrations of sucrose (20-30-40-50-60%) and then collecting each concentration for analysis after centrifugation. Each concentration of sucrose has a different density, and the VLPs migrate to the zone with the same density, purifying them from other debris that could not be removed in previous steps. Iodixanol is a self-forming density gradient medium used in place of sucrose to complete purification by density gradient ultracentrifugation (Van Veldhoven, Baumgart, & Mannaerts, 1996).

3.3.1.2 Chromatography

Chromatography can also be used to purify influenza VLPs. To date, most of the purification for influenza VLPs has been done with ultracentrifugation using sucrose or iodixanol gradients. These techniques are well established and convenient to use for small-scale production, especially when chromatography-based purification has not yet been fully developed and explored. However, ultracentrifugation is quite labour intensive and has poor scalability (Vicente et al., 2011). Therefore, as the influenza VLP field grows, there have been recent reports of influenza VLP purification using chromatography steps (D'Aoust et al., 2010; GE_Healthcare, 2012). These include size exclusion chromatography, and ion-exchange protocols.

3.4 Quantification

Quantification methods for influenza VLP and virus can be categorized into two general classes. The first provides information on antigen quantity, in the amount of HA (SRID, HA assay) or of enzymatic NA activity, but currently there is no commercial vaccine with quantified NA. The other quantification type gives information on the morphology and concentration of VLPs. Techniques used for particle quantification of viruses (qPCR, TCID50) are not applicable for VLPs due to their lack of genome and infectivity. Currently, the only method available to quantify total VLPs is counting by electron microscopy. There is a relationship between the HA assay and the number of influenza particles that could be used to estimate VLP total particle titers but this correlation cannot be used with confidence as outlined by Thompson *et al* (2013). In the following sections, methods used to quantify and characterize influenza VLPs are described in greater detail.

3.4.1 Hemagglutination (HA) assay

The hemagglutination assay was the first method proposed to quantify the influenza virus based on its agglutination property (Hirst, 1942). This method has remained largely unchanged since it was first developed and has been used for the quantification of HA activity in viral preparations (Kalbfuss, Knöchlein, Kröber, & Reichl, 2008; Petiot et al., 2011). Although this assay is not considered a standard method by health authorities, many production and purification yields of

influenza VLPs use this technique (Pushko et al., 2005, 2011; Quan et al., 2007; Schmeisser et al., 2012). The basis of agglutination is HA's ability to bind sialic acid on erythrocytes (RBC). This is crucial for influenza virus because the virus must bind to sialic acid to enter the cell and begin the infection cycle (Samji, 2009). This point is not significant for VLPs, as they are non-infectious, but their ability to bind sialic acid shows that HA is in the correct conformation and active. To complete the assay, serial dilutions of VLPs are made which RBCs are added. Based on the last well that has hemagglutination, which corresponds to the minimal amount of virus particles that cause complete hemagglutination, the titer of HA in terms of HA units (HAU) can be calculated.

3.4.2 Electron Microscopy

Historically, electron microscopy (EM) has been used for virus observation and influenza whole virus quantification (Isaacs & Donald, 1955). EM has also been used to verify the presence and to characterize influenza VLPs in terms of morphology and size (Krammer, Nakowitsch, et al., 2010; Pushko et al., 2005; Schmeisser et al., 2012). In order to quantify, negative stain electron microscopy (NSEM) is used where samples are prepared, fixed on a grid, and stained for enhanced visualization. Particles are counted within the gridlines and compared to a quantified standard of silicon beads that are also present on the grid.

3.4.3 Single Radial Immunodiffusion (SRID)

Current human influenza vaccine doses are determined from the single radial immunodiffusion (SRID) assay, the only validated potency test used for the quantification of HA protein in trivalent influenza vaccines (Pincus, Boddapati, Li, Sadowski, & Pincus, 2010). This assay measures the radial diffusion of HA in an agarose gel containing specific antibodies. The diameter of the ring is then compared against quantified standards to determine its amount. In contrast to the hemagglutination assay, this method measures the HA content expressed in μg of HA/ml and has a limit of detection of approximately 3-5 μg/ml (Schild, Wood, & Newman, 1975). This method is widely used for VLP characterization (Bright et al., 2007; Easterbrook et al., 2012; Landry et al., 2010; López-Macías et al., 2011; Mahmood et al., 2008; Pushko et al., 2011).

3.4.4 Western Blot

Western blot is used to verify the presence of the proteins that make up the VLPs. This is the only method available that can identify the presence of influenza matrix proteins. Western blot is a well-established method, simple to complete and can also give indication of the amount of contaminating proteins with the appearance of non-specific bands. However, this method is really only suited for purified or semi-purified samples, making analysis complicated with in-process samples.

Chapter 4: Research Objectives

Most of the studies thus far have focused on the proof of concept that VLPs can be produced and on the immunogenicity of influenza VLPs to support their candidacy as potential vaccines (Latham & Galarza, 2001; Pushko et al., 2005). Bright *et al* (2007) showed that influenza VLPs are able to elicit a broader immune response than inactivated whole virus inactivated or recombinant hemagglutinin vaccines; and Mahmood *et al* (2008) showed that an H5N1 vaccine induced protection in ferrets against a lethal injection from H5N1 virus. Additionally, VLPs have been used as a model to gain insight into the minimal requirements for influenza virus budding (B. J. Chen et al., 2007). With all the work done in this field to date, little attention has been paid to the bioprocessing aspect of VLP production. However, studies of this nature are starting to surface, Krammer *et al.* completed an investigation on the comparison of Sf9 and High Five cells for VLP production and found that High Five cells were more productive with less contamination from baculovirus (Krammer, Schinko, et al., 2010). This result agrees with Aucoin *et al*, however Sf9 cells have the ability to operate at high cell densities, which could compensate for the higher productivity of High Five at lower densities (Aucoin, Mena, & Kamen, 2010). Additionally, a study by Tang *et al*. (2011) highlighted a potential solution to contaminating baculovirus with production of VLPs in mammalian cells by Bacmam transduction (Tang et al., 2011). Finally, Vincente *et al* (Vicente et al., 2011) outlined the steps and potential methods to complete large scale production and purification of VLP vaccines, however the focus was not specifically on influenza VLPs but VLPs in general.

In line with the theme of studying influenza VLPs from a bioprocressing point of view, this study aims to characterize quantitatively two of the production platforms tried thus far for VLP production, and to critically analyze the pros and cons of each system.

Objective #1: Produce influenza VLPs with the insect cell-baculovirus and mammalian cell-bacmam systems

- Determine the best production condition for each system with the use of western blot, GFP fluorescence and HA assay

Objective #2: Investigate VLP production from the insect cell-baculovirus production and mammalian cell-bacmam from a bioprocessing standpoint

- Determine production values for each platform in terms of total VLPs produced per production volume, μg HA/ml and HAU/ml from both of their best production conditions
- Quantify the amount of contaminant baculovirus from the Sf9-baculovirus production

Chapter 5: Methods

5.1 Construct design

The DNA sequence of H1N1 A/Puerto Rico/8/1934 HA (AB671289.1), NA (AB671290.1) and M1 (CY033578.1) were obtained from NCBI's influenza database. Sequences were sent to BioBasic (Markham, Canada) for construction in the vector pUC with XbaI and BglII restrictions sites on the C- and N-terminal of each gene. Each vector was then amplified in E.Coli and purified using the Qiagen miniprep system (Venlo, Netherlands). Each vector was digested with XbaI and BglII restriction enzymes from New England Biolabs (Ipswich, USA) and HA, NA and M1 inserts isolated using agarose gel electrophoresis and purified. To make baculoviruses, the BD bioscience (Franklin Lakes, USA) BaculoGold™ system was used. pVL1393 vectors were amplified in E.Coli and purified using Qiagen's miniprep system and further digested in the multiple cloning site with restriction enzymes XbaI and BglII. The remaining vector was then isolated by separation with agarose gel electrophoresis and purified. pVL1393 and the HA, NA and M1 inserts were ligated with T4 Ligase (New England Biolabs), amplified and purified using Qiagen's maxiprep kit to yield pVL1393-HA, pVL1393-NA and pVL1393-M1. All three genes are under the control of the polyhedron promoter (polh)

The construct used for HEK 293 was kindly donated by Dr. Ted Ross at the University of Pittsburg. Its construction can be found in Tang *et al* (2011). Briefly, it was made using the Bac-to-Bac baculovirus construction system (Carlsbad, USA). Each influenza protein, HA, NA and M1 were under CMV control to create a baculovirus that is able to express proteins in mammalian cells (BacMam). Additionally, green fluorescent protein (GFP) was coded under its own CMV promoter to use as a marker. Finally, to promote transduction, baculovirus was pseudotyped with VSVG under polyhedron control.

5.2 Cells and Medium

The HEK 293SF (referred to as HEK 293 in this document) cell line used for VLP production was previously adapted to suspension and serum-free culture (Côté, Garnier, Massie, & Kamen, 1998). Working cell banks were made from a vial of the master cell bank, which was developed

under Good Manufacturing Practices (cGMP). HEK 293 cells were sub-cultured every three days and discarded after 2 months, when a new aliquot from the working bank was thawed for use. HEK 293 cells were grown at 37 °C and 5% CO_2, in animal and serum free SFM4Transfx 293TM (HyQ) medium (HyClone, Waltham, MA, USA) with shaking at 120 rpm. Cells were counted using a hemacytometer or the Cedex Cell Counter (Innovatis Roche Applied Science, Penzberg, Germany) when they were subcultured.

Insect *Spodoptera frugiperda* (Sf9) cells were maintained in serum free Sf900 II media (GIBCO, Burlington, ON, Cananda), in shake flasks at 27 °C with shaking at 110 rpm. Cells were sub-cultured twice each week and maintained for 2-3 months before discarding for a fresh vial from the working sock. Cell density was measured using the Cedex Cell Counter (Innovatis Roche Applied Science, Penzberg, Germany).

5.3 Viral stock production

5.3.1 Amplification

To make recombinant baculoviruses, pVL1393-HA, pVL1393-NA and pVL1393-M1 were all mixed with BaculoGold™ baculovirus linearized DNA at a ratio of 4:1 to give a total of 2 µg DNA. Sf9 cells at $1x10^6$ cells/ml were transfected with Polyethylenimine (PEI) and the DNA mix at a ratio of 2.5:1 and left to incubate for 5 days at 27 °C. Each supernatant was harvested and 2 ml of this stock (called P0) was used to infect 200 ml of Sf9 cells at $2.6x10^6$ cells/ml. Cell density, viability and cell diameter for each amplification were measured every 24 hours with a Cedex Cell counter from Roche Diagnostics (Basel Switzerland). Culture supernatants were harvested after 72 hours at a viability of 60%, 56%, and 39% for P1-BacHA, P1-BacNA, P1-BacM1, respectively. Each was filtered with a 0.22 µm filter and stored in the dark at 4°C. Protein expression was verified with western blot analysis and each virus was titered for total and infectious particles.

The bacmam virus was amplified in a similar way except it was constructed in the Bac-to-Bac system. Sf9 cells were seeded at $0.5x10^6$ cells/ml and PEI and bacmid DNA were mixed at a ratio of 2.5:1 and left to incubate at 27°C for 5 days. Supernatant was harvested and 1 ml was used to infect 100 ml of Sf9 cells at $2.4x10^6$ cells/ml.

5.3.2 Working Stock Production: 3 L Bioreactor

A second round of amplification was done in an A3-3L bioreactor Chemap SG type bioreactor (Mannedorf, Switzerland) to create a working stock (P2) for each virus. The working volume was 2.7 to 2.8 L and the bioreactor was equipped with two sets of 45º pitched-blade impellers with a ratio of impeller to bioreactor diameter of 0.5 and three top-mounted vertical baffles. The temperature was maintained at 27ºC by a water jacket. The partial pressure of oxygen (pO_2) was measured with a polarographic oxygen electrode (Mettler-Toledo, Urdorf, Switzerland) and dissolved oxygen (DO) was maintained at 40% by surface aeration with a gas mixture of nitrogen and oxygen at a total flow rate of 300 cm^3/minute (ccm). The stirring speed was maintained with the chemap control unit at 110 rpm. The pH was measured with a gel-filled electrode (Mettler-Toledo) and culture capacitance was measured with a Biomass Monitor 220 (Aber Instruments, Aberystwyth, UK). The bioreactors were seeded at $0.5x10^6$ cells/ml in Sf900 II media and cells were allowed to grow until reaching a density of approximately $4\text{-}5\times10^6$ cells/ml, after which they were diluted with fresh Sf900 II media to $2\text{-}2.5x10^6$ cells/ml. Cultures were then infected at this concentration by direct addition of baculovirus virus (MOI = 0.1-2) to the culture. Samples were taken twice a day to be counted and measure their viability and average cell diameter.

5.4 Viral Stock Titering

5.4.1 Flow Cytometry: Total Particle Analysis

All P1 and P2 baculovirus stocks were titered for total viral particles using flow cytometry (FC). First, stocks were diluted 100 x with 1x PBS buffer to create the working stock. 100 µl of the working stock virus was added to 850 µl 1x PBS, 20 µl 5% paraformaldehyde and incubated at 4°C for 1 hour to complete fixation of viral particles. Fixed samples were frozen in a mixture of dry ice and ethanol for 10 minutes, and then thawed in a water bath. Next, the fixed viral particles were permeabilized with the addition of 10 µl of 10% Triton-X for 5 minutes. After permeabilization, samples were stained with 20 µl of $5x10^{-3}$ diluted stock of Invitrogen SYBR Green I (Carlsbad, USA). Samples were heated in the dark in a 80°C water bath for 10 minutes, and cooled at room temperature for 5 minutes, before being transferred to polystyrene tubes for analysis. Samples were analyzed with a flow cytometer (EPICS XL-MCL, discriminator: green,

voltage and gain of multiplier: 650 V and 2, threshold: 0 and acquisition time: 30 sec) and compared against the flowset standard that contained $1x10^6$ particles/ml. Flow cytometer profiles looked similar for each virus with minimal amount of aggregation. Total particle concentration was calculated as shown in Appendix 1a.

5.4.2 Easy Titer: Infectious Particles Analysis

All viral stocks were titered for infectivity using Sf9 ET/GFP (Easy Titer) cells with a method developed by Hopkings *et al* (2009). This method was made to replace the TCID50 assay for infectious particles and is based on GFP expression from Sf9 ET/GFP cells once infected with baculovirus. GFP is introduced under polyhedron control, which is turned on during the early replication cycle of the virus. Virus stocks were diluted 1:500 using Thermoscientific SFX HyClone insect cell medium (Waltham, USA) as a diluent. Plates were filled with 100 µl of diluent in rows A-H columns 2-10 and then 125 µl of diluted virus stock in rows A-H, column 1. The virus was serially diluted 1:5 in each column from 1-9 and column 10 was left blank as a control. The Sf9 ET/GFP cells were seeded into each well with 100 µl of working stock for a final cell concentration of $7.4x10^4$ cells/well using a multichannel pipette. Plates were placed in a plastic storage container with a damp towel to maintain moisture and incubated for 5 days at 27 °C. Then TCID50 values were determined by scoring GFP positive wells for each virus stock. Based on GFP positive wells, the infectious titer was calculated (Appendix 1b). Table 5.1 shows the infectious and total particle titers of each viral stock calculated using this method and the FC method previously described.

Table 5.1: Total and infectious titers of each virus stock made.

Virus Stock	Total Virus Particles/ml	Infectious Virus Particles/ml	Total Particles: Infectious Particles
P1 HA Baculovirus polh	$5.79x10^9$	$9.22x10^8$	6.28
P2 HA Baculovirus polh	$6.46x10^8$	$1.02x10^8$	6.33
P1 NA Baculovirus polh	$4.74x10^8$	$1.62x10^8$	2.93
P2 NA Baculovirus polh	$1.92x10^9$	$1.15x10^8$	16.7
P1 M1 Baculovirus polh	$1.21x10^9$	$3.18x10^8$	3.81
P2 M1 Baculovirus polh	$3.51x10^9$	$1.34x10^8$	26.2
P1 HA+NA+M1 Bacmam CMV	$2.88x10^9$	$5.83x10^7$	49.4
P2 HA+NA+M1 Bacmam CMV	$3.79x10^9$	$1.21x10^9$	3.1

In order to calculate the multiplicity of infection (MOI) for VLP production, the infectious titer must be known. MOI represents the number of infectious virus particles (IVP) added per cell in culture. It is calculated with the following equation

$$MOI = \frac{Infectious\ Titer\ \left(\frac{IVP}{mL}\right) \times Virus\ Volume\ (mL)}{Cell\ concentration\ \left(\frac{Cells}{mL}\right) \times Total\ Volume\ (mL)}$$

5.5 VLP Production

5.5.1 Mammalian Platform

Cells were transduced with the P2 working stock at a density of 1.0-2.0x10^6 cells/ml with MOIs ranging from 1-200 at 37°C. Twice a day to every 24 hours, cell density, viability and average cell diameter were measured using the Cedex Cell Counter (Innovatis Roche Applied Science, Penzberg, Germany).

5.5.1.1 μ-24 MOI and Additive Study

MOI and additive runs were completed in a 6 ml μ-24 microbioreactor (Pall, New York, USA) with a 5 ml working volume. 48 hours before transduction, 1 ml of media was added to each well to calibrate the pH and temperature probes. 24 hours prior to transduction, each well was seeded with cells at a concentration of 0.5-0.75x10^6 cells/ml so they could be transduced the following day between 1.0-1.5x10^6 cells/ml. DO was controlled at 40% with the addition of oxygen and inert gas, pH was monitored and controlled at 7.2 with CO_2 addition, and the cassette was mixed by shaking at 500 rpm. Baculovirus was added to give MOIs ranging between 1-200 followed by the addition of butyric acid or valproic acid for a final working concentration of 0.25-5 mM. Cell density was measured 24, 30 and 48 hpt using a cedex cell couter or hemacytometer. Cells were harvested 48-72 hours post transduction and cells were analyzed for GFP expression and influenza protein expression by western blot.

5.5.1.2 Shake Flask Production

All other runs were completed in shake flasks (0.250-2 L with 60-400 ml working volume, respectively). Cells were transduced at 1.0-2.0x10^6 cells/ml with baculovirus at an MOI of 60, followed by addition of butyric acid for a final concentration of 5 mM. After 48 or 72 hours the cells were clarified by slow centrifugation at 300 x g for 5-10 minutes. The supernatant was concentrated via sucrose cushion ultracentrifugation and analyzed by western blot, HA assay, NSEM and SRID. SCC-VLPs were further purified using iodixanol density gradient ultracentrifugation.

5.5.2 Insect Platform

VLP productions were completed in shake flasks (0.250-2 L flasks with 60-400 ml working volume, respectively). Cells were infected with P2 working stocks at a density of 2.0-2.5x10^6 cells/ml with a total MOI of 0.3-2.1 at 27°C. Every 24 hours, cell density, viability and average cell diameter were determined using the Cedex Cell Counter (Innovatis Roche Applied Science, Penzberg, Germany). Cells were harvested after the viability started to decline but before it reached 50%, preferably around 70%. Upon harvest, cells were separated from the supernatant with slow centrifugation at 300 x g for 5-10 minutes. The supernatant was concentrated via sucrose cushion ultracentrifugation and analyzed by western blot, HA assay, NSEM and SRID. Further purification was achieved using density gradient ultracentrifugation.

5.5.3 Cell Pellet Analysis

To explore the possibility of VLPs trapped within or attached to Sf9 or HEK 293 cells and to develop an appropriate method of release, the cell pellet obtained after slow centrifugation was re-suspended in a solution of 1x PBS and 10 µg/ml of TPCK-trypsin and slowly shook at 37°C for 30 minutes. Cells were pelleted via slow centrifugation and the cell pellet wash was collected for analysis by western blot, HA assay and NSEM. To explore the possibility of internally budded VLPs, cell pellets were frozen at -80°C and thawed to induce cell lysis and the supernatant was removed via centrifugation at 1000 x g for 5 min. The supernatant was analyzed using western blot, HA assay and NSEM.

5.6 VLP Purification by Ultracentrifugation

5.6.1 Sucrose Cushion Ultracentrifugation

Concentration by sucrose cushion ultracentrifugation works as to both concentrate and semi-purify by removing free proteins found in the supernatant. 200 ml of supernatant from VLP productions in both Sf9 and HEK 293 cells were loaded into cold 250ml ultracentrifugation bottles. If there was not 200 ml of supernatant available, the volume was completed to 200 ml using 20 mM Tris-HCl at pH 7.5. The VLP supernatants were under layered with 10% of the VLP supernatant volume with 20 mM Tris-HCl 25% sucrose at pH 7.5 (i.e 20 ml 25% sucrose solution for 200 ml VLP supernatant). This was spun at a speed of 37 000 x g for 3 hours (Sorvall Discovery SE 100 ultracentrifuge, A621 rotor, Thermo Scientific, Waltham, USA) at 4°C. The supernatants were then discarded and the remaining VLP pellet was re-suspended in 20 mM Tris-HCl, 1% sucrose, 2 mM $MgCl_2$ overnight at 4°C to give a total concentration factor of 20-75x. Sucrose cushion VLP solutions were then aliquoted and stored at either -80°C, 4°C or subjected to further purification by iodixanol density gradient ultracentrifugation.

5.6.2 Iodixanol Density Gradient Ultracentrifugation

Iodixanol density gradient ultracentrifugation works by separating particles based on their density. A 40% w/v working stock was made using 20 g of 60% w/v Optiprep Iodixanol solution (Axis-Sheild, Oslo, Norway) with 10 g of 60 mM Tris-HCl pH 7.5. A 25.5% working stock was made using 19.13 g of the 40% working stock with 10.87 g of 20 mM Tris-HCl pH 7.5. Next, 13 ml of the 25.5% working stock and 3.51 ml sucrose cushion purified VLPs were combined and subjected to slow mixing to give a final iodixanol concentration of 20% and VLP dilution of 4.7x. The VLP-iodixanol solution was then loaded into 13 ml ultracentrifuge tubes, sealed and spun at 350 000 x g for 6 hours at 4°C (Sorvall Discovery SE 100 ultracentrifuge, 65V13 rotor, Thermo Scientific, Waltham, USA). After ultracentrifugation, 1 ml fractions were taken from the bottom of the tube and weighed to determine the density and iodixanol concentration in each. Each fraction was analyzed by western blot, HA assay and NSEM.

5.7 VLP Quantification and Detection

5.7.1 Western Blot

30 µl of 1.4 M DTT was added to 250 µl SDS-sample buffer from Bio-Rad (Hercules, USA). Samples were then added at a ratio 2:1 to the reduced sample buffer and left to equilibrate at room temperature for 5 minutes. Samples were boiled at 100 °C for 5 minutes and left to equilibrate for 5 minutes at room temperature. Samples were then centrifuged for 30 seconds at 13 000 x g and loaded into a Bio-Rad mini-protean Tris-Glycine 4-15% electrophoresis gel with 1x running buffer (25 mM Tris, 192 mM Glycine, 3.5 mM SDS). The gel was run for 40 minutes at 200 V and then washed 3 times with Towbin transfer buffer (25 mM Tris, 192 mM Glycine, 20% Methanol pH 8.3) before being transferred to a nitrocellulose membrane via semi-dry western transfer with a Bio-Rad Trans-Blot 3D semi-dry transfer cell for 1 hour at 10 V. After the transfer the membranes were incubated with 5% non-fat milk solution in 0.1% Tween 1x TBS pH 7.5 (50 mM Tris, 150 mM NaCl, 0.1% Tween-20) for 1 hour. The membrane was washed 3 times for 10 minutes with 0.1% Tween TBS pH 7.5 and then incubated with its respective antibody at a concentration of 1/1000 overnight at 4 °C. The membranes were washed again 3 times for 10 minutes with 0.1% Tween TBS pH 7.5 then incubated for 1 hour with 1/1000 secondary antibodies. Finally, the membranes were washed once again with 0.1% Tween TBS pH 7.5 4 times for 10 minutes and then a picture of each was taken with as DS Image Station 440CF (Kodak, Rochester, USA).

Table 5.2: List of Antibodies used for western blots

Antibody	Type	Manufacturer
Anti-HA	Primary Polyclonal sheep serum	NIBSC, London, United Kingdom
Anti-NA	Primary Polyclonal sheep serum	NIBSC, London, United Kingdom
Anti-HA	Primary Monoclonal Mouse	Santa Cruz Biotechnology, Santa Cruz, USA
Anti-M1	Primary Monoclonal Mouse	AbCam, Cambridge, United Kingdom
Anti-GP64	Primary Monoclonal Mouse	eBioscience, San Diego, USA
Donkey anti-sheep IgG	Secondary HRP	Jackson ImmunoResearch, West Grove, USA
Donkey anti-mouse IgG	Secondary HRP	Jackson ImmunoResearch, West Grove, USA

5.7.2 Hemagglutinin (HA) Assay

The assay was completed in 96 well v-bottom plates. Plates were filled with 100 µl of 1x PBS solution in rows A-H, column 2-12. Each sample took up two rows (A and B, C and D, etc) and was serially diluted with VLP samples from the supernatant, sucrose cushion and iodixanol purifications. Once the wells were serially diluted, 100 µl of red blood cells at a concentration of $2x10^7$ cells/ml were added to each well in the plate for a final concentration of 1.25%. The plates were left in a plastic container for 3 hours to overnight and scored. If hemagglutination of the RBCs by the VLPs has occurred, then the solution in the well will be light red and homogenous. If hemagglutination did not occur, there will be a cell pellet at the bottom of the well of RBCs, referred to as a button. There exists a grey area when reading the plates, based on the size and shape of the dot, where some may consider that hemagglutination still partially occurs. Section 6.4 explains this point further. Calculations to determine HA units/ml can be found in Appendix 2.

5.7.3 SRID assay

To a 1% agarose solution in 1x PBS, equilibrated to 50 °C in a water bath, Anti-HA sheep serum (NIBSC, London, United Kingdom) was added and mixed. The agarose-antibody mixture was cast and left to cool in a Bio-Rad gel-casting module for at least 15 minutes. Once the gel was set, 4 mm wells were punched into the gel. Purified recombinant A/H1N1/Puerto Rico/8/1934 from Protein Sciences Corporation (Meriden, USA) at 30, 20, 15 and 7 µg/ml was used as a standard. Treatment with 1% Zwittergent for 15 minutes on a rocker platform was used to help break up VLPs or VLP aggregates to allow for better diffusion. 20 µl of each sample was added to its own well and left at room temperature for 18-24 hours. The gel was dried using Whatman #3 filter paper (Kent, United Kingdom) and paper towels to absorb the liquid. After removing and replacing the paper towel 3 times (but keeping the filter paper on top of the gel), the gel was placed in a 37°C incubator for 15 minutes before removing the filter paper and continuing the incubation until the gel was transparent. The gel was rinsed with deionized water and stained with Coomassie Blue R-250 for 15 minutes and distained using a 7.5% acetic acid and 10% ethanol solution. The gel was photogrpahed and the diameter of the reference standards and samples were calculated using Image-J software (Pixel-aspect ratio = 1, known distance = 4mm). A calibration curve based on the area of the immunoprecipitation ring from the standard ring diameters can be found in Appendix 3.

5.7.4 NSEM

NSEM analysis and quantification was completed by Micheline Letarte at INRS Institut Armand Frappier in Laval, Quebec. Samples were diluted with TEN buffer (10 mM Tris, 1 mM EDTA, 100 mM NaCl pH 8.0) to an appropriate concentration. Diluted samples were then placed in 240 µl microtubes with carbon and polyvinyl formal coated grids inserted at the bottom of the tubes. The tubes were centrifuged at 20 000 x g for 5 minutes. Recovered grids were dried and stained with 3% phosphotungstic acid, pH 6.0. Samples were then visualized under a transmission electron microscope.

Chapter 6: Production of Influenza VLPs Using the BacMam System

Production of influenza VLPs in mammalian cells using the BacMam system have been previously reported by Tang *et al* (2010). From the literature and our own experience, it seems plausible that manipulation of production conditions has the potential to increase VLP production. In particular, the addition of butyric acid, valproic acid, and increasing cell concentration at transduction to achieve increased production. To examine these factors, sequential experiments were completed; by varying the concentrations from 1-5 mM and 0.25-2 mM of butyric acid and valproic acid, respectively; and increasing cell concentration at transduction from $0.5x10^6$ cells/ml to $2x10^6$ cells/ml. Conditions were probed for VLP production with the aid of western blots of HA, visual inspection of reporter GFP expression and the HA assay. The starting point used the optimal conditions found in Tang *et al* (2010). Typical growth curves during VLP production can be found in Appendix 4a.

6.1 Butyric Acid and Valproic Acid Additives

To try and increase protein production, one dose of butyric acid or valproic acid was added to VLP production directly after addition of the BacMam virus. We assumed that both additives remained in the culture for the duration of the experiment, as cell growth was either completely arrested or slowed down compared to the control culture, which is one of the side effects of the addition of butyric and valproic acids. Visual inspection of GFP expression, as shown in Figure 6-1 was analyzed to compare protein expression with and without the addition of butyric acid during VLP production at an MOI of 60 (three independent replicates were completed). Because of unique CMV promoter control of GFP and the influenza genes, expression profiles of GFP and the influenza proteins were expected to be similar. It should be noted however, that VLP production does not necessarily follow the same profile as simple protein production.

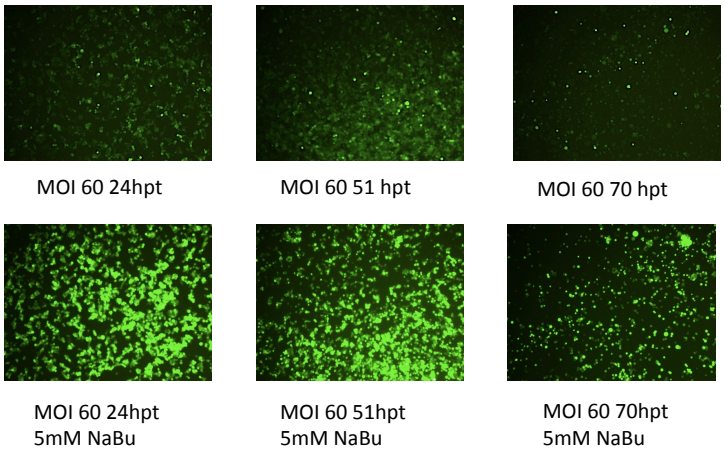

Figure 6.1: GFP expression with and without the addition of 5mM butyric acid.
The top row shows pictures for GFP expression in culture taken at 24, 51 and 70 hpt without the addition of butyric acid. The bottom row shows GFP expression in culture taken at 24, 51 and 70 hpt with the addition of butyric acid.

As shown in Figure 6.1, GFP expression is enhanced with the addition of 5 mM butyric acid at each time point. Figure 6.2 shows the HA activity (normalized to production values) measured from productions completed with and without the addition of butyric acid.

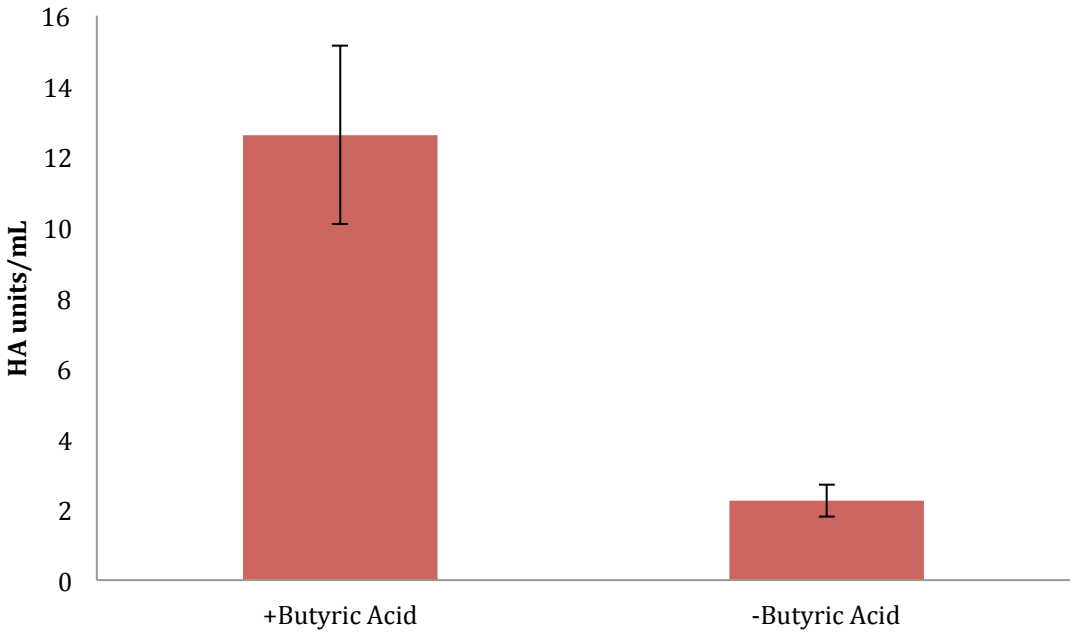

Figure 6.2: HA activity (HAU/ml) of sucrose cushion purified HEK 293 VLPs produced with and without butyric acid.

More information on the appropriate time of harvest was also gained from this study as it was observed that the GFP signal decreased after 70 hours post transduction (hpt), possibly due to the degradation of the baculovirus viral DNA inside the cell, and started discussions of the appropriate time of harvest discussion, as Tang *et al* (2011) harvested their VLP production at 72 hpt. At 72 hpt, cell viability was still over 90%, however there was a large amount of cell clumping observed, making counting difficult. Experiments from this point on were harvested around 48 hpt to avoid cell clumping and take advantage of maximum protein production based on GFP expression at 48 hpt.

Valproic acid and butyric acid addition at different concentrations (one experiment of 0-2.5mM and 1-5mM for valproic acid and butyric acid, respectively) were assessed visually based on GFP fluorescence as shown in Figure 6.3. These concentrations were used based on the concentrations of butyric acid used in the previous study by Tang *et al* (2011) and from concentrations that have been previously tested in the past by members of our group for protein production in mammalian cells. Under the range of conditions tested, valproic acid did not appear to have a significant effect on GFP expression where 5mM butyric acid resulted in the most intense signal.

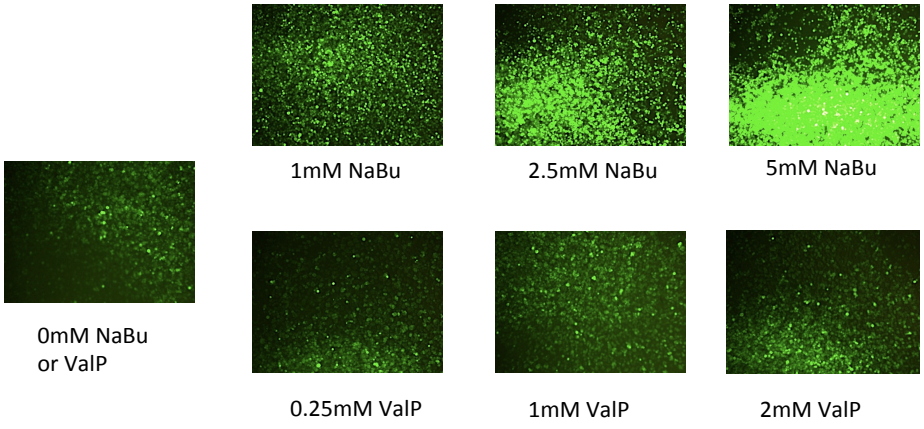

Figure 6.3: GFP expression with the addition of butyric acid and valproic acid for HEK 293 VLP production.
The top row shows GFP expression from cultures with butyric acid addition (NaBu) at concentrations from 1-5 mM. The bottom row shows GFP expression from cultures with valropic acid (ValP) at concentrations from 0.25-2 mM.

6.2 Multiplicity of Infection (MOI)

Different MOIs were tested to pinpoint the one leading to the highest GFP and HA protein expression (three independent replicates). Figure 6.4 shows GFP expression at different MOIs. MOIs of 120 and 200 showed the most intense GFP signal in this study. These MOIs were chosen partly based on those used previously by Tang *et al* (2011) and also depended on the concentration of the BacMam that we produced. We did not want to add more than 10% BacMam by volume to the culture, so MOI 200 was the upper limit that allowed us to stay within these boundaries without further concentration of the virus stock.

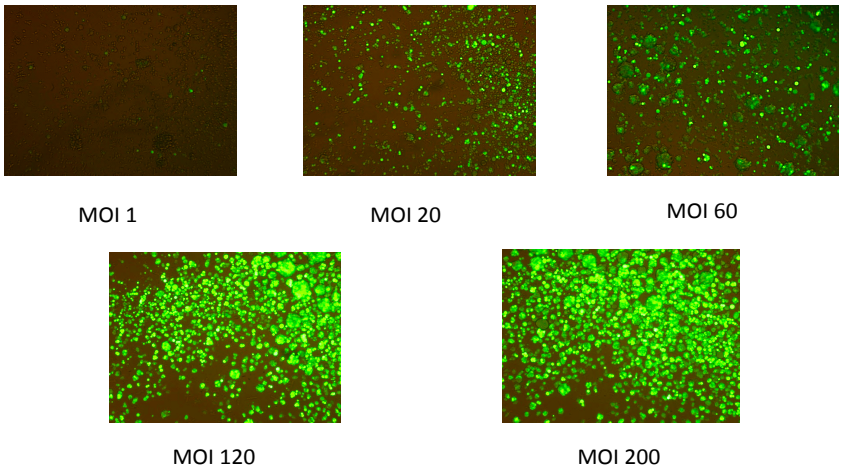

Figure 6.4: GFP expression at different MOIs ranging from 1-200 for HEK 293 VLP production.

Western Blot analysis revealed that while MOIs of 120 and 200 had the strongest GFP signal, MOIs of 60 and 120 had similar HA band intensity as shown in Figure 6.5. This result matches Tang *et al* (2011), who observed that, above an MOI of 60, influenza protein production saturated, based on their NA western blot analysis (Tang et al., 2011). From this result, an MOI of 60 was chosen for subsequent studies.

1 2 3 4 5

Figure 6.5: HA western blot for MOIs of 1-200 for HEK 293 VLP production.
Labels 1-5 represent MOIs of 1, 20, 60, 120 and 200, respectively. MOI 60 was chosen as the condition that produced the greatest amount of HA protein.

6.3 Cell Concentration at Transduction

VLP production was compared during production at two different concentrations, $1.0x10^6$ cells/ml and $2.0x10^6$ cells/ml. Higher cell densities were not explored because of in-house data that showed that productivity of HEK 293 cells reached a plateau at $2.0x10^6$ cells/ml for influenza virus production. Sucrose cushion concentrated supernatants were compared using the HA assay as shown in Figure 6.6. VLP production with a starting cell concentration of $2.0x10^6$ cells/ml had a higher HA activity than production with a starting concentration of $1.0x10^6$ cells/ml. Transduction at a cell density of $2.0x10^6$ cells/ml was chosen for subsequent studies.

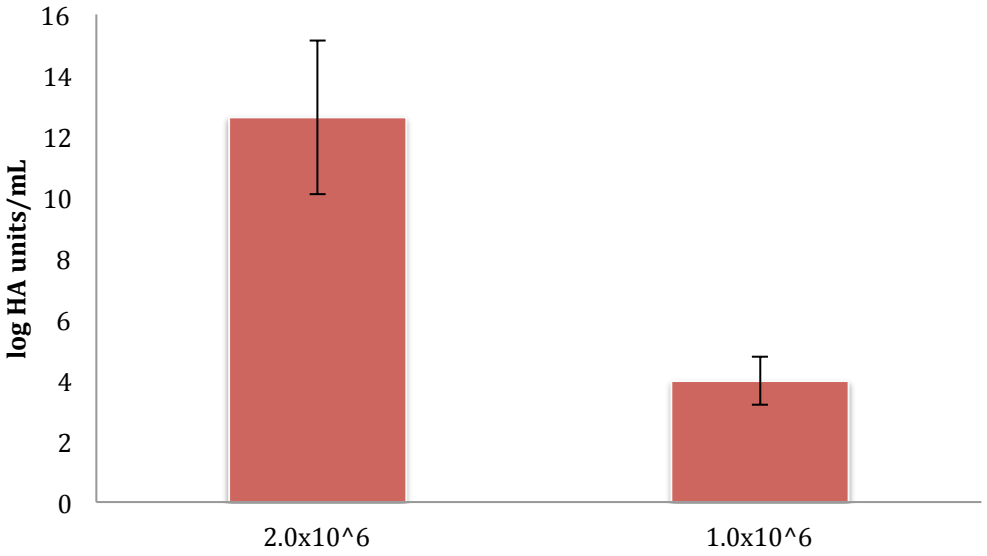

Figure 6.6: HA activity (HAU/ml) of sucrose cushion purified HEK 293 VLPs at different cell concentrations.

6.4 VLP Characterization

In order to verify the presence of VLPs, harvested supernatants were concentrated with a sucrose cushion and analyzed for presence of HA, NA and M1 proteins by western blot. Any free influenza or cell proteins in the supernatant should not be captured in the sucrose cushion pellet containing VLPs, thereby also serving as a partial purification step. HA activity was verified with the HA assay and the SRID assay. The physical presence of VLPs was verified and quantified by NSEM.

Analysis by western blot confirmed the presence of HA and NA proteins in VLPs (Figure 6.7). HA0 is found just under 75kDa and overlaps with contaminant proteins labeled through non-specific binding (shown in Appendix 5). The positive control, H1N1 A/Puerto Rico/8/1934 (influenza WT), does not match the HA0 band in the VLP sucrose cushion (SC) lane because it was produced in the presence of trypsin, which cleaves HA0 into HA1 and HA2 (J. Chen et al., 1998). Although WT virus needs to be produced in the presence of trypsin in cell culture to ensure infectivity (Le Ru et al., 2010), it is not required for the production of non-infectious VLPs. Therefore, HA in VLPs should remain in its uncleaved form, HA0. NA was present at approximately 55kDa in the VLP sample, but for the WT two extra bands at 37kDa and at 25 kDa were also labeled. These bands could potentially be truncated forms of NA from trypsin cleavage during production (Air & Laver, 1989). M1 is only present in the sucrose cushion in very low amounts, and was confirmed to be present in the pellet by western blot shown in Figure 6.15.

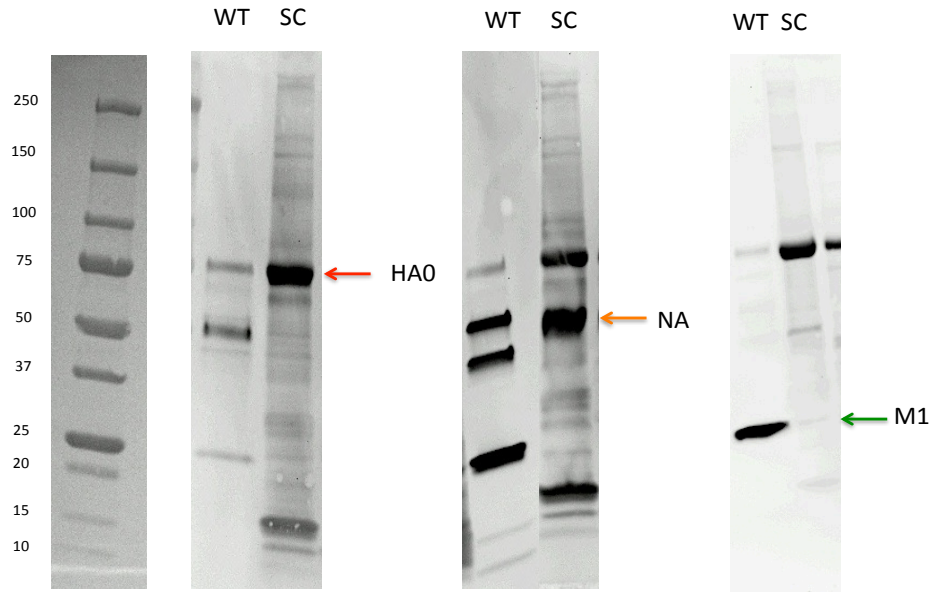

Figure 6.7: HA, NA, M1 western blot of HEK SCC-VLPs and influenza H1N1/A/PR/8/1934. WT is supernatant from H1N1/A/PR/8/1934 and SC is SCC-VLPs, both produced in-house from HEK 293 cells.

The HA assay was completed to show the agglutination activity of sucrose cushion purified VLPs. Figure 6.8 shows a typical profile that was obtained when completing this assay. One observation from this assay was that there exists a grey area, where partial agglutination occurred as described previously (Killian, 2008). The red circle on the left without a red drop represents the lower limit of agglutination, where complete agglutination of the red blood cells occurred. The wells enclosed by the black lines have small red dots that do not tear when the plate is inclined and this is where partial agglutination occurred. Finally, the last well with a non-tearing drop is the upper limit of agglutination. In this study, we adopted a similar methodology to Tang *et al* (2011), where they took the upper limit of agglutination as the HA titer. HA titers of 630 HAU/ml for a 50x concentrated VLP sample that corresponds to a production value of 12.6 HAU/ml were obtained.

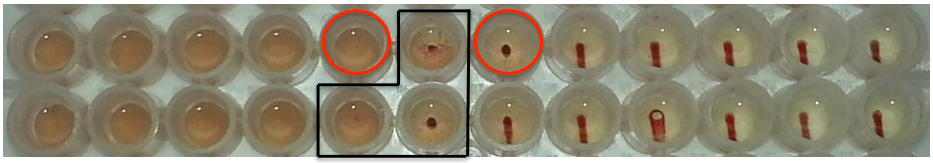

Figure 6.8: HA assay results completed with sucrose cushion HEK 293 VLPs and 1.25% chicken red bloods cells.
The circle on the left represents the point where complete agglutination occurs, and the circle on the right is where incomplete agglutination occurs. The area between the circles outlined by the box represents incomplete agglutination.

The SRID assay was used to quantify the amount of HA in µg/ml. Figure 6.9A shows a picture of the diffusion pattern observed. The observed ring is very small, but was able to be quantified as 4.6 µg HA/ml in a 50x concentrated VLP sample and a production value of 0.09 µg HA/ml. The ring does not follow the standard pattern that SRID rings usually follow (shown in Figure 6.9B). This could be because sucrose cushion material, which was only partially purified, was used instead of fully purified material (the standards). The debris in the sample could precipitate in the well resulting in the dark stain around the circumference[1].

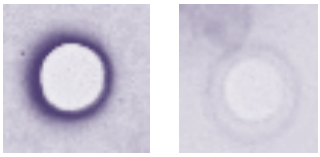

Figure 6.9: SRID rings observed with HEK 293 VLPs (A) and recombinant H1N1/A/PR/8/1934 protein (B).

SCC-VLPs and influenza virus were analyzed by visual inspection and quantified for total particles/ml by NSEM. Figure 6.10 and 6.11 shows zoomed-in images of both VLPs and virus produced in-house in HEK 293 cells (marked with black arrows). VLPs were identified as

[1] At first, we assumed there was actually no diffusion ring, but after adjusting the contrast on the picture, we could see that the outer ring was very close to the inner precipitation ring that it appeared there was only one ring.

particles with a fringe or spike around the outside, which was assumed to be made up of influenza glycoproteins HA and NA. VLPs were counted to be at a concentration of $7.9x10^9$ VLPs/ml in a 50x concentrated sample, or $1.58x10^8$ VLPs/ml during production. Influenza virus produced in cell culture is pleomorphic and consists mainly of spherical and elongated particles with an average size of 100 +/- 20 nm (Le Ru et al., 2010). Based on the way VLPs were identified and quantified for this analysis, their morphology also falls into this classification however the average size ranged from 100 to 300 nm by NSEM analysis. Figure 6.11 shows a zoomed out image of SCC-VLPs and influenza virus. In the virus sample, it was easier to identify influenza particles, as it is already widely known what influenza particles look like. However, it is clear that in the virus sample there are particles with a fringe (marked with white arrows) that would have been identified as VLPs had they been in the VLP sample.

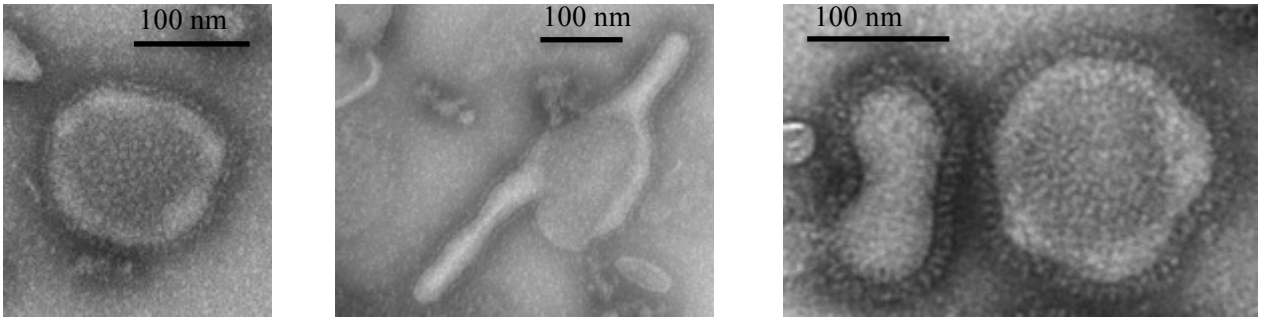

Figure 6.10: NSEM images of VLPs (A, B) and influenza virus H1N1 A/PR/8/1934 (C) at 40 000x magnification.
VLPs from image A resembles typical influenza particles produced in cell culture, as shown in image C. However, image B shows particles with unique morphology.

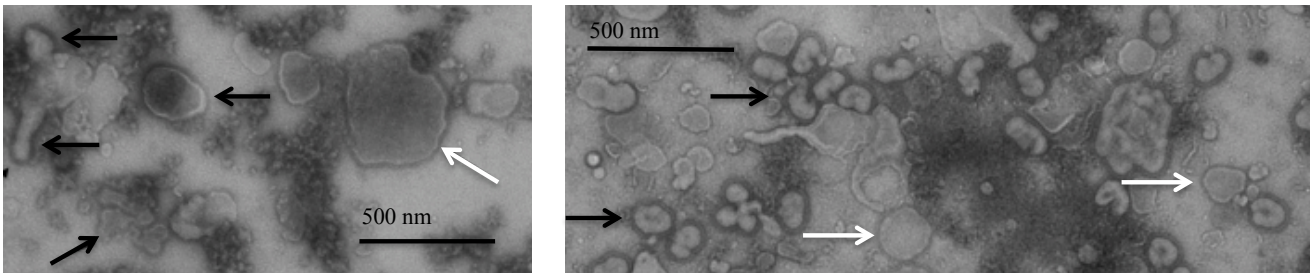

A B

Figure 6.11: NSEM images of SCC-VLP and virus samples.
Black arrows represent the particles identified as VLPs (image A) or influenza virus (image B). White arrows represent similar looking larger particles with a fringe that could also be identified as VLPs that were found in both samples.

In order to gain insight on how to store VLPs mid-process, SCC-VLPs were either stored at -80 °C or 4 °C and analyzed after 3 weeks. Both samples showed the same HA activity (12.6 HA units/ml), indicating that particles can be stored at either temperature with no detectable effect on HA activity during purification.

6.5 VLP Purification by Iodixanol Gradient

SCC-VLP samples were purified further using ultracentrifugation with an iodixanol gradient. Fractions (12 or 13 x 1ml) were collected from the bottom of the tube and analyzed with western blot, HA assay and NSEM. Figure 6.12 is the HA western blot of fractions collected from the iodixanol gradient ultracentrifugation. HA0 is the middle band just under 75 kDa and present in the iodixanol fractions at the bottom of the tube (fractions 1, 2, 3, first lanes on the left in Figure 6.12) and the top of the tube (fractions 11 and 12, the last two lanes on the right in Figure 6.12). The density at the bottom of the tube was 1.2-1.1 g/ml where at the top was 1.0 µg/ml. Particles (including VLPs) migrate to fractions of higher density and free protein to those of lower density. Western blots for NA agreed with the pattern for HA while M1 was only found in fraction #1 (NA and M1 western blots shown in Appendix 6a). The HA band in top fractions show that there was a high amount of free HA protein present in the sucrose cushion starting material released from VLPs during iodixanol purification.

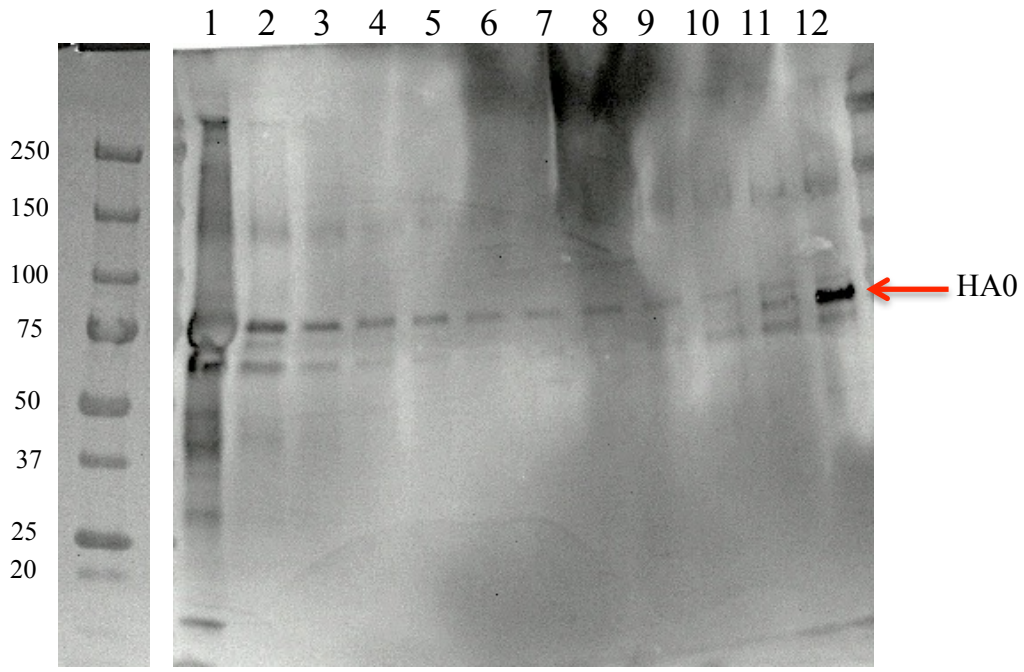

Figure 6.12: HA western blot of collected iodixanol gradient purified VLP fractions.
Fraction #1 corresponds to those of higher density taken from the bottom of the ultracentrifugation tube and fraction #12 to those of lower density from the top of the tube.

Collected iodixanol fractions where analyzed by the HA assay. Figure 6.13 shows their agglutination ability in HAU/ml. HA activity agrees with HA identification from the western blot, with the highest HA activity detected in the bottom and top fractions of the iodixanol gradient.

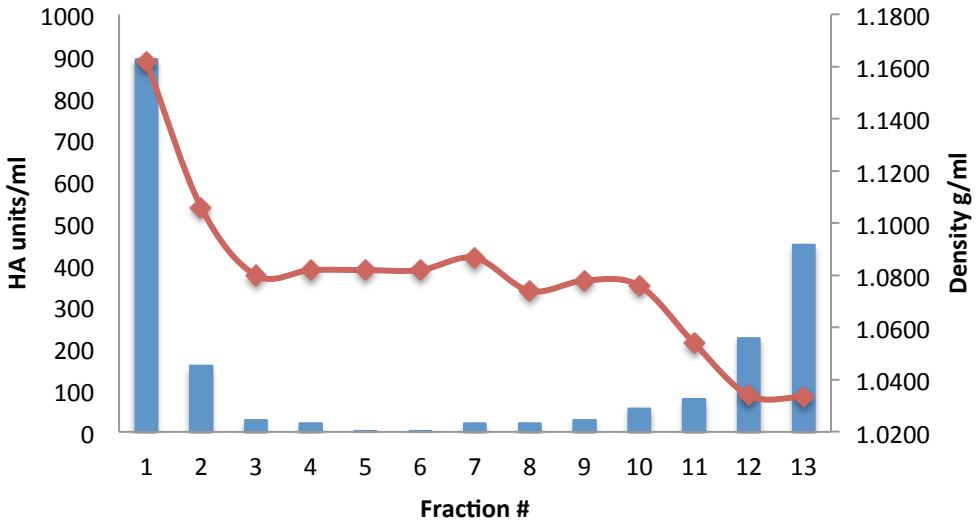

Figure 6.13: HA activity (blue bars, left axis) and density (red line, right axis) in iodixanol fractions #1-13.

Iodixanol fractions of high and low density were visually analyzed by NSEM and quantified. Figure 6.14 shows NSEM images at 40 000 x magnification. Fraction #1 contained the highest amount of VLPs quantified. In addition, this fraction contained many small white particles (that could possibly be identified as aggregated HA proteins, or HA rosettes (Ruigrok et al., 1988)) as well as a baculovirus particle (rod shaped particle), both indicated by the white arrows. Fraction #2 and #3 both contain less white protein aggregates and less VLPs. Fraction #3 contained less contaminant and a more homogenous population of VLPs around 100 nm. Fraction #12 however, contained very large pieces of membrane and fringed particles along with VLPs. The heterogeneity of this sample made quantification difficult, but it was found to contain 1.84×10^9 VLP/ml. This fraction also elicited a strong response on the western blot and HA assay, either from the fringed particles or in the form of free HA that migrated to the fractions of lower density. The agglutination ability of VLPs in terms of particle concentration is given in Table 6.1 and varied from 8.20×10^6 – 1.21×10^8 VLP/HAU. Fraction #1 contained the small white particles, which could be HA rosettes, fraction #12 contained the larger pieces of membrane. Larger particles or pieces of membrane will naturally have a better agglutination ability than small rosettes, as they require less to agglutinate RBCs. Issacs & Donald (1955) state a similar observation, where they saw that filamentous influenza had a different agglutination ability than spherical-like, based on its larger size. Fractions 2 and 3 had similar

VLP/HAU values and also contained similar looking VLPs, and did not contain rosettes or large pieces of membrane with HA spikes in the NSEM images like fractions #1 and #12.

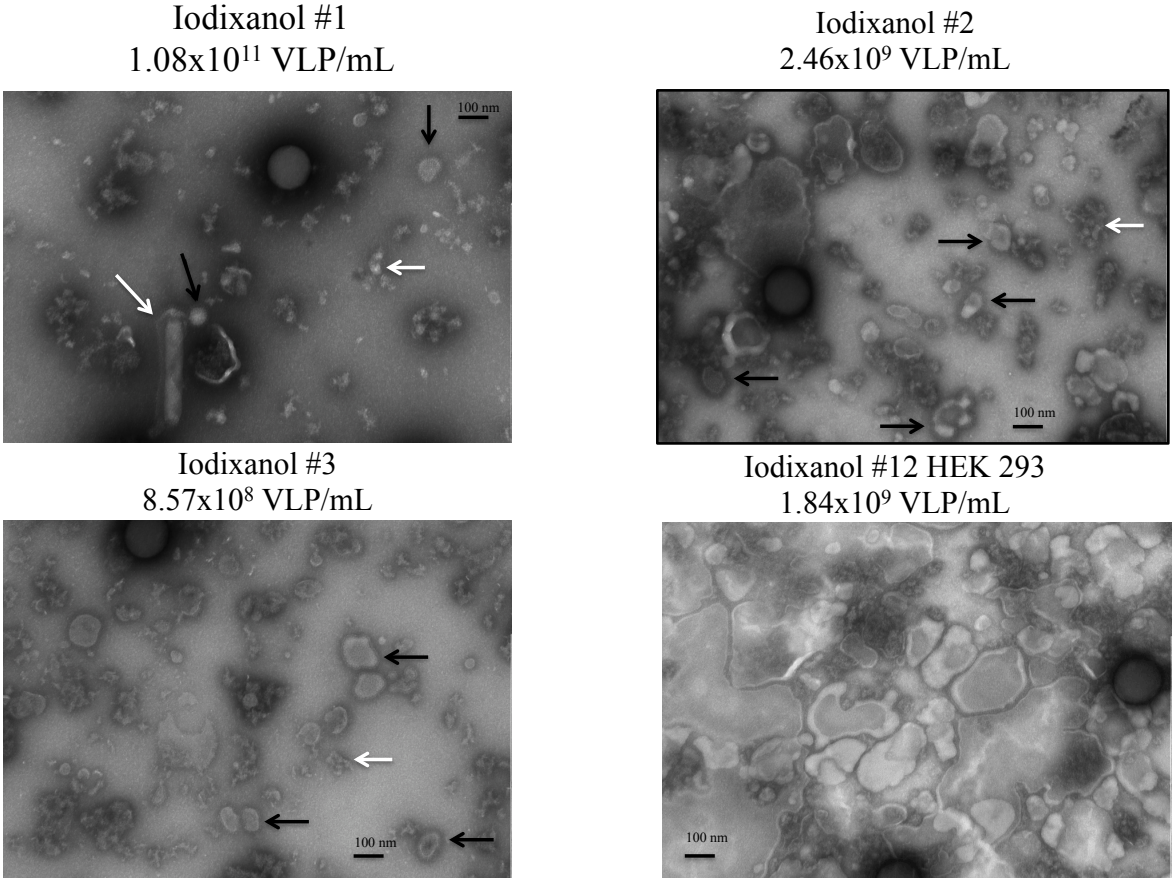

Figure 6.14: NSEM images of iodixanol purified VLPs at 40000x magnification.
Black arrows indicate VLPs. White arrows indicate HA rosettes and baculovirus particles (image #1), and debris (image #2).

Table 6.1: VLP/HAU for different fraction of the iodixanol density gradient

Fraction	VLP/HAU
1	1.21×10^8
2	1.55×10^7
3	3.03×10^7
12	8.20×10^6

6.6 Cell Pellet Analysis

To try and achieve the highest possible yield, the cell pellet was examined to see if VLPs were still attached to the cell. Excessive cell clumping was observed during VLP production trials, which could have trapped VLPs. To address this issue, the cell pellet was washed with 10 µg/ml TPCK-trypsin to favor the break-up of cell clumps and the release of trapped VLPs. In addition, cells were lysed with a freeze thaw cycle to explore the possibility of internally budded or intracellular trapped VLPs. Analysis was completed with western blot, HA assay and NSEM.

Figure 6.15 is the HA, NA and M1 western blot of SCC-VLPs, cell pellet wash and lysate. Western blot analysis of the cell pellet washes showed bands for HA0 and NA near the 70kDa and 50kDa mark, respectively, and a very faint signal for M1 at 25kDa. All proteins were detected in the cell lysate with more intense bands compared to the cell wash and sucrose cushion (sucrose cushion western blot is shown in Figure 6.7).

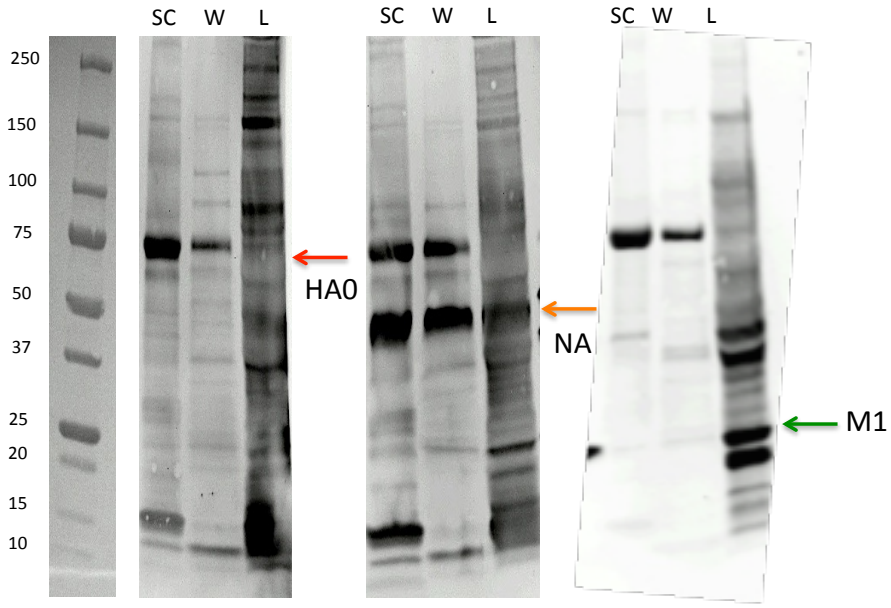

Figure 6.15: Western Blot of SCC-VLP (SC), cell pellet wash (W) and cell pellet lysate (L). NIBSC anti-HA and NA and Abcam anti-M1 antibodies were used for each protein.

Analysis with the HA assay shown in Figure 6.16 indicated that there was active HA released from the cell pellet wash and found in the cell lysate. The amount of active HA released into the supernatant was slightly higher than that found in the pellet.

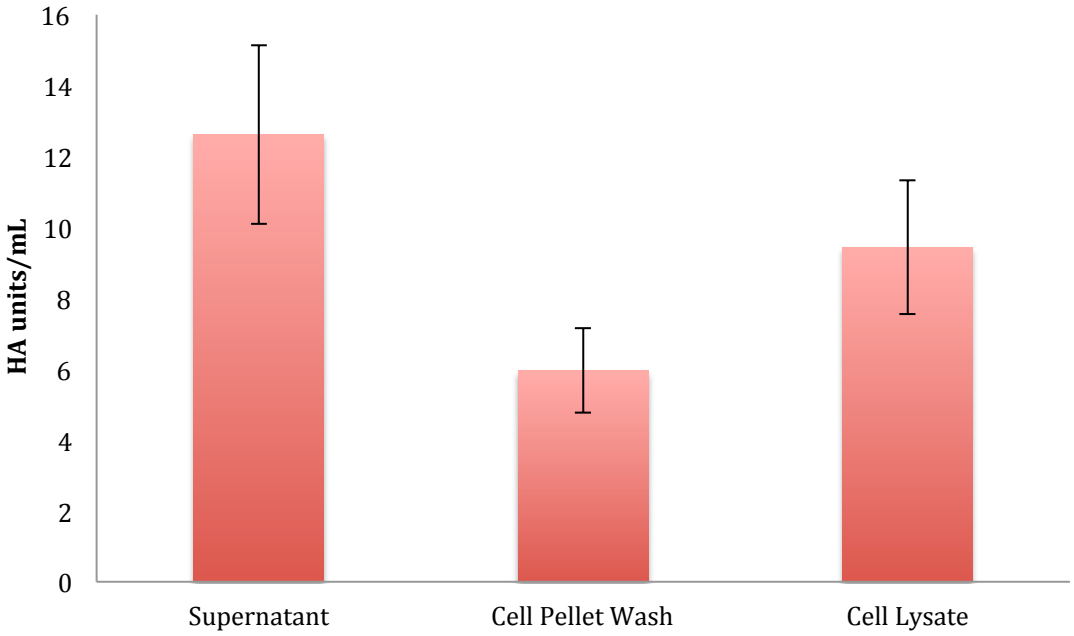

Figure 6.16: HA activity of SCC-VLPs, supernatants from cell pellet wash and cell lysate (normalized).

To check if there were any VLPs associated with the pellets and that the HA activity detected in the pellet (wash or lysate) was not only from the release of HA in the form of free protein, samples were analyzed with NSEM for VLPs and quantified. Figure 6.17 shows NSEM images of released particles from the cell wash at 40000x magnification (A) and zoomed in (B). The cell pellet wash showed a wide range of particles with a fringe, including a cluster of round particles just under 100 nm that closely resembled influenza virus particles (black arrow), as well as very large particles up to 400 nm (white arrows). They were quantified as 3.07×10^8 VLPs/ml, which is actually higher than the sucrose cushion. HA activity was lower for the cell wash compared to the sucrose cushion, indicating that particles with a fringe in the cell wash sample may have been misidentified as VLPs. Nevertheless, this confirmed that the HA activity found was not only from free protein, but from trapped VLPs that were released from the non-lysed cell pellet.

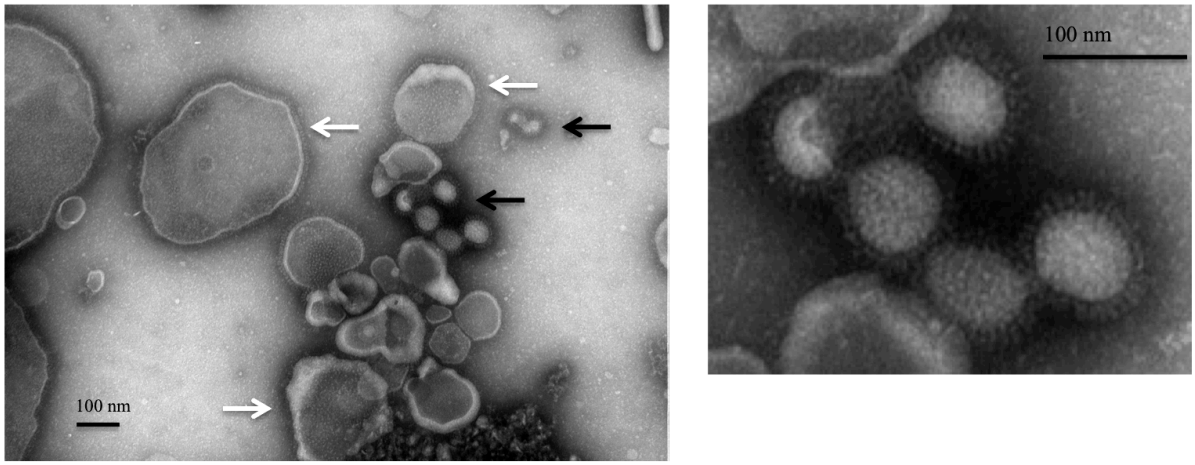

A B

Figure 6.17: NSEM images of VLP particles from the cell pellet wash.
Image A is was done at 40000x magnification and image B shows a zoomed in view of a cluster of VLPs identified by the black arrows in image A. White arrows indicate large particles with a fringe that were not identified as VLPs due to their large size.

As for the cell lysate, particles with a fringe were also present, as shown in Figure 6.18. They were counted to be present at a concentration of 1.43×10^8 VLPs/ml, about the same level as what was observed in the sucrose cushion purified VLPs. Like other samples, both round and pleomorphic particles were found.

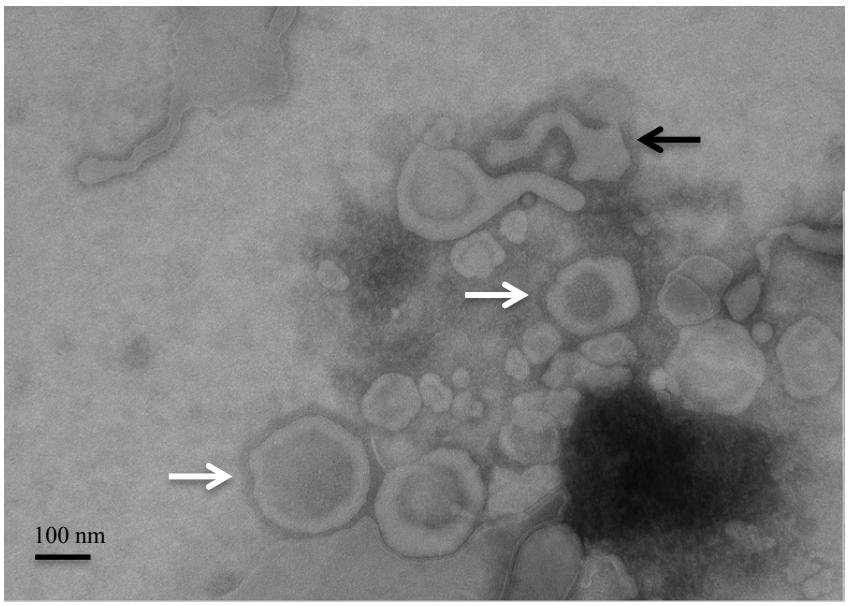

Figure 6.18: NSEM image of released particles from the cell lysate.
Those counted as VLPs are marked with back arrows and white arrows indicate particles not counted due to their large size.

Chapter 7: Production of Influenza VLP using the BEVS

In order to compare with the VLP production in HEK293 cells, a series of experiments varying MOI and time of harvest were completed to probe for the best condition. VLP production was completed with MOIs chosen ranged from 0.3-2.1 (Table 7.1), and the best found was HA = 1, NA = 0.1, M1 = 1, or a total of 2.1, based on western blot analysis (Appendix 7). Cell density at infection was $2.0x10^6$ cells/ml and a higher MOI was chosen in order to harvest before viability dropped below 70%. Conditions were analyzed for the presence of influenza proteins in the supernatant by western blot. Typical growth curves and cell diameter profile during VLP production can be found in Appendix 4b.

Table 7.1: Different combinations of MOI probed for the best VLP production in Sf9 cells

Protein	HA	NA	M1	Total MOI
MOI	1	1	1	3
	0.5	0.5	0.5	1.5
	0.1	0.1	0.1	0.3
	1	0.1	0.1	1.2
	0.1	1	0.1	1.2
	0.1	0.1	1	1.2
	1	0.1	1	2.1

7.1 VLP Characterization

To verify the presence of VLPs, harvested supernatants were concentrated with a sucrose cushion and analyzed for the presence of HA, NA and M1 proteins by western blot. HA activity was verified with the HA assay and the SRID assay. SCC-VLPs were also analyzed with NSEM.

Analysis of SCC-VLPs by western blot confirmed the presence of HA, NA and M1 proteins in the VLPs (Figure 7.1). HA0 is between the 75 and 50 kDa marker, NA is present at 50 kDa markers and also in truncated forms at 37 and 25 kDa. M1 is present at 25 kDa and GP64 between 75 kDa and 50 kDa.

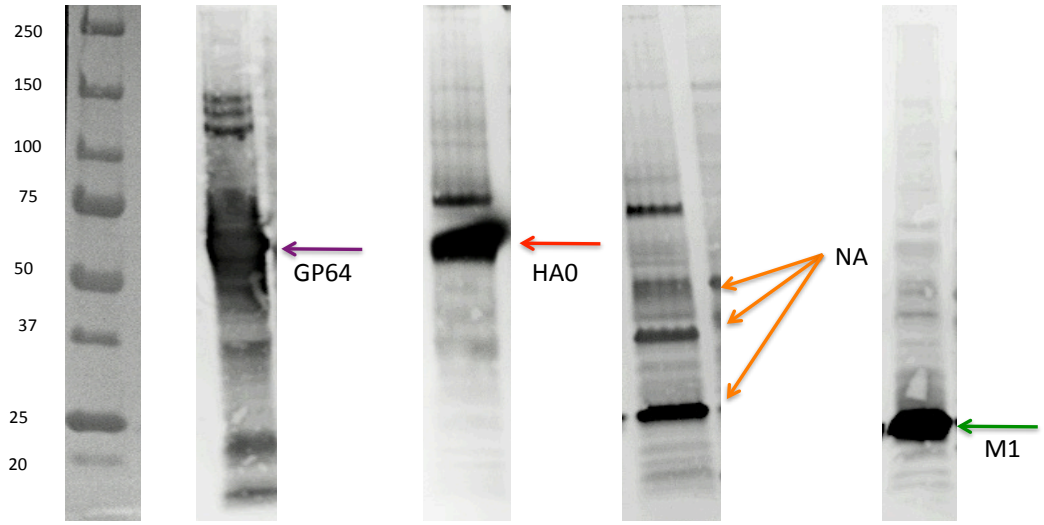

Figure 7.1: GP64, HA, NA, and M1 western blot of Sf9 SCC-VLP.
NIBSC anti-HA and NA, Abcam anti-M1 and eBioscience anti-GP64 antibodies were used.

SCC-VLPs and virus were analyzed by visual inspection and quantified for total particles/ml by NSEM. Figure 7.2 shows images of both VLPs and influenza virus produced in-house from the Sf9 and HEK 293 systems, respectively. VLPs were identified as particles with a fringe around the outside, which is assumed to be made up of influenza glycoproteins HA and NA. A concentration of 2.34×10^{11} VLPs/ml in a 40x sample, corresponding to a production value of 5.85×10^{9} VLPs/ml was observed. Baculovirus particles are clearly present in both images in a higher amount than VLPs. Total baculovirus particles were quantified to be present at a production concentration of 1.21×10^{11} BV/ml, which corresponds to 20x more total BV particles than VLPs. The morphology of VLPs produced from Sf9 cells was uniform, consisting of spherical particles around 100 nm in size.

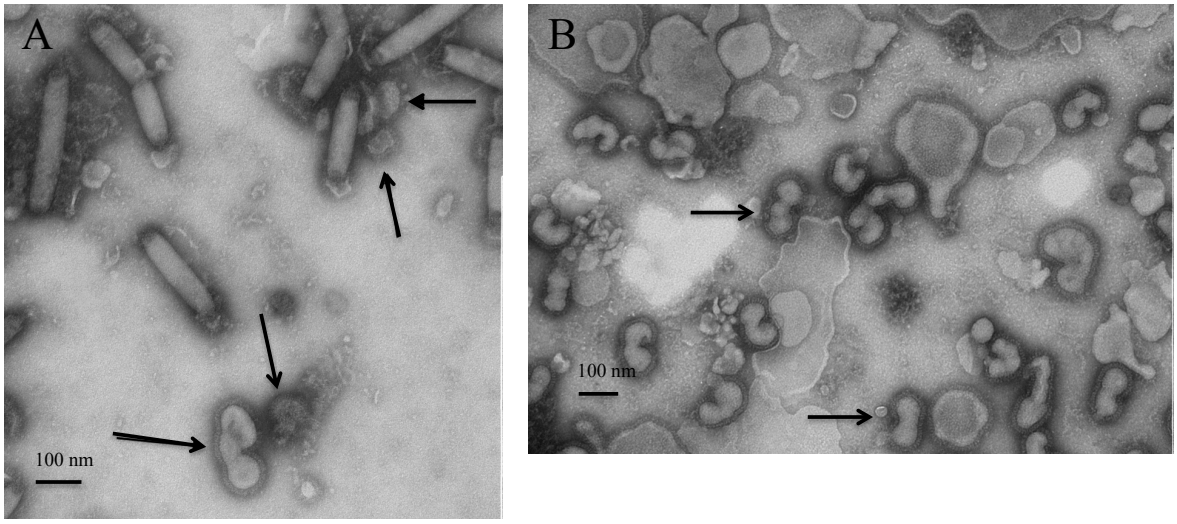

Figure 7.2: NSEM images of Sf9 SCC-VLP (A) and H1N1/A/PR/8/1934 (B) samples. Black arrows indicate VLPs and virus particles.

The HA titer for Sf9 produced VLPs was 336 HAU/ml. Based on ratio of BV/VLP made from NSEM quantification, an estimation of the HA activity from VLP particles was roughly calculated to be 15.6 HAU/ml or 3.78×10^8 VLP/HAU. However, these values were calculated (Appendix 2) based on the assumption that both particles have the same agglutination ability. It may not be completely accurate to say that because the physical concentration ratio of BV:VLP is 20:1, that the HA activity from BV particles is 20 times stronger than the HA activity from VLPs. Agglutination ability largely depends on the size of the particle. An HAU is defined as the number of particles needed to agglutinate red blood cells, and it is currently unknown if it is the same for influenza VLPs and BV tagged with HA. Thus, this caveat illustrates the complications with influenza VLP quantification, especially in the case when HA-tagged contaminants are present.

To gain insight on how to store VLPs mid-process, SCC-VLP VLPs were either stored at -80 °C or 4 °C for 3 weeks before analysis by the HA assay. Samples stored at -80 °C had an HA activity of 400 HA units/ml while 4 °C samples had 530 HA units/ml. There is not a huge difference in HA activity, although storage of sucrose cushion samples at 4 °C appears to be the best option during purification steps. The activity before storage was not tested, however the lower HA activity from storage at -80 °C could be due to the thawing step. Both VLPs and BV could have HA activity associated with them and despite the fact that 1% sucrose was used as a

cryoprotectant in the re-suspension buffer, there still could be loss of functionality due to the freeze/thaw cycle.

From the SRID assay, 15.15 µg HA/ml was detected in a 40x concentrated VLP sample, which corresponds to a production value of 0.38 µg HA/ml. The ring formed in this case followed the same pattern as that of the purified standard (Figure 6.9b). This is could be from the low about of cell debris found in the NSEM images of the SSC-VLPs.

7.2 Purification by Iodixanol Gradient

SCC-VLP samples were purified using ultracentrifugation with an iodixanol gradient. Fractions of 1 ml were collected from the bottom of the tube and analyzed with western blot, HA assay and NSEM.

Figure 7.3 shows the HA western blot of fractions collected. HA0 was present in all fractions, showing poor separation with this method, however higher band intensity was still seen in the bottom and top fractions. These bands represent free HA, HA associated with VLPs and HA associated with BV. The density at the bottom of the tube was 1.2-1.1 g/ml where at the top it was 1.09 µg/ml. Figure 7.4 shows the profile of the baculovirus envelope protein, GP64. Following a similar pattern to HA, GP64 is in every fraction, concentrating in the bottom and top fractions. Particles (including VLPs and BV) should migrate to fractions of higher density and free protein to those of lower. Western blots for NA and M1 agreed with the pattern seen here for HA (NA and M1 western blots can be found in Appendix 6b). It is not surprising that baculovirus is co-purified with influenza VLPs, as it is a common problem previously reported by other studies (Margine et al., 2012; Pushko et al., 2005).

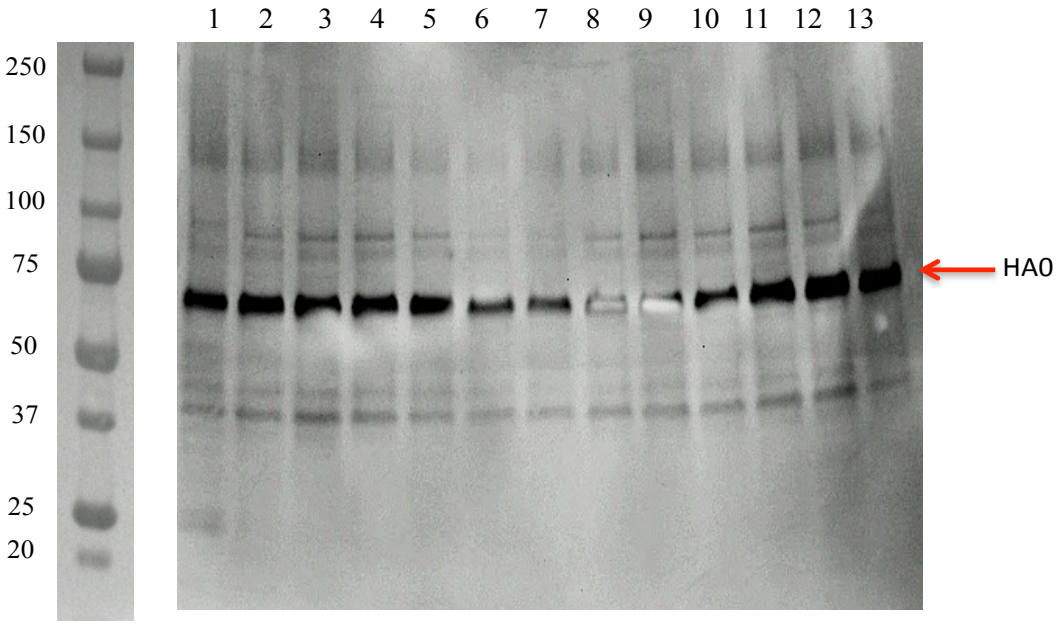

Figure 7.3: HA western blot of collected iodixanol gradient purified Sf9 VLP fractions (#1, bottom to #13, top) with NIBSC anti-HA sheep serum.

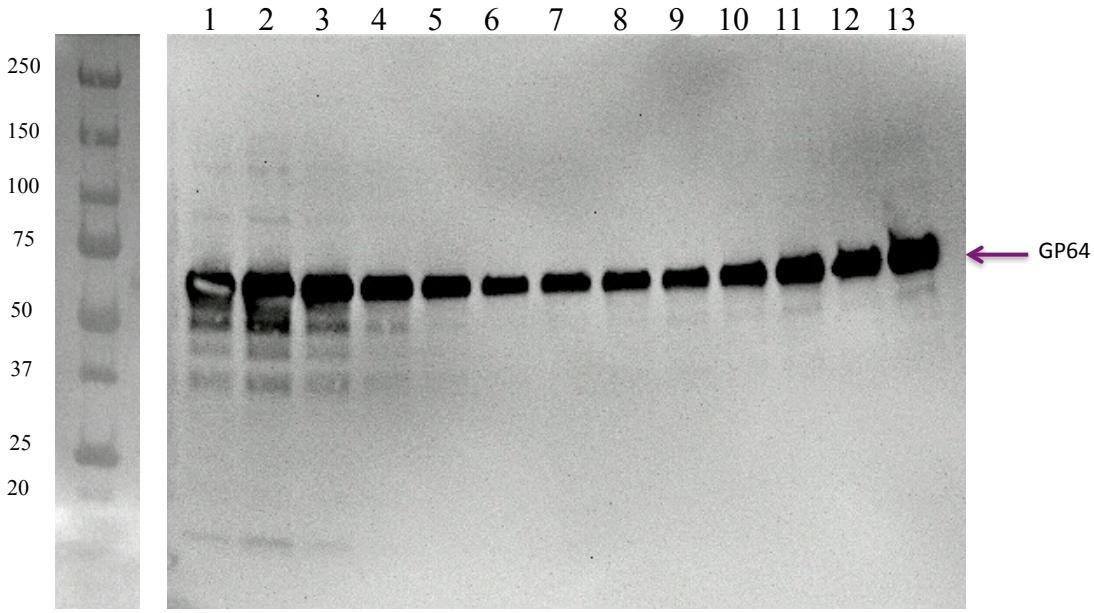

Figure 7.4: HA western blot of collected iodixanol gradient purified Sf9 VLP fractions (#1, bottom to #13, top) with eBioscience anti-GP64 sheep serum.

Collected iodixanol fractions were analyzed by HA assay (Figure 7.5). All fractions had HA activity, which agrees with the western blot of iodixanol fractions. This is likely due to inefficient separation of VLPs, host cell components or BV associated with HA. However, the pattern shows the highest HA activity in fractions 1-4 and 11 and 12. This result also matches the GP64 western blot, which has the strongest bands in fractions 1-4 and 11-13.

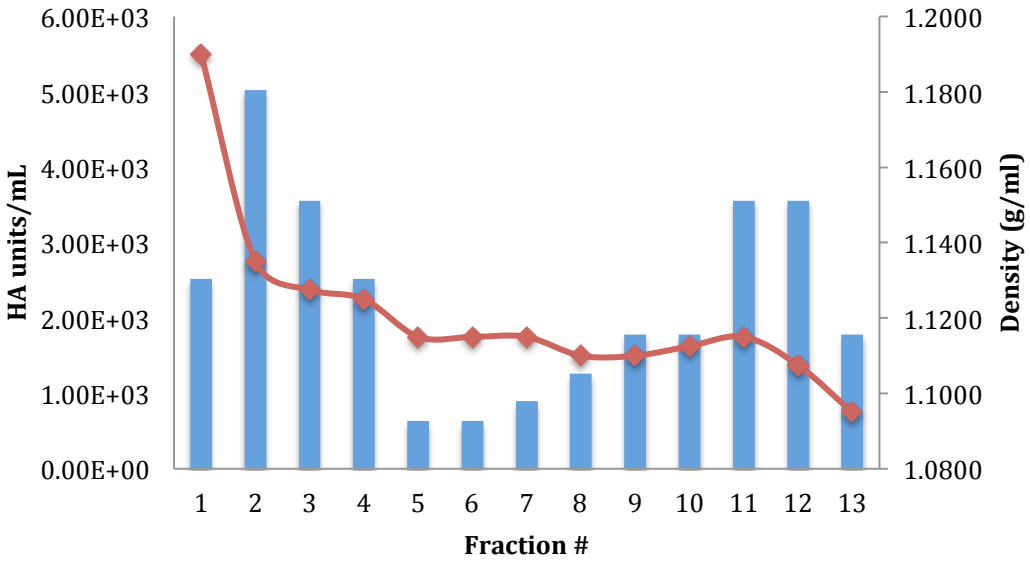

Figure 7.5: HA activity (blue bars, left axis) and density (red line, right axis) in iodixanol fractions #1-13.

Iodixanol fractions (2, 3, 9, 12) were analyzed by NSEM (Figure 7.6, 40 000x magnification). VLPs had similar concentrations in each of these fractions, from 1.89-2.86x10^{10}. Baculovirus particles on the other hand, were mainly migrating to fraction #9, as indicated by the BV to VLP ratio shown in Figure 7.7. Fraction #9, which contained the lowest HA activity of those fractions sent for NSEM quantification, had the highest BV count at 1.3x10^{12} VLP/ml, 69 times higher than VLPs. Fraction #2 had the lowest count with 2.61x10^{11} BV/ml, still 9 x higher than VLPs. The sucrose cushion starting material had a BV to VLP ratio of 20, showing that the iodixanol gradient separated BV from VLPs, but as previously shown on the western blot, not completely.

The agglutination ability of the VLPs in each fraction is illustrated in Table 7.2 and shows that the VLP agglutination ability is not very consistent ranging from 5.76x10^{7} to 7.40x10^{8}

VLP/HAU. This could be due to the distribution of BV throughout the gradient, which may not have a consistent amount of HA taken into its membrane, but still contributes to this value, skewing the VLP/HAU calculated value.

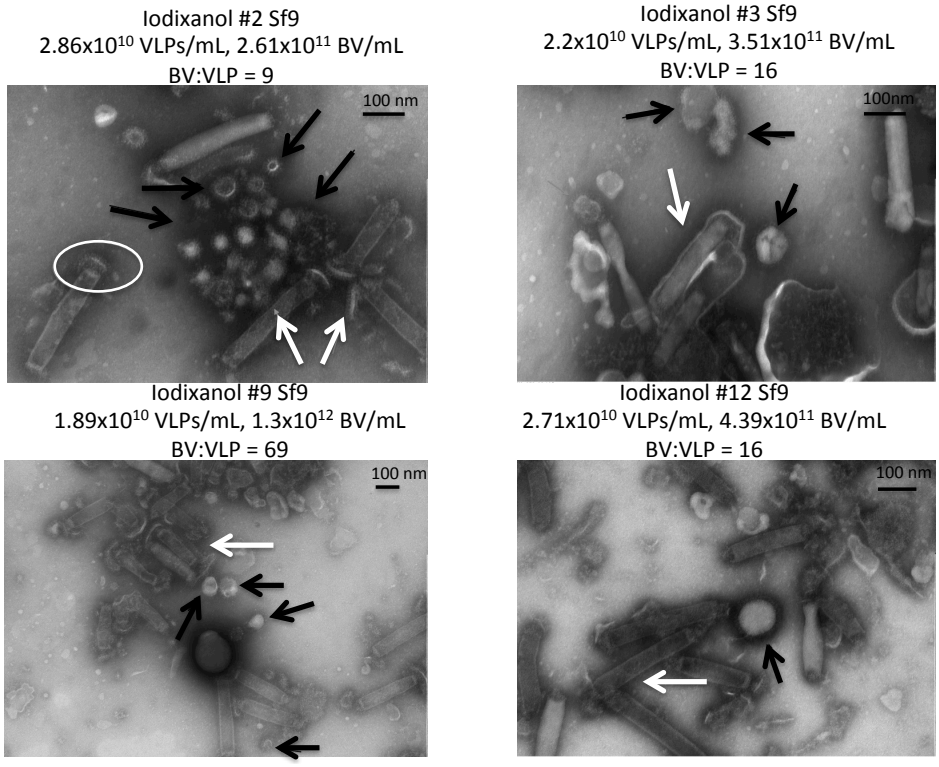

Figure 7.6: NSEM images of iodixanol purified Sf9 VLPs.
Black arrows indicate VLPs, white arrows indicate baculovirus particles and the white circle in Iodixanol #2 shows the glycoprotein spikes on the baculovirus particle.

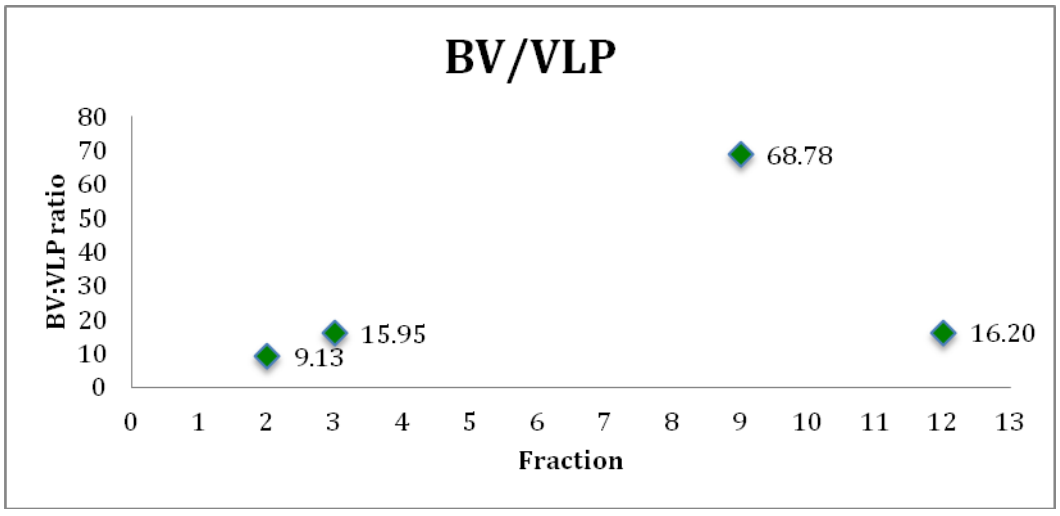

Figure 7.7: BV to VLP ratio in NSEM quantified Sf9 VLP iodixanol fractions.

Table 7.2: VLP/HAU values for fractions of the iodixanol density gradient

Fraction	VLP/HAU
2	$5.76x10^7$
3	$1.08x10^8$
9	$7.40x10^8$
12	$1.31x10^8$

7.3 Cell Pellet Analysis

From western blot analysis, there was a significant amount of HA, NA and M1 proteins found to be in the cell lysate. TPCK-trypsin cell pellet wash and cell lysate analysis was performed to determine if there were internally budded VLPs or some stuck to the cells during production. Western blot and HA assay were used to analyze samples.

Western blot analysis revealed release of each influenza VLP proteins and GP64 in the wash and lysate as identified in Figure 7.8.

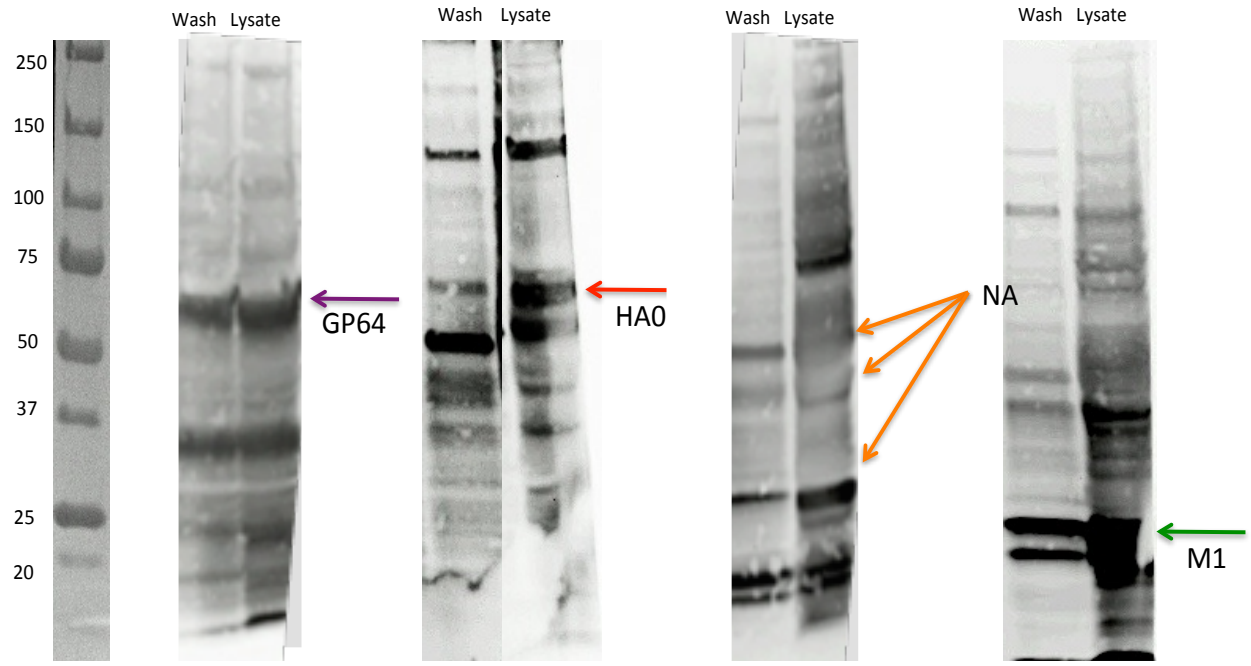

Figure 7.8: HA, NA, M1 and GP64 western blot of cell pellet wash and cell pellet lysate. NIBSC anti-HA and anti-NA, Abcam anti-M1 and eBioscience anti-GP64 antibodies were used.

Analysis of the wash and cell lysate for Sf9 produced VLPs shows that the HA activity from sucrose cushion concentrated VLPs is much stronger than both the cell wash and lysate (all normalized based on concentration factor), as depicted in Figure 7.9. This indicates that HA protein was released from the wash and was also present in the cell pellet, in agreement with western blot results. However, it also shows that the HA is not as functional in terms of agglutination ability as those released into the supernatant with VLPs or BV.

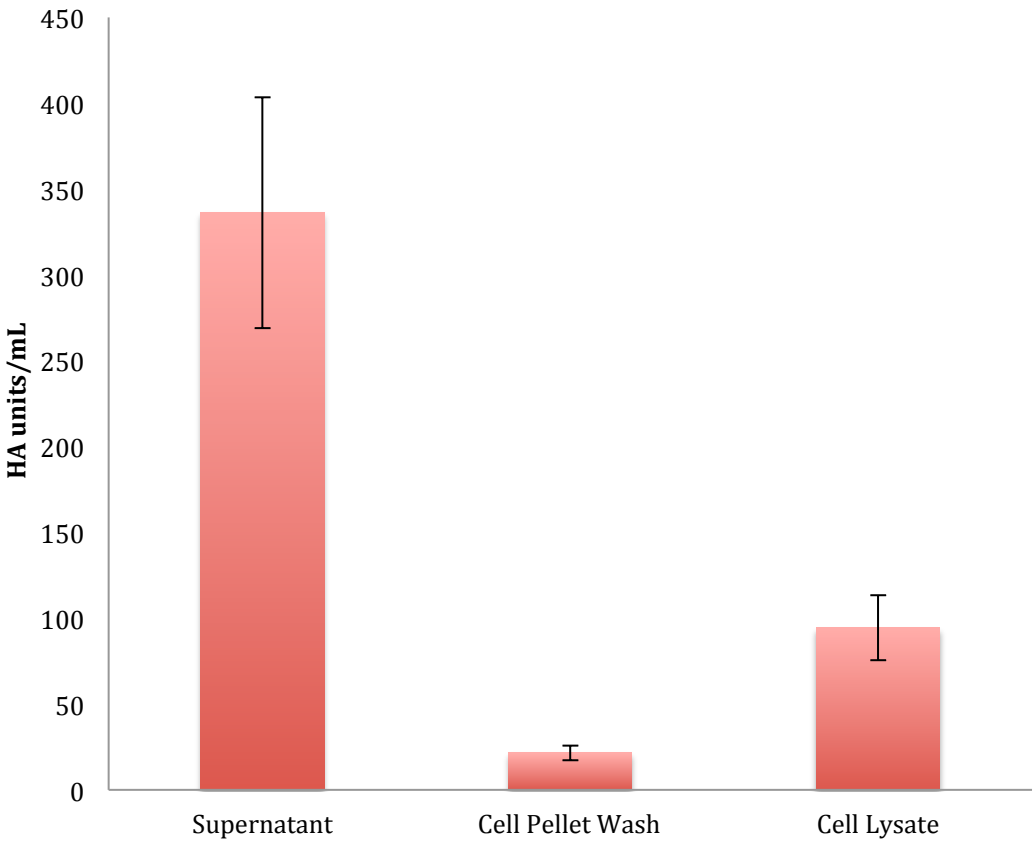

Figure 7.9: HA activity (HAU/ml) of sucrose cushion purified Sf9 VLPs, supernatant from cell pellet wash and cell lysate.

Chapter 8: Discussion

8.1 Identification/Quantification Limitations

The methods used to identify the best conditions from a designed experimental space were qualitative (western blot, GFP visual inspection), and were only based on the presence of influenza antigens associated with the VLP (western blot and HA assay), giving no information on their physical characteristics or the number of total particles. These results highlight the difficulties that researchers currently face regarding quantification of influenza VLP process development. To further optimize both systems, clearer objectives and limitations need to be outlined during experimentation such as the minimum MOI that will give the highest production of VLPs in the smallest time period. However, in order to complete such an optimization, appropriate quantification techniques are in need.

An ideal quantification or identification method to be used in process development needs to be compatible with crude samples. To be compatible the method must be able to discriminate the end production from other material (debris, cellular proteins, vesicles, baculovirus particles) that could cause some kind of interference, have a low enough detection/quantification limit and be relatively quick in order to process a large number of samples in a reasonable amount of time. One of the main problems of current protocols is the low limit of detection. For example, during production with the Bacmam system, crude samples were tested with the HA assay which resulted in zero HA activity in part due to a limit of detection of 40 HA units/ml (Hirst, 1942; Szretter, Balish, & Katz, 2006). A 50x SCC-VLP sample had a reading of 630 HA units/ml, which corresponds to 12.6 HA units/ml when normalized to the volume of the supernatant. This problem can be overcome with sample concentration, but creates other problems which still limit process development such as laborious sample preparation, potential loss due to unknown product stability, and the general treatment of the step from concentration to assay readout as a black box because it is not possible to identify where product loss or low HA values are coming from; the production conditions or the downstream processing steps. Another constraint for this method is related to the purity of samples; HA activity from contaminant particles in samples containing HA (i.e vesicles, baculovirus) can enhance the HA activity, as this method cannot differentiate between HA activity from VLPs or other sources. When HA activity values were

reported in previous influenza VLP studies they have not considered the contribution from HA-labeled baculovirus. The problem of baculovirus contamination is widely acknowledged in purification strategies and immunization challenges and has lead to regulatory consideration (Haynes, 2009; Krammer, Schinko, et al., 2010; Margine et al., 2012; Palomares & Ramírez, 2009; Vicente et al., 2011). Given that there is still contamination at the end of purification, it is clear that having in-line quantification tools that can discriminate between influenza VLPs and baculovirus are needed.

Although the SRID assay is heavily relied upon, HEK 293 SCC-VLPs were difficult to analyze by the SRID assay due to their small ring diameter (Figure 6.9a). Additionally, the ring was abnormally dark, which could indicate the presence of precipitation. HA is prone to aggregation, especially in concentrated mixtures, which VLPs usually are. Large aggregates may prevent proper diffusion, precipitation and interfere with readings (Apostolov & Fishman, 1967). Additionally, this method requires a long processing time (1-1.5 days), and has low sensitivity (Nilsson et al., 2010; Wood et al., 1999; Wood, Schild, Newman, & Seagroatt, 1977). The WHO is encouraging development of alternative methods that can replace SRID-based quantification (WHO, 2006). This initiative is targeted towards quantification of influenza virus-derived vaccines, but VLP process development could greatly benefit from these advances as well.

With regards to the western blot, another commonly used method for VLP characterization; interference from contaminating material is a problem, especially when non-purified samples are tested. For HA and NA, polyclonal anti-HA or NA sheep serum were used, which resulted in labeling many non-specific bands. This makes analysis confusing and time consuming. Monoclonal antibodies alleviate some of these problems, however there is still non-specific labeling from secondary antibodies. Therefore, western blot is not a suitable method for in-process sample analysis.

Electron microscopy is the only method currently available that gives information on total particles, in terms of morphology, size and concentration. The drawbacks of this technique are the price of equipment and level of expertise needed to analyze and run samples. Additionally, as microscopy counts are based on visual enumeration, samples need to be pure enough, making this method difficult for the analysis of crude samples collected upstream of purification. Currently, there is no other option to validate the physical presence of VLPs. Past studies that have used this

method do not give the production or final concentration of total VLPs/ml, and focused more on morphological aspects of the particles (Krammer, Schinko, et al., 2010). Additionally, most pictures given thus far of VLPs have been very close up images of just the VLPs, not giving any indication what the rest of the sample may contain. Total concentration of VLPs is an important number to report, as the concentration of total particles in the vaccine formulation is one of its defining characteristics, apart from the amount HA present. Additionally in terms of process development, the concentration of total VLPs produced can be a good marker for process efficiency. A quantification method that can report total VLP concentration accurately and rapidly would greatly aid the process development process. Thompson *et al* (Thompson et al., 2013) indicate several potential methods for total and antigenic methods that could fill this need.

8.2 HEK 293 vs. Sf9 IVLP Production

Production values for influenza VLP from the Sf9 and HEK 293 systems are presented in Table 8.1

Table 8.1: IVLP Production HEK 293 vs. Sf9

	SRID (ug HA/ml)	**HA Assay (HAU/ml)**	**VLP/HAU (Iodixanol Fractions 2,3)**	**VLP/ml**	**VLP/cell**	**Contamination**
HEK	0.09 +/- 0.01	12.6 +/- 2.50	$5.76x10^{7}$	$1.58x10^{8}$	79	Vesicles, trace BV particles
Sf9	0.38 +/- 0.04	336 +/- 67.2	$1.55x10^{7}$	$5.85x10^{9}$	2925	$1.21x10^{11}$ BV/ml

Sf9 produced VLPs at a concentration of $5.85x10^{9}$ VLP/ml while HEK 293 produced VLPs at a concentration of $1.58x10^{8}$ VLP/ml. Therefore, it appears the Sf9 system is better in terms of productivity of VLPs/cell (both produced at $2.0x10^{6}$ cells/ml over a course of 48 hours). In

terms of HA activity, the Sf9 SCC-VLP sample had 336 HAU/ml and HEK 293 had 12.6 HAU/ml. However, the large amount of BV present in Sf9 SCC-VLPs must be taken into consideration when looking at this value, as the true amount of HA activity from VLPs or BV is not completely clear. By pairing NSEM quantification values and those from the HA assay, the agglutination ability (i.e the number of particles that it takes to agglutinate red blood cells, VLP/HAU) were calculated to estimate the quality of the VLPs produced. The HEK 293 SSC-VLP sample had a better agglutination ability than the Sf9 SCC-VLP sample ($9.60x10^6$ vs. $4.48x10^8$ VLP/HAU). This can be attributed to the contribution from the large particles with HA spikes (100 < VLP < 400 nm in diameter) found in the HEK 293 VLP samples, as larger particles have a better agglutination ability. However, in iodixanol fraction 2 and 3 for both systems, similar agglutination ability was observed, $1.55x10^7$ VLP/HAU for HEK 293 and $5.76x10^7$ VLP/HAU for Sf9. In these fractions, there was the least amount of contaminant in the form of BV or large particles with HA spikes, showing that their actual agglutination ability may be closer when contaminants are not skewing the values. However, these calculations are just an estimation, as they are based on the overarching assumption that BV and VLPs have the same agglutination ability (calculated with NSEM ratios to distinguish the difference between BV and VLP HA activity, Appendix 2) and do not take into account the fact that some HA activity could also be from free, aggregated, rosette-form HA or large vesicles with HA spikes not accounted for with VLP quantification by NSEM. Despite its limitations, the HA assay is the only method currently available to characterize VLPs from different production systems from a quality point of view (i.e amount of active HA antigen). Even though higher level calculations are based on shaky assumptions, overall the HA assay is still able to give a readout to compare the two systems, which tells us that the Sf9 system produces more active HA than the HEK 293 platform, but from the HA ability calculated in iodixanol fraction 2, that the VLPs produced are of similar quality.

From analysis of the Sf9 cell pellet (Figures 7.11), it is clear that the HA that remains in the pellet, while large in quantity by western blot analysis, is not very functional. However, in the HEK 293 system (Figure 6.16), the HA in the pellet had similar activity to its counterpart in the supernatant, indicating that VLPs were still attached to the pellet or inside the cell in the correct formation in vesicles. This brings up the question of where these VLPs were coming from, either attached to the cell after budding/incomplete budding or from inside the cell. Influenza particles bud from

the cell membrane (Rossman & Lamb, 2011), and there are no reports of internally budded influenza particles. However, there are cases of HIV particles budding from internal multi-vesicular bodies (Welsch et al., 2007), where they should normally bud from the plasma membrane, like the influenza virus. Considering that more than one influenza protein has the potential to induce budding (Rossman & Lamb, 2011) this explanation may hold some merit in a VLP system. In addition, the presence of particles that are physically similar to what we identified as VLPs in the virus sample, could mean that system vesicles from the HEK 293 system have taken HA or NA into their membrane. These vesicles may have budded from the cell membrane, but also may have budded from internal membranes, then released upon cell death.

Overall, Sf9 VLPs are produced at a higher level than HEK 293 when comparing production at the same cell density (Table 8.1). The Sf9 system has the challenge of baculovirus contamination, and the HEK 293 may also have a similar problem but in terms of cell vesicles (Section 8.4). The next step in these studies would be to compare the immune response generated by each particle. Margine et al (Margine et al., 2012) completed a study of this type but did not purify out the BV. In order to truly compare the two systems, a purified sample of VLPs from both systems need to be compared.

8.3 Structural Matrix Protein

One of the main differences between Sf9 VLPs and HEK 293 VLPs was the presence of the matrix protein (M1) in Sf9 VLPs. M1 was not present on the western blot of HEK 293 SCC-VLPs, but was in the pellet. For Sf9 VLPs, it was present in both the sucrose cushion purified samples and the cell pellet. Previous reports indicate that M1 is able to form VLPs on its own (Gómez-Puertas, Albo, Pérez-Pastrana, Vivo, & Portela, 2000; Latham & Galarza, 2001) however this was later implied to be a result of the production system used (B. J. Chen et al., 2007). M1 does not possess the signal for transport to the cell membrane, but is assumed to be recruited by binding to the cytoplasmic tails of HA, NA and/or M2. However, M2 has the only verified sequence to which M1 binds (B. J. Chen, Leser, Jackson, & Lamb, 2008). Chen *et al* (B. J. Chen et al., 2007) showed in a mammalian plasmid-transfection system that HA in combination with M1 resulted in VLPs, but the addition of M2 enhanced VLP production. Additionally, Tang *et al*'s study of Bacmam VLP production in HEK 293 adherent cells also

found M1 in the supernatant without expression of M2. It is still not clear why M1 remained in the pellet for the case of VLP production in HEK 293 suspension cells. The addition of M2 could potentially increase yields, but the presence of HA and NA, based on previous studies, should be enough to recruit M1 to the cell membrane for VLP formation. This has lead to hypothesize that some intracellular function is blocking the recruitment of M1 to the cell membrane for incorporation during budding in this cell system.

Regardless of the reason why M1 is or is not incorporated into the VLP, its presence or lack thereof could have a lasting effect on the VLPs produced. It may not be of significance in terms of its antigenic potential, but particles could be structurally compromised as M1 is the structural backbone of the influenza virus (Rossman & Lamb, 2011). This is an important point for bioprocessing, where producing stable particles that can withstand downstream processing is sought.

This may also be an explanation for the large amount of debris present in sucrose cushion and iodixanol purified HEK 293 VLPs (Figure 8.1).

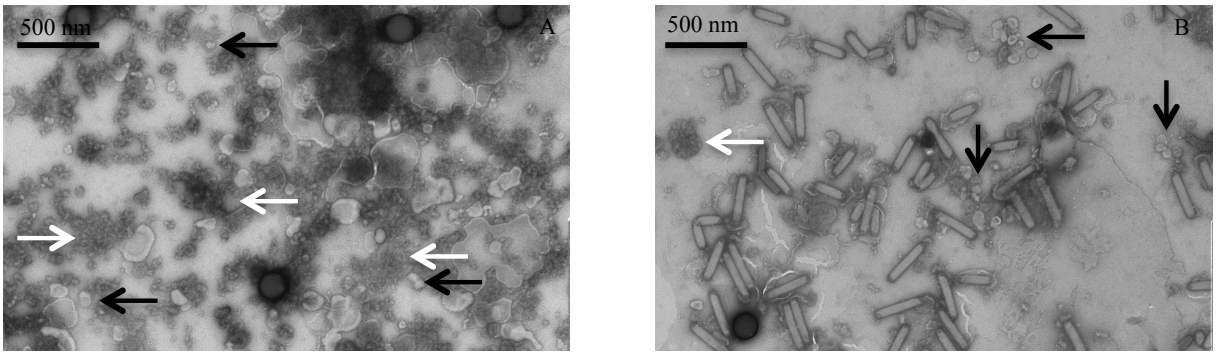

Figure 8.1: 10 000x magnification images of HEK 293 SCC-VLP (A) and Sf9 SCC-VLP (B). Black arrows represent VLPs and white arrows cell debris.

This study has not verified that some of the debris in the NSEM images was free HA protein (i.e protein that was associated with VLPs but was released due to particle destruction), however there is a reason to believe it could be as there was a large HA band in the lower density fractions of the iodixanol gradient purification. Free protein will migrate to lower density compared to VLPs, which are heavier. The potential presence of free protein in both the sucrose cushion and iodixanol purified samples could indicate two important points about HEK 293 VLP stability. The particles that were pelleted during the sucrose cushion could have

collapsed, resulting in the presence of free HA. Next, during the iodixanol gradient purification, the existing free HA could have migrated to the lower density fractions plus any new free HA from destroyed particles that could not withstand the second ultracentrifugation. Sf9 VLPs did not have as much debris in their pictures and were produced at a level of 1.5 logs higher than their counterparts produced in HEK 293. The hypothesis that the presence of M1 increases particle stability and thus yields is partially supported from our observations of both systems. Chen *et al* (B. J. Chen et al., 2007) have shown that when M1 is expressed with HA, rather than HA alone, VLP production was increased. Additionally, the presence of M1 could be the reason for a more uniform and traditional cell culture influenza-like particle morphology in the Sf9 system, as it has been shown that the structure of M1 further determines whether the virus particle is spherical or filamentous (Calder, Wasilewski, Berriman, & Rosenthal, 2010).

Another hypothesis connected to the strong presence of M1 in the Sf9 system and higher production levels could be due to the construct used for VLP production. One baculovirus containing all three genes in addition to GFP was on present on the Bacmam construct, while in the insect cell system three separate baculoviruses were used to produce each influenza protein. This could be a large amount of stress on the baculovirus, and limit protein production, resulting in lower levels of VLP production, or insufficient amounts of M1 produced. Considering that the Sf9 system used three separate baculovirues for VLP production, a more accurate comparison may be with three separate bacmam constructs. However, given that the difference in production was significantly higher, at 1.5 logs, it is possible that the Sf9 system will still prove to be superior despite upstream improvements made by changing the bacmam constructs.

8.4 Contamination

The motivation behind producing VLPs in HEK 293 cells was to avoid contamination with baculovirus (Tang et al., 2011). However, we encountered potential contamination from another source with this production system. Western blots of uninfected HEK 293 cell culture showed a contaminating band at 75 kDa (Appendix 5). It is hypothesized that this band could be from cellular proteins associated with secreted vesicles, which are budded particles that perform a variety of functions in a cell's secretory system (Denzer, Kleijmeer, Heijnen, Stoorvogel, &

Geuze, 2000). Past studies on the development of purification of retroviruses produced in cell culture have shown the presence of contaminating cell membrane vesicles (Abe, Miyanohara, & Friedmann, 1998; Bess, Gorelick, Bosche, Henderson, & Arthur, 1997; Gluschankof, Mondor, Gelderblom, & Sattentau, 1997; Segura, Garnier, & Kamen, 2006). Gluschankof *et al* state they are between 50-500 nm in size and make up 50-75% of total particles produced according to NSEM analysis. Considering the particles present in the NSEM influenza image that could be labeled as VLPs (Figure 6.11 b), there exists the possibility that these particles are vesicles that have taken up HA or NA during budding. This observation brings up an important point of how to define VLPs. On a western blot, HA assay or SRID assay, a vesicle or VLP would be indistinguishable, if they have both incorporated HA and/or NA during the budding process and are co-purified together. NSEM analysis however, allows for visual inspection of the particles. If VLPs are identified as particles with a fringe, then mainly all the vesicles could be identified as VLPs. Additionally, under this definition it could be argued that vesicles could be used as a tool to aid VLP production, and increase overall yield. However, secretory vesicles could contain cell waste, including proteins and nucleic acids that need to be quantified and removed or inactivated in final vaccine formulations. Therefore, there is the possibility that accompanying vesicles could end up to be more of a burden, than an aid during VLP process development. If VLPs are defined as particles that fall into the same shape and size of influenza virus, then vesicles will not fall into this definition, and current production of VLPs is overestimated. The presence of these particles could also complicate purification, resulting in a similar contamination problem that exists with VLP production in the baculovirus-insect cell system. Finally, the question of whether these particles have the ability to induce an immune response is another important consideration that will need to be eventually addressed.

For Sf9 VLPs, it is clear here that the major contaminant is baculovirus, as vesicles were not detected in the NSEM images. Previous reports by Krammer *et al* (Krammer, Schinko, et al., 2010) report the presence of BV contamination in supernatant VLP samples at a level of 10^8 and 10^6 PFU/ml from Sf9 and High Five cells, respectively. Our report of 10^{11} total particles/ml is higher than previously mentioned. This could be due to variation between titering methods, which have shown when completed at different times by different operators has lead to 1-2 logs variation in titer (Shen, Meghrous, & Kamen, 2002). Furthermore, quantification is done in PFU, which is always less than total particles. Margine *et al* (Margine et al., 2012) report an enhanced

immune response from BEVS derived VLPs compared to mammalian produced VLPs, but attribute this enhanced immunogenicity to contaminant baculovirus that triggers the innate immune response. As a consequence of this finding, past immunological studies done with VLP preparations from the BEVS system do not communicate the true immune response associated with influenza VLPs, but rather that from VLPs and BV. Additionally, in the study of HEK 293 VLPs produced by Bacmam transduction, Tang *et al* (Tang et al., 2011) have contradictory results to Margine *et al* for the immunogenicity of mammalian produced VLPs, which were much stronger compared to what was found from the transfection based system that Margine *et al* used. Tang *et al* do mention that there was not any infectious residual BV in VLP formulations, but BV DNA was detected by PCR, which could still mean the presence of defective BV particles that could trigger an immune response. In our purified samples from Bacmam productions, residual BV was detected in NSEM images. Therefore, immunological studies with VLPs from any BV system (infection or transduction) should be completed with purified VLPs free of any viral contaminant that may skew results.

Considering the concern from regulatory agencies with human vaccines containing any live virus or genomes, BV must either be inactivated or removed for these VLPs to be considered human vaccine candidates. Chemical and UV inactivation has been shown to eliminate both interferon and immune-enhancing activity of BV (Hervas-Stubbs, Rueda, Lopez, & Leclerc, 2007) and GE healthcare has shown that baculovirus can be separated from influenza VLPs using Capto Q ion-exchange chromatography in flow through mode (GE_Healthcare, 2012), where BV and DNA, which are assumed to be more negatively charged, bind to the column but the VLPs are allowed to flow through and are collected before subsequent elution of contaminant material. They do not indicate if the starting material was pre-purified or concentrated and how much BV was initially present, however, efficiency of BV separation does depend on the condition of the VLP feed and contaminant concentrations. VLP recovery varies from 60-80% for H5N1 VLPs and 39-43% for H1N1 VLPs. One of the benefits of purifying VLPs in flow-through mode is reducing potential shear forces and stress from binding and elution that could affect the stability of the VLPs. Another potential method would to use affinity chromatography in flow through mode, here BV or vesicles would bind to the column but VLPs are allowed to pass through. For this to work efficiently the column would have to target BV proteins or vesicles proteins (i.e GP64, VP39, heat shock proteins). However a potential problem would arise if VLPs have taken a considerable

amount of BV or vesicle proteins in their membrane during budding, allowing for the VLPs to bind to the column as well. Another study (Gerster et al., 2013) showed that baculovirus can be purified from cell culture supernatant on a HPLC monolithic system by salt elution at 450 mM. An in-house HPLC method developed by our lab (data not shown) has found that infectious influenza particles elute from the same column at 650 mM salt. This could provide a potential method for separation. Other existing chromatography protocols for influenza virus purification include affinity, size exclusion and anion-exchange in flow through mode (GE_Healthcare, 2012; Kalbfuss, Wolff, Morenweiser, & Reichl, 2007; Opitz, Salaklang, Büttner, Reichl, & Wolff, 2007). Additionally, Medicago Inc purifies plant-produced influenza VLPs with affinity chromatography (D'Aoust et al., 2008). All of this data should be a good starting point to begin to develop a separation technique for VLP and BV, or even just purification of VLPs from other platforms without such significant contamination as scalable methods need to be developed. The monolithic and flow-through modes seem to be the most promising in terms of binding capacity and maintaining particle stability.

Chapter 9: Conclusions and Recommendations

Based on the results from this work, there are multiple conclusions and directions in which to move forward. It is evident from comparing the two production systems that the BEVS VLP production system is superior in terms of VLP production ability and quality of particles produced. It produced VLPs at a concentration of 5.85×10^9 VLP/ml while the concentration achieved with the Bacmam HEK 293 system was 1.21×10^8 VLP/ml. Additionally, VLPs produced in insect cells were more homogeneous and resembled influenza particles produced in cell culture, while the VLPs produced in mammalian cells were more heterogeneous in shape and size. From this conclusion, two other can be drawn; firstly that the incorporation of M1 in the VLP has an influence on the type of VLP produced. The VLPs found in the supernatant produced in the HEK 293 system had very little or no M1 as detected by western blot, even though it was included in the expression cassette. This unexpected finding leads to the conclusion that the lack of M1 may have played a role in terms of the quality of VLPs produced from this system. M1 is the structural backbone of the influenza virus, linking the envelope glycoproteins to the RNA inside the particle. Additionally, it has been hypothesized that M1 determines the shape of the influenza particle (Calder et al., 2010). Without this important protein, VLPs of varying size and lacking structural stability could have been produced. Secondly, the wide variation of shape and size for mammalian produced VLPs could have been influenced by the production of cellular vesicles that take up HA and/or NA in their envelope when exiting the cells. The production of cellular vesicles with influenza proteins was not a problem in the Sf9 system as shown by NSEM images. However, there was a problem of BV contamination in the Sf9 system, where BV was produced at a level of 1.21×10^{11} BV/ml. This is the first time to our knowledge that these production values (VLPs/mL and BV/ml) have been given.

With regards to quantification, throughout this project it was made very clear to us how difficult VLP process development is without a proper quantification method to complement these studies. Current quantification protocols are more suitable for purified material, which makes the analysis of in-process samples challenging due to the presence of contaminants and insufficient levels of identification/quantification.

To move forward in VLP process development, multiple steps need to be completed. Firstly, a quantification technique that is appropriate for in-process samples is needed. However, in order to fully develop such a method, a purified "gold standard" VLP will be needed for validation. As a result, more work needs to be done on separating VLPs from BV. There have been some preliminary studies and protocols (GE_Healthcare, 2012; Gerster et al., 2013), but this is only the beginning of many more studies that need to be completed. Another route is to use a system where the BV is able to infect the cell and deliver genes of interest, but unable to complete the budding process (Marek, van Oers, Devaraj, Vlak, & Merten, 2011). In the case of mammalian produced VLPs, where BV contamination is not a problem, ultracentrifugation purification should be sufficient for a purified sample, but the large amount of debris and system vesicles needs to be separated.

Once a quantification protocol has been developed, process optimization in bioreactors assessing aspects such as DO, agitation rate, time of harvest, MOI, and temperature can be further optimized. Finally, this will also allow further comparisons for production systems such as mammalian transfection vs. insect, plant vs. insect or mammalian vs. plant. Finally, VLP stability and storage conditions need to be assessed.

.

References

Abe, A., Miyanohara, A., & Friedmann, T. (1998). Enhanced Gene Transfer with Fusogenic Liposomes Containing Vesicular Stomatitis Virus G Glycoprotein. *Journal of virology*, *72*(7), 6159–63.

Acheson, N. H. (2007). *Fundamentals of Molecular Virology*. (K. Witt, Ed.) (1st ed.). Hoboken: John Wiley & Sons, Inc.

Air, G. M., & Laver, W. G. (1989). The neuraminidase of influenza virus. *Proteins: Structure, Function and Genetics*, *6*(4), 341–56.

Apostolov, K., & Fishman, B. (1967). Purification and concentration of influenza virus by auto-aggregation. *Nature*, 1287–88.

Aucoin, M. G., Mena, J. A., & Kamen, A. A. (2010). Bioprocessing of baculovirus vectors: a review. *Current Gene Therapy*, *10*(3), 174–86.

Backliwal, G., Hildinger, M., Kuettel, I., Delegrange, F., Hacker, D. L., & Wurm, F. M. (2008). Valproic acid: a viable alternative to sodium butyrate for enhancing protein expression in mammalian cell cultures. *Biotechnology and bioengineering*, *101*(1), 182–9.

Barut, M., Podgornik, A., Urbas, L., & Al, E. (2008). Methacrylate-based short monolithic columns: enabling tools for rapid and efficient analyses of biomolecules and nanoparticles. *Journal of separation science*, *31*(11), 1867–80.

Bernal, V., Carinhas, N., Yokomizo, A. Y., Carrondo, M. J. T., & Alves, P. M. (2009). Cell density effect in the baculovirus-insect cells system: a quantitative analysis of energetic metabolism. *Biotechnology and bioengineering*, *104*(1), 162–80.

Bess, J. W., Gorelick, R. J., Bosche, W. J., Henderson, L. E., & Arthur, L. O. (1997). Microvesicles are a source of contaminating cellular proteins found in purified HIV-1 preparations. *Virology*, *230*(1), 134–44.

Bright, R. A., Carter, D. M., Daniluk, S., Toapanta, F. R., Ahmad, A., Gavrilov, V., … Ross, T. M. (2007). Influenza virus-like particles elicit broader immune responses than whole virion inactivated influenza virus or recombinant hemagglutinin. *Vaccine*, *25*(19), 3871–8.

Calder, L. J., Wasilewski, S., Berriman, J. A., & Rosenthal, P. B. (2010). Structural organization of a filamentous influenza A virus. *Proceedings of the National Academy of Sciences of the United States of America*, *107*(23), 10685–90.

Carrat, F., & Flahault, A. (2007). Influenza vaccine: the challenge of antigenic drift. *Vaccine*, *25*(39-40), 6852–62.

Chen, B. J., Leser, G. P., Jackson, D., & Lamb, R. a. (2008). The influenza virus M2 protein cytoplasmic tail interacts with the M1 protein and influences virus assembly at the site of virus budding. *Journal of virology*, *82*(20), 10059–70.

Chen, B. J., Leser, G. P., Morita, E., & Lamb, R. A. (2007). Influenza virus hemagglutinin and neuraminidase, but not the matrix protein, are required for assembly and budding of plasmid-derived virus-like particles. *Journal of virology*, *81*(13), 7111–23.

Chen, C.-Y., Lin, C.-Y., Chen, G.-Y., & Hu, Y.-C. (2011). Baculovirus as a gene delivery vector: Recent understandings of molecular alterations in transduced cells and latest applications. *Biotechnology advances*, *29*(6), 618–31.

Chen, J., Lee, K. H., Steinhauer, D. a, Stevens, D. J., Skehel, J. J., & Wiley, D. C. (1998). Structure of the hemagglutinin precursor cleavage site, a determinant of influenza pathogenicity and the origin of the labile conformation. *Cell*, *95*(3), 409–17.

Chua, J. V, & Chen, W. H. (2010). Bench-to-bedside review: vaccine protection strategies during pandemic flu outbreaks. *Critical care*, *14*(2), 218–26.

Chun, S., Li, C., Van Domselaar, G., & Al., E. (2008). Universal antibodies and their applications to the quantitative determination of virtually all subtypes of the influenza A viral hemagglutinins. *Vaccine*, *26*(48), 6068–76.

Cohen, J. (2009). Out of Mexico? Scientists Ponder Swine Flu's Origins. *Science*, *324*, 700–3.

Côté, J., Garnier, A., Massie, B., & Kamen, A. (1998). Serum-free production of recombinant proteins and adenoviral vectors by 293SF-3F6 cells. *Biotechnology and bioengineering*, *59*(5), 567–75.

Cox, M. M. J., & Hollister, J. R. (2009). FluBlok, a next generation influenza vaccine manufactured in insect cells. *Biologicals : journal of the International Association of Biological Standardization*, *37*(3), 182–9.

D'Aoust, M.-A., Couture, M. M.-J., Charland, N., Trépanier, S., Landry, N., Ors, F., & Vézina, L.-P. (2010). The production of hemagglutinin-based virus-like particles in plants: a rapid, efficient and safe response to pandemic influenza. *Plant biotechnology journal*, *8*(5), 607–19.

D'Aoust, M.-A., Lavoie, P.-O., Couture, M. M.-J., Trépanier, S., Guay, J.-M., Dargis, M., … Vézina, L.-P. (2008). Influenza virus-like particles produced by transient expression in Nicotiana benthamiana induce a protective immune response against a lethal viral challenge in mice. *Plant biotechnology journal*, *6*(9), 930–40.

De Vries, R. P., Smit, C. H., de Bruin, E., Rigter, A., de Vries, E., Cornelissen, L. a H. M., … de Haan, C. a M. (2012). Glycan-dependent immunogenicity of recombinant soluble trimeric hemagglutinin. *Journal of virology*, *86*(21), 11735–44.

Denzer, K., Kleijmeer, M. J., Heijnen, H. F., Stoorvogel, W., & Geuze, H. J. (2000). Exosome: from internal vesicle of the multivesicular body to intercellular signaling device. *Journal of cell science*, *113 Pt 19*, 3365–74.

Easterbrook, J. D., Schwartzman, L. M., Gao, J., Kash, J. C., Morens, D. M., Couzens, L., … Taubenberger, J. K. (2012). Protection against a lethal H5N1 influenza challenge by intranasal immunization with virus-like particles containing 2009 pandemic H1N1 neuraminidase in mice. *Virology*, *432*(1), 39–44.

Elias, C. B., Zeiser, A., Bédard, C., & Kamen, A. A. (2000). Enhanced growth of Sf-9 cells to a maximum density of 5.2 x 10(7) cells per mL and production of beta-galactosidase at high cell density by fed batch culture. *Biotechnology and bioengineering*, *68*(4), 381–8.

FDA. (2012). FDA approves first seasonal influenza vaccine manufactured using cell culture technology. Retrieved March 26, 2013, from http://www.fda.gov/newsevents/newsroom/pressannouncements/ucm328982.htm

FDA. (2013). FDA approves new seasonal influenza vaccine made using novel technology. Retrieved March 26, 2013, from http://www.fda.gov/newsevents/newsroom/pressannouncements/ucm328982.htm

Feng, S. Z., Jiao, P. R., Qi, W. B., Fan, H. Y., & Liao, M. (2010). Development and strategies of cell-culture technology for influenza vaccine. *Applied microbiology and biotechnology*, *89*, 893–902.

GE_Healthcare. (2012). Removal of DNA and baculovirus from influenza virus-like particles using Capto ^{TM} Q. GE Healthcare.

Genzel, Y., Behrendt, I., Rödig, J., Rapp, E., Kueppers, C., Kochanek, S., … Reichl, U. (2013). CAP, a new human suspension cell line for influenza virus production. *Applied microbiology and biotechnology*, *97*(1), 111–22.

Gerdil, C. (2003). The annual production cycle for influenza vaccine. *Vaccine*, *21*(16), 1776–79.

Gerster, P., Kopecky, E.-M., Hammerschmidt, N., Klausberger, M., Krammer, F., Grabherr, R., … Jungbauer, A. (2013). Purification of infective baculoviruses by monoliths. *Journal of chromatography. A*, *1290*, 36–45.

Gluschankof, P., Mondor, I., Gelderblom, H. R., & Sattentau, Q. J. (1997). Cell membrane vesicles are a major contaminant of gradient-enriched human immunodeficiency virus type-1 preparations. *Virology*, *230*(1), 125–33.

Gómez-Puertas, P., Albo, C., Pérez-Pastrana, E., Vivo, A., & Portela, A. (2000). Influenza virus matrix protein is the major driving force in virus budding. *Journal of virology*, *74*(24), 11538–47.

Gravel, C., Li, C., Wang, J., Hashem, A. M., Jaentschke, B., Xu, K., … Li, X. (2010). Qualitative and quantitative analyses of virtually all subtypes of influenza A and B viral neuraminidases using antibodies targeting the universally conserved sequences. *Vaccine*, *28*(36), 5774–84.

Hancioglu, B., Swigon, D., & Clermont, G. (2007). A dynamical model of human immune response to influenza A virus infection. *Journal of theoretical biology*, *246*(1), 70–86.

Haynes, J. R. (2009). Influenza virus-like particle vaccines. *Expert review of vaccines*, *8*(4), 435–45.

Held, P. G. (BioTek). (2006). Nucleic Acid Purity Assessment using A 260 / A 280 Ratios. Bioteck.

Hervas-Stubbs, S., Rueda, P., Lopez, L., & Leclerc, C. (2007). Insect Baculovirus Strongly Potentiate Adaptive Immune Responses by Inducing Type I IFN. *Journal of Immunology*, *178*, 2361–69.

Hirst, G. K. (1942). The quantitative determination of influenza virus and antibodies by means of red cell agglutination. *J Exp Med.*, *75*(1), 49–64.

Hopkins, R., & Esposito, D. (2009). A rapid method for titrating baculovirus stocks using the Sf-9 Easy Titer cell line. *BioTechniques*, *47*(3), 785–8.

Isaacs, A., & Donald, H. B. (1955). Particle counts of haemagglutinating viruses. *Journal of general microbiology*, *12*(2), 241–7.

Jarvis, D. L. (2009). Baculovirus-insect cell expression systems. In *Methods in Enzymology* (1st ed., Vol. 463, pp. 191–222). Elsevier Inc.

Jordan, I., Vos, A., Beilfuss, S., Neubert, A., Breul, S., & Sandig, V. (2009). An avian cell line designed for production of highly attenuated viruses. *Vaccine*, *27*(5), 748–56.

Kalbfuss, B., Knöchlein, A., Kröber, T., & Reichl, U. (2008). Monitoring influenza virus content in vaccine production: Precise assays for the quantitation of hemagglutination and neuraminidase activity. *Biologicals*, *36*(3), 145–61.

Kalbfuss, B., Wolff, M., Morenweiser, R., & Reichl, U. (2007). Purification of cell culture-derived human influenza A virus by size-exclusion and anion-exchange chromatography. *Biotechnology and Bioengineering*, *96*(5), 932–44.

Kang, S.-M., Song, J.-M., Quan, F.-S., & Compans, R. W. (2009). Influenza vaccines based on virus-like particles. *Virus research*, *143*(2), 140–6.

Killian, M. L. (2008). Hemagglutination Assay for the Avian Inlfuenza Virus. In *Methods In Molecular Biology* (Vol. 436, pp. 47–52). Humana Press.

Kistner, O., Barrett, P. N., Mundt, W., Reiter, M., Schober-Bendixen, S., & Dorner, F. (1998). Development of a mammalian cell (Vero) derived candidate influenza virus vaccine. *Vaccine*, *16*(9-10), 960–8.

Kost, T. A., Condreay, J. P., & Jarvis, D. L. (2005). Baculovirus as versatile vectors for protein expression in insect and mammalian cells. *Nature biotechnology*, *23*(5), 567–75.

Krammer, F., & Grabherr, R. (2010). Alternative influenza vaccines made by insect cells. *Trends in molecular medicine*, *16*(7), 313–20.

Krammer, F., Nakowitsch, S., Messner, P., Palmberger, D., Ferko, B., & Grabherr, R. (2010). Swine-origin pandemic H1N1 influenza virus-like particles produced in insect cells induce hemagglutination inhibiting antibodies in BALB/c mice. *Biotechnology journal*, *5*(1), 17–23.

Krammer, F., Schinko, T., Palmberger, D., Tauer, C., Messner, P., & Grabherr, R. (2010). Trichoplusia ni cells (High Five) are highly efficient for the production of influenza A virus-like particles: a comparison of two insect cell lines as production platforms for influenza vaccines. *Molecular biotechnology*, *45*(3), 226–34.

Kruh, J., & Saint, F. (1982). Effects of sodium butyrate , a new pharmacological agent , on cells in culture I . Introduction The interest in studies concerning sodium buty-, *82*, 65–82.

Landry, N., Ward, B. J., Trépanier, S., Montomoli, E., Dargis, M., Lapini, G., & Vézina, L.-P. (2010). Preclinical and clinical development of plant-made virus-like particle vaccine against avian H5N1 influenza. *PloS one*, *5*(12), e15559.

Latham, T., & Galarza, J. M. (2001). Formation of Wild-Type and Chimeric Influenza Virus-Like Particles following Simultaneous Expression of Only Four Structural Proteins. *Society*, *75*(13), 6154–6165.

Le Ru, A., Jacob, D., Transfiguracion, J., Ansorge, S., Henry, O., & Kamen, A. a. (2010). Scalable production of influenza virus in HEK-293 cells for efficient vaccine manufacturing. *Vaccine*, *28*(21), 3661–71.

Lohr, V., Rath, A., Genzel, Y., Jordan, I., Sandig, V., & Reichl, U. (2009). New avian suspension cell lines provide production of influenza virus and MVA in serum-free media: studies on growth, metabolism and virus propagation. *Vaccine*, *27*(36), 4975–82.

López-Macías, C., Ferat-Osorio, E., Tenorio-Calvo, A., Isibasi, A., Talavera, J., Arteaga-Ruiz, O., … Glenn, G. (2011). Safety and immunogenicity of a virus-like particle pandemic influenza A (H1N1) 2009 vaccine in a blinded, randomized, placebo-controlled trial of adults in Mexico. *Vaccine*, *29*(44), 7826–34.

Lorbetskie, B., Wang, J., Gravel, C., Allen, C., Walsh, M., Rinfret, A., … Girard, M. (2011). Optimization and qualification of a quantitative reversed-phase HPLC method for

hemagglutinin in influenza preparations and its comparative evaluation with biochemical assays. *Vaccine*, *29*(18), 3377–89.

Mahmood, K., Bright, R. a, Mytle, N., Carter, D. M., Crevar, C. J., Achenbach, J. E., … Ross, T. M. (2008). H5N1 VLP vaccine induced protection in ferrets against lethal challenge with highly pathogenic H5N1 influenza viruses. *Vaccine*, *26*(42), 5393–9.

Marcelin, G., DuBois, R., Rubrum, A., Russell, C. J., McElhaney, J. E., & Webby, R. J. (2011). A contributing role for anti-neuraminidase antibodies on immunity to pandemic H1N1 2009 influenza A virus. *PloS one*, *6*(10), e26335 1–10.

Marek, M., van Oers, M. M., Devaraj, F. F., Vlak, J. M., & Merten, O.-W. (2011). Engineering of baculovirus vectors for the manufacture of virion-free biopharmaceuticals. *Biotechnology and bioengineering*, *108*(5), 1056–67.

Margine, I., Martinez-Gil, L., Chou, Y., & Krammer, F. (2012). Residual Baculovirus in Insect Cell-Derived Influenza Virus-Like Particle Preparations Enhances Immunogenicity. (P. Zhou, Ed.)*PLoS ONE*, *7*(12), e51559.

Mehtali, M., Champion-Arnaud, P., & Arnaud, L. (2006). Process of manufacturing viral vaccines in suspension avian embryonic derived stem cell lines.

Michaelis, M., Doerr, H. W., & Cinatl, J. (2009). Novel swine-origin influenza A virus in humans: another pandemic knocking at the door. *Medical microbiology and immunology*, *198*(3), 175–83.

National Network For Immunization Information. (2010). Vaccines, Influenza. Retrieved July 20, 2013, from http://www.immunizationinfo.org/vaccines/influenza

Neumann, G., Noda, T., & Kawaoka, Y. (2009). Emergence and pandemic potential of swine-origin H1N1 influenza virus. *Nature*, *459*(7249), 931–9.

Nilsson, C. E., Abbas, S., Bennemo, M., Larsson, A., Hämäläinen, M. D., & Frostell-Karlsson, A. (2010). A novel assay for influenza virus quantification using surface plasmon resonance. *Vaccine*, *28*(3), 759–66.

Noda, T. (2011). Native morphology of influenza virions. *Frontiers in microbiology*, *2, Article*(January), 1–5.

Ohnishi, S. (1983). Hemolytic activity of influenza virus hemagglutinin glycoproteins activated in mildly acidic environments Biochemistry : *PNAS*, *80*(June), 3153–7.

Oksanen, H. M., Domanska, A., & Bamford, D. H. (2012). Monolithic ion exchange chromatographic methods for virus purification. *Virology*, *434*(2), 271–7.

Opitz, L., Salaklang, J., Büttner, H., Reichl, U., & Wolff, M. W. (2007). Lectin-affinity chromatography for downstream processing of MDCK cell culture derived human influenza A viruses. *Vaccine*, *25*(5), 939–47.

Palomares, L. a., & Ramírez, O. T. (2009). Challenges for the production of virus-like particles in insect cells: The case of rotavirus-like particles. *Biochemical Engineering Journal*, *45*(3), 158–67.

Patriarca, P. (2007). Use of Cell Lines for the Production of Influenza Virus Vaccines: An Appraisal of Technical, Manufacturing, and Regulatory Considerations. Geneva, Switzerland: World Health Organization.

Pau, M. G., Ophorst, C., Koldijk, M. H., Schouten, G., Mehtali, M., & Uytdehaag, F. (2001). The human cell line PER.C6 provides a new manufacturing system for the production of influenza vaccines. *Vaccine*, *19*(17-19), 2716–21.

Petiot, E., Jacob, D., Lanthier, S., Lohr, V., Ansorge, S., & Kamen, A. A. (2011). Metabolic and kinetic analyses of influenza production in perfusion HEK293 cell culture. *BMC biotechnology*, *11*(84), 1–12.

Pincus, S., Boddapati, S., Li, J., Sadowski, T., & Pincus, B. S. (2010). Release and Stability Testing Programs for a Novel Virus-Like Particle Vaccine. *BioPharm International Supplements*, *October*, 26–34.

Pushko, P., Pearce, M. B., Ahmad, A., Tretyakova, I., Smith, G., Belser, J. a, & Tumpey, T. M. (2011). Influenza virus-like particle can accommodate multiple subtypes of hemagglutinin and protect from multiple influenza types and subtypes. *Vaccine*, *29*(35), 5911–8.

Pushko, P., Tumpey, T. M., Bu, F., Knell, J., Robinson, R., & Smith, G. (2005). Influenza virus-like particles comprised of the HA, NA, and M1 proteins of H9N2 influenza virus induce protective immune responses in BALB/c mice. *Vaccine*, *23*(50), 5751–9.

Quan, F.-S., Huang, C., Compans, R. W., & Kang, S.-M. (2007). Virus-like particle vaccine induces protective immunity against homologous and heterologous strains of influenza virus. *Journal of virology*, *81*(7), 3514–24.

Racaniello, V. (2009). Structure of Influenza Virus. *Virology Blog: About Viruses and Viral Disease*. Retrieved July 25, 2013, from http://www.virology.ws/2009/04/30/structure-of-influenza-virus/

Rathore, A. S., Yu, M., Yeboah, S., & Sharma, A. (2008). Case study and application of process analytical technology (PAT) towards bioprocessing: use of on-line high-performance liquid chromatography (HPLC) for making real-time pooling decisions for process chromatography. *Biotechnology and bioengineering*, *100*(2), 306–16.

Rossman, J. S., & Lamb, R. a. (2011). Influenza virus assembly and budding. *Virology*, *411*(2), 229–36.

Ruigrok, R. W., Aitken, A., Calder, L. J., Martin, S. R., Skehel, J. J., Wharton, S. A., … Wiley, D. C. (1988). Studies on the structure of the influenza virus haemagglutinin at the pH of membrane fusion. *The Journal of general virology*, *69*, 2785–95.

Samji, T. (2009). Influenza A: understanding the viral life cycle. *The Yale journal of biology and medicine*, *82*(4), 153–9.

Schild, G. C., Wood, J. M., & Newman, R. W. (1975). A single-radial-immunodiffusion technique for the assay of influenza haemagglutinin antigen. Proposals for an assay method for the haemagglutinin content of influenza vaccines. *Bulletin of the World Health Organization*, *52*(2), 223–31.

Schmeisser, F., Adamo, J. E., Blumberg, B., Friedman, R., Muller, J., Soto, J., & Weir, J. P. (2012). Production and characterization of mammalian virus-like particles from modified vaccinia virus Ankara vectors expressing influenza H5N1 hemagglutinin and neuraminidase. *Vaccine*, *30*(23), 3413–22.

Sedova, E. S., Shcherbinin, D. N., Migunov, a I., Smirnov, I. a, Logunov, D. I., Shmarov, M. M., … Gintsburg, a L. (2012). Recombinant influenza vaccines. *Acta naturae*, *15*(4), 17–27.

Segura, M. D. L. M., Garnier, A., & Kamen, A. (2006). Purification and characterization of retrovirus vector particles by rate zonal ultracentrifugation. *Journal of virological methods*, *133*(1), 82–91.

Shen, C. F., Meghrous, J., & Kamen, A. (2002). Quantitation of baculo v irus particles by flow cytometry, *105*.

Szécsi, J., Boson, B., Johnsson, P., Dupeyrot-Lacas, P., Matrosovich, M., Klenk, H. D., … Cosset, F. L. (2006). Induction of neutralising antibodies by virus-like particles harbouring surface proteins from highly pathogenic H5N1 and H7N1 influenza viruses. *Virology journal*, *3*, 70.

Szretter, K. J., Balish, A. L., & Katz, J. M. (2006). Influenza: Propagation, Quantification and Storage. In *Current Prtotocols in Microbiology* (pp. 1–22). John Wiley & Sons, Inc.

Tancevski, I., Wehinger, A., Patsch, J. R., & Ritsch, A. (2006). In vivo application of adenoviral vectors purified by a Taqman Real Time PCR-supported chromatographic protocol. *International journal of biological macromolecules*, *39*(1-3), 77–82.

Tang, X.-C., Lu, H.-R., & Ross, T. M. (2010). Hemagglutinin displayed baculovirus protects against highly pathogenic influenza. *Vaccine*, *28*(42), 6821–31.

Tang, X.-C., Lu, H.-R., & Ross, T. M. (2011). Baculovirus-produced influenza virus-like particles in mammalian cells protect mice from lethal influenza challenge. *Viral immunology*, *24*(4), 311–9.

Taubenberger, Jeffery K., Morens, D. M. (2008). The Pathology of Influenza Virus Infections. *Annu Rev Pathol*, (3), 499–22.

Thompson, C. M., Petiot, E., Lennaertz, A., Henry, O., & Kamen, A. A. (2013). Analytical technologies for influenza virus-like particle candidate vaccines: challenges and emerging approaches. *Virology journal*, *10*(141), 1–14.

Transfiguracion, J., Mena, J. a, Aucoin, M. G., & Kamen, A. a. (2011). Development and validation of a HPLC method for the quantification of baculovirus particles. *Journal of chromatography. B, Analytical technologies in the biomedical and life sciences*, *879*(1), 61–8.

Van Veldhoven, P. P., Baumgart, E., & Mannaerts, G. P. (1996). Iodixanol (Optiprep), an improved density gradient medium for the iso-osmotic isolation of rat liver peroxisomes. *Analytical biochemistry*, *237*(1), 17–23.

Vicente, T., Roldão, A., Peixoto, C., Carrondo, M. J. T., & Alves, P. M. (2011). Large-scale production and purification of VLP-based vaccines. *Journal of invertebrate pathology*, *107 Suppl*, S42–8.

Voeten, J. T., Brands, R., Palache, a M., van Scharrenburg, G. J., Rimmelzwaan, G. F., Osterhaus, a D., & Claas, E. C. (1999). Characterization of high-growth reassortant influenza A viruses generated in MDCK cells cultured in serum-free medium. *Vaccine*, *17*(15-16), 1942–50.

Welsch, S., Müller, B., & Kräusslich, H.-G. (2007). More than one door - Budding of enveloped viruses through cellular membranes. *FEBS letters*, *581*(11), 2089–97.

WHO. (2006). *Global pandemic influenza action plan to increase vaccine supply*. Geneva, Switzerland: Department of Immunization Vaccines and Biologicals.

WHO. (2009). Influenza (Seasonal). Retrieved March 26, 2013, from http://www.who.int/mediacentre/factsheets/fs211/en/

Wood, J., Dunleavy, U., Newman, R., Riley, A., Robertson, J., & Minor, P. (1999). The influence of the host cell on standardisation of influenza vaccine potency. *Dev Biol Stand.*, *98*, 183–8.

Wood, J., Schild, G., Newman, R., & Seagroatt, V. (1977). an improved single-radial-immunodiffusion technique for the assay of influenza haemagglutinin antigen: application for potency determinations of inactivated whole virus and subunit vaccines. *Jounal of Biological Standardization*, *5*, 237–47.

Wu, C. Y., Yeh, Y. C., Yang, Y. C., Chou, C., Liu, M. T., Wu, H.-S., … Hsiao, P. W. (2010). Mammalian expression of virus-like particles for advanced mimicry of authentic influenza virus. *PloS one*, *5*(3), e9784.

Appendix 1A: Flow Cytometry Total Baculovirus Particle Calculation

The concentration of total baclovirus particles was calculated based on the following (1):

$$\frac{\text{Viral Particle Concentration}}{\text{ml}} = \frac{C_v \times D \times 1000 \times 50000}{C_F \times \text{Vol}} \qquad (1)$$

Where:

CV and CF: average particle counts for viral particles and flowset, respectively.

D: dilution rate of the viral solution

Vol: volume (ul) of the diluted solution taken for the sample preparation

1000: final volume of the sample.

50000: particle concentration of the diluted flowset

Three counts were taken for each virus that was quantified. An example of particle counts is given below for the P2 viral stock of HA under polyhedron control.

Appendix 1A Table 1.1: FC BV and flow set counts

Count #	Particle Count (CV)	Flow Set Standard Count (FS)
1	1194	794
2	1223	973
3	1086	944
Average	1167.666667	903.6666667

Appendix 1B: Easy Titer Calculation

This section explains the calculations used to quantify the infectious baculovirus titer using the Titer less method described in section 5.4.2.

First, the wells were scored for GFP activity. Wells that had any GFP were marked as positive, and those without as negative.

Appendix 1B Table 1.1: Typical reading observed with the titerless assay.

	1	2	3	4	5	6	7	8	9	10	11	12
A	+	+	+	+	+	+	+	-	-	-	-	
B	+	+	+	+	+	+	-	+	-	-	-	
C	+	+	+	+	+	+	+	-	-	-	-	
D	+	+	+	+	+	+	+	-	+	-	-	
E	+	+	+	+	+	+	+	+	-	-	-	
F	+	+	+	+	+	+	-	+	-	-	-	
G	+	+	+	+	+	+	+	-	-	-	-	
H	+	+	+	+	+	+	+	+	-	-	-	
# +	8	8	8	8	8	8	6	4	1	0	0	

In columns 7 and 8 the % ratio of infected wells changes from above 50% to below 50%. To begin the infectious particle calculation, the proportionate distance (PD) must be calculated based on the % ratio above 50% infected and below.

$$\text{Proportionate Distance (PD)} = \frac{(\%\ \text{ratio above } 50\%) - 50}{(\%\ \text{ratio above } 50\%) - (\%\ \text{ratio below } 50\%)}$$

The % ratio above and below 50% was calculated as shown in Table 2.

Appendix 1B Table 1.2: Calculation for above and below 50% values

	Virus Dilution	Neg. Log	Infected Wells	Non-Inf. Wells	Cumulative Inf. Wells	Cumulative non-infected Wells	% Infected
1	1:1000	10^{-3}					
2	1:5000	$10^{-3.7}$					
3	1:25000	$10^{-4.4}$					
4	1:125000	$10^{-5.1}$					
5	1:625000	$10^{-5.8}$					
6	1:3125000	$10^{-6.5}$	8	0	19	0	100%
7	1:15626000	$10^{-7.2}$	6	2	11	2	**85%**
8	1:78125000	$10^{-7.9}$	4	4	5	6	**45%**
9	1:390630000	$10^{-8.6}$	1	7	1	13	7%

Therefore, column 7 has 85% of the wells infected and column 8 has 45% and the PD is calculated as follows:

$$\text{PD} = \frac{85 - 50}{85 - 45} = 0.875$$

To complete the calculation for infectious titer, the following calculations were then completed:

$$\text{PD (corrected)} = \text{DP}_\text{C} = \text{DP} \times \text{Difference in dilution factor at turning point}$$

$$\text{DP}_\text{C} = 0.875 \times (7.9 - 7.2) = 0.61$$

$$\frac{\text{Virus Titer}}{0.2\text{ml}} = 10^{\text{DP}_\text{C} + \log \text{ of dilution at \% ratio above 50\%}}$$

$$\frac{\text{Virus Titer}}{0.2\text{ml}} = 10^{0.61+7.2} = 10^{7.81}$$

$$\text{Virus Titer} = 3.23 \times 10^8 \text{ pfu/ml}$$

Appendix 2: HA Assay Calculations

The HA titer is calculated based on the last well without agglutination of the red blood cells.

Appendix 2 Table 2.1: Typical HA assay agglutination pattern

Column	**1**	**2**	**3**	**4**	**5**	**6**	**7**	**8**	**9**	**10**	**11**	**12**
Dilutions	1:1	1:2	1:4	1:8	1:16	1:32	1:64	1:128	1:256	1:512	1:1024	1:2048
							●	●	●	●	●	●

Therefore, if column 6 were the last well with agglutination, where the dilution is 1/32, the amount of HA would be calculated as follows:

$$\frac{\text{Log HA units}}{100\text{ ul}} = \log(32) = 1.5\log\frac{HA\ units}{100ul}$$

$$\frac{1000\text{ul}}{1\text{ ml}} \times 1.5\log\frac{HA\ units}{100ul} = 10\times 1.5\log\frac{HA\ units}{ml} = 2.5\log\frac{HA\ units}{ml}$$

$$2.5log\frac{HA\ units}{ml} = 10^{2.5}\ HA\frac{units}{ml} = 316.23\ HA\frac{units}{ml}$$

One HA unit is the equal to the minimum number of virus particles that cause complete agglutination.

Based on NSEM quantification, particle concentration per HAU was calculated as follows:

For the Sf9 system:

$$\text{Total HA Activity} = \text{HA activity from BV} + \text{HA activity from VLP}$$

For Iodixanol fraction #2, the ratio of BV/VLP was 9:1

$$\text{Total HA Activity} = \text{HA activity from BV} + \frac{1}{9}\ (\text{HA activity from BV})$$

$$\text{Total HA Activity} = \frac{10}{9}\ (\text{HA activity from BV})$$

$$4520.7\ \frac{\text{HAU}}{\text{ml}}\text{HA activity from BV}$$

And for the activity from the VLPs,

$$5023\ \frac{\text{HAU}}{\text{ml}} = 9\ (\text{HA activity from VLP}) + \ \text{HA activity from VLP}$$

$$5023\ \frac{\text{HAU}}{\text{ml}} = 10\ (\text{HA activiy from VLP})$$

$$502.3\ \frac{\text{HAU}}{\text{ml}} = \text{HA activity from VLP}$$

Appendix 3: SRID Calibration Curve

To calculate the amount of HA in VLP, a standard curve must be made with known concentrations of HA protein. The standard used was recombinant HA from from Protein Sciences Corporation (USA). Concentrations used were 7.5, 15, 20 and 30 µg/ml. The diffusion ring diameter of each well was measured both horizontally and vertically. Then the average of was calculated and used to find the area of the ring. A standard curve based on these values was made (Appendix 3 Figure 3.1) to calculate the amount of HA in each sample. This standard curve was repeated each time the assay was done.

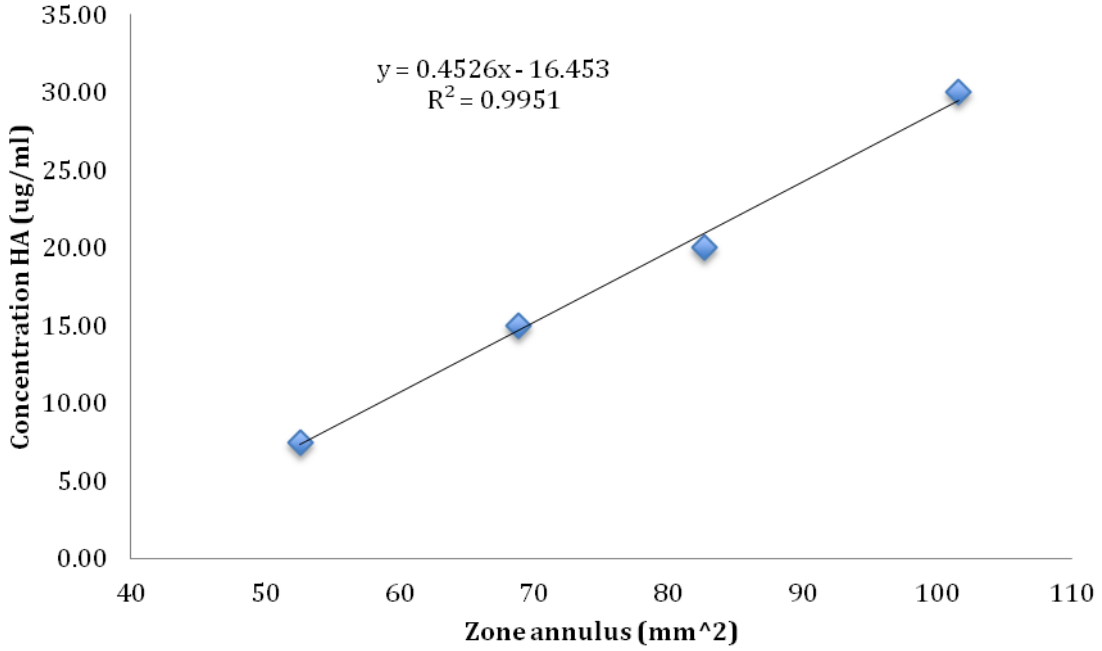

Appendix 3 Figure 3.1: SRID standard curve with recombinant H1/A/PR/8/1934 protein from Protein Sciences corporation.

Appendix 4A: HEK 293 VLP Production Growth Curves

Typical growth curves for VLP production at different MOIs in HEK 293 cells and non-transduced cells are shown in Figure 1.0 of this section. Cells were transduced with baculovirus containing genes under CMV control just under $1.0x10^6$ cells/ml and Butyric acid was added for a final concentration of 5mM to each VLP production but not the control. For transduced cultures, growth was greatly reduced, due to the addition of butyric acid, which halts cell growth. The control cells grew as they usually do, doubling after 24 hours and slowing growth after $2.0x10^6$ cells/ml. The viability profile is also shown in Figure 2.0 of this section, and illustrates that the control culture remained close to 100% viability after 48 hours, while VLP productions began to decrease in viability up to 80% at harvest.

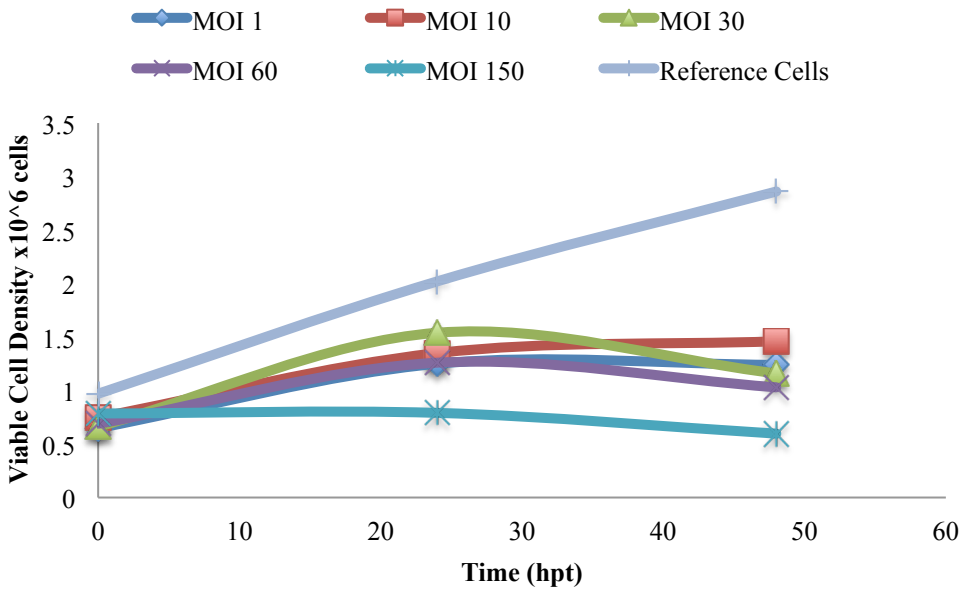

Appendix 4A Figure 4.1: Viable cell growth curve for HEK 293 VLP production

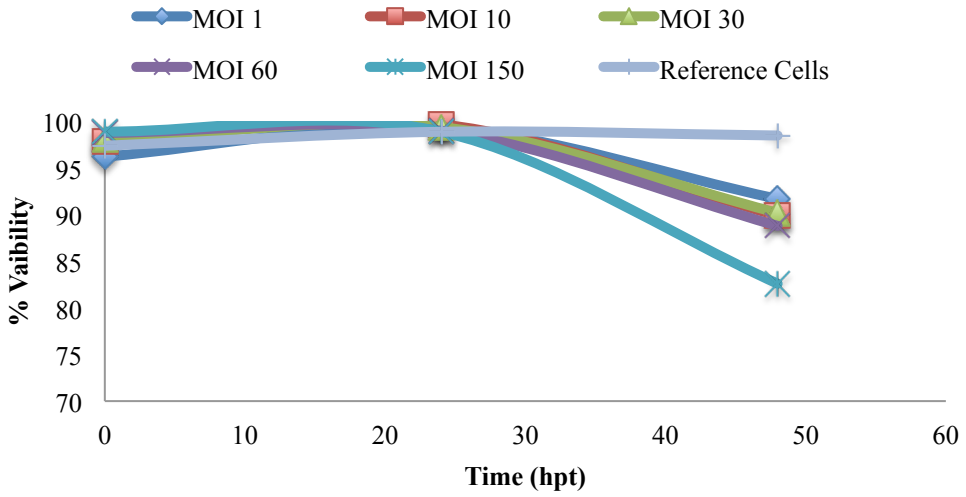

Appendix 4A Figure 4.2: Viability curve for HEK 293 VLP production

Appendix 4B: Sf9 VLP Production Growth Curves

Typical growth curves for VLP production at different MOIs in Sf9 cells and uninfected cells are shown in Figure 1.0 of this section. Cells were infected with individual baculoviruses containing influenza genes under polh control at $2.0x10^6$ cells/ml. For infected cultures, growth was greatly reduced, due to baculovirus infection, which halts cell growth. The control cells grew as they usually do, almost doubling every 24 hours. The viability profile is also shown in Figure 2.0 of this section, and illustrates that the control culture remained close to 100% viability after 48 hours, while VLP productions began to decrease in viability up to 60% at harvest. In addition to growth and viability curves, average cell diameter of the cells during production is shown in Figure 3.0. The uninfected culture remain at a diameter of 15um for the duration of the experiment while the infected cultures cell size increases up to 19.5 um, indicating baculovirus infection.

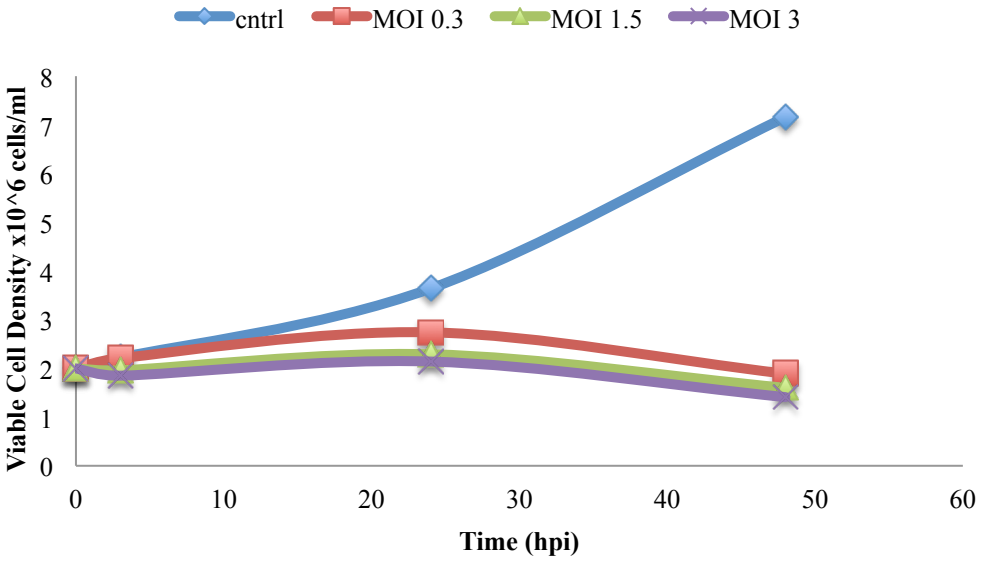

Appendix 4B Figure 4.1: Viable cell growth curve for Sf9 VLP production

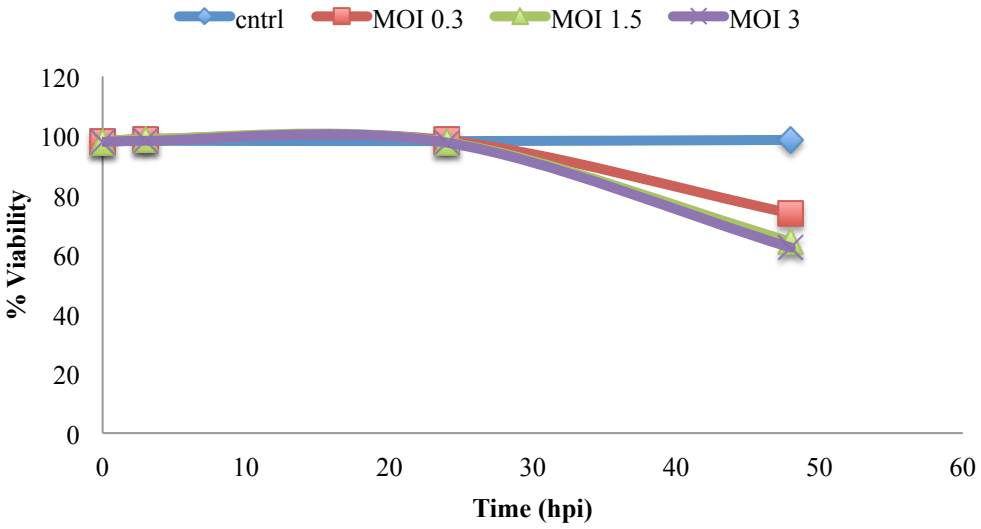

Appendix 2B Figure 4.2: Viability curve for Sf9 VLP production

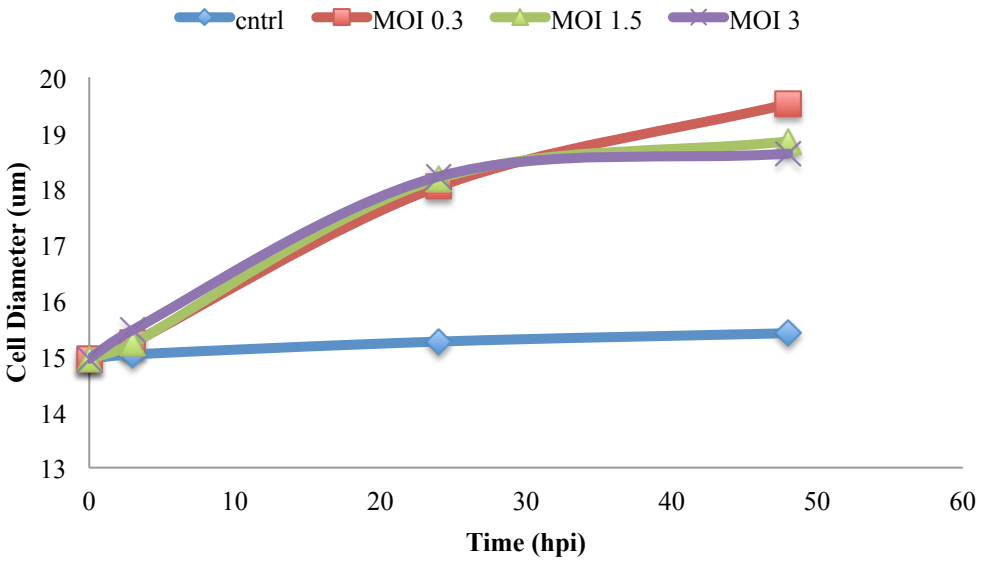

Appendix 2B Figure 4.3: Cell diameter curve for Sf9 VLP production

Appendix 5: HEK 293 Western Blot Non-Specific Bands

During process optimization, a contaminant band around 70 kDa was observed in the western blots of control cultures. This was worrisome because HA0 was expected to be at 70 kDa as well. However, during iodixanol purification it was verified that this contaminating band was simply overlapping with HA0. Figure 1.0 of this section shows the iodixanol western blot for HA with NIBSC anti-HA polyclonal antibody. The control well, to the right of the ladder, shows two bands above and below 75 kDa, none of which are believed to be HA0 as the control virus was produced in the presence of TPCK-trypsin, which cleaves HA0 into HA1 and HA2. VLPs however, will still have intact HA0 and lane 1 shows a large band at 75 kDa and another smaller one just under 75 kDa. Lane 2 then reveals that three bands exist at 75 kDa, above, at and below. This is illustrated more closely in Figure 2.0. Lanes 4 to 9 show that the middle band disappears and is present again in lanes 10-12. Additionally, the NA western blot that used the same secondary antibody (anti-sheep HRP) also has these bands above and below 75 kDa, but not the middle one (Figure 3.0). From these observations, this middle band is believed to be HA0. The other two bands may be heat shock proteins that are known to be expressed when cells are under stress, and have been shown to associate themselves with vesicles (De Maio, 2010).

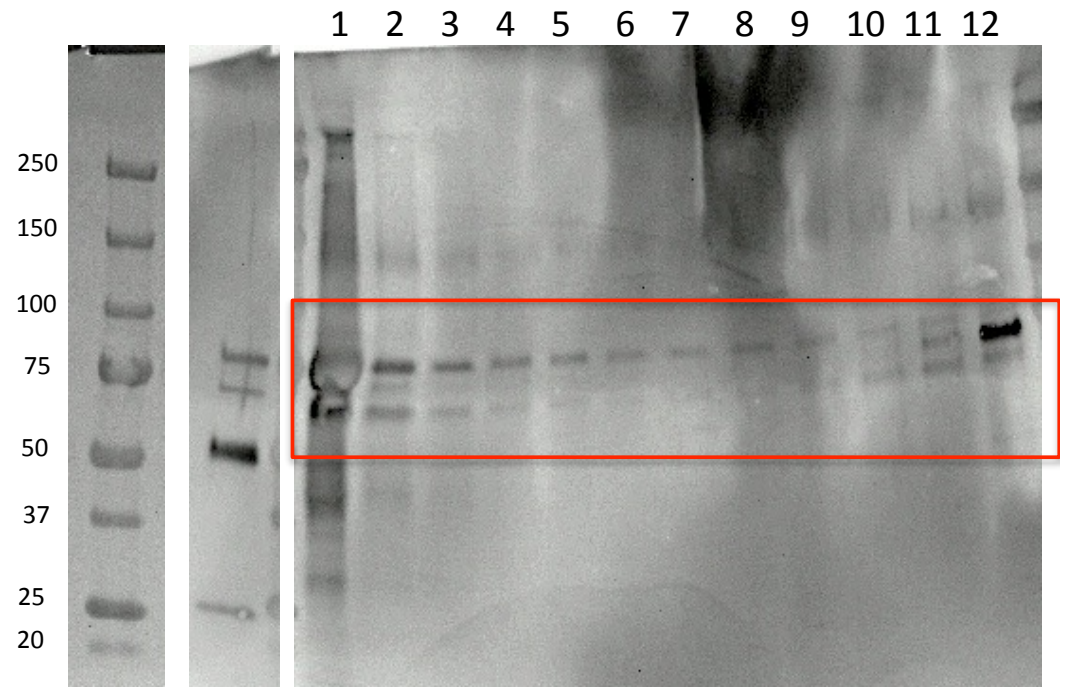

Appendix 5 Figure 5.1: HA iodixanol western blot HEK 293 VLP

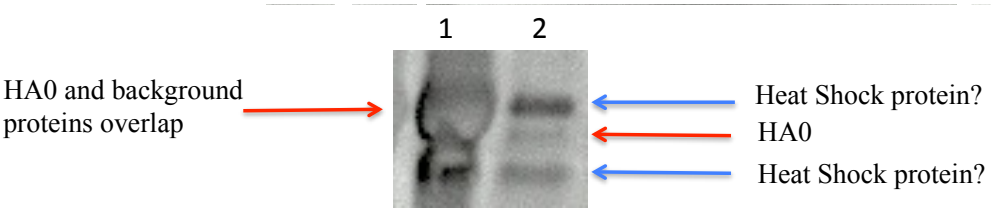

Appendix 5 Figure 5.2: HEK 293 VLP HA iodixanol western blot, lanes 1 and 2 zoomed in

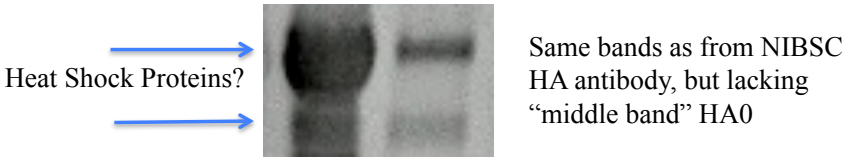

Appendix 5 Figure 5.3: HEK 293 VLP NA iodixanol western blot, lanes 1 and 2 zoomed in

Appendix 6A: HEK 293 VLP NA and M1 Iodixanol Western Blots

The iodixanol western blots for NA and M1 show the same information as the HA iodixanol western blot. Mainly, for the NA blot (Figure 1.0 in this section), there are NA signals at 55 kDa in fractions 1-4 and 8-10 (outlined by the orange box), and are strongest in the lower and upper fractions. The M1 blot (Figure 2.0) only has a band for M1 at 25 kDA, and bands at 75 kDa from the secondary antibodies. However, there is a band at 50 kDa that could be a M1 dimer.

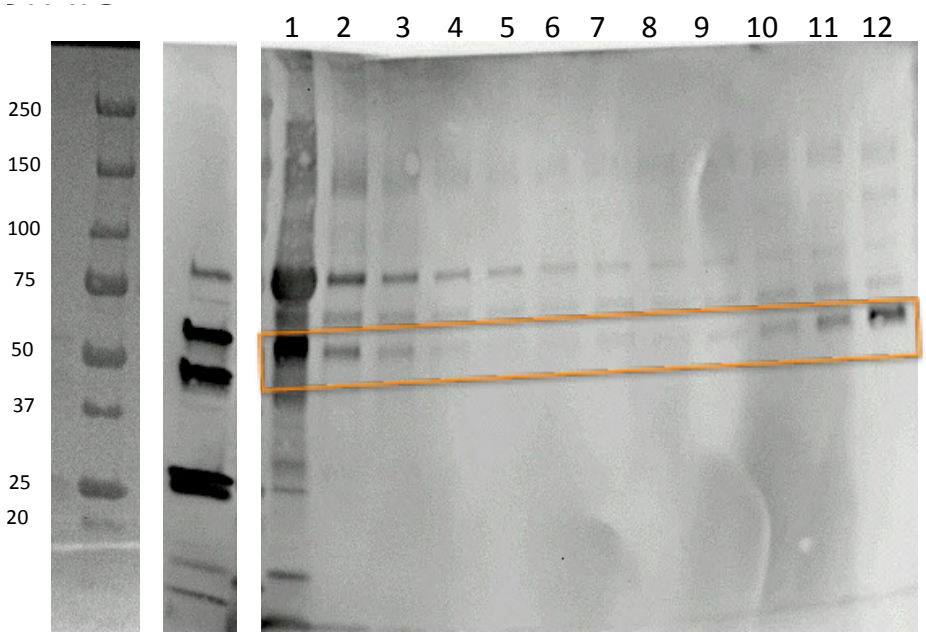

Appendix 6A Figure 6.1: HEK 293 VLP NA Iodixanol western blot

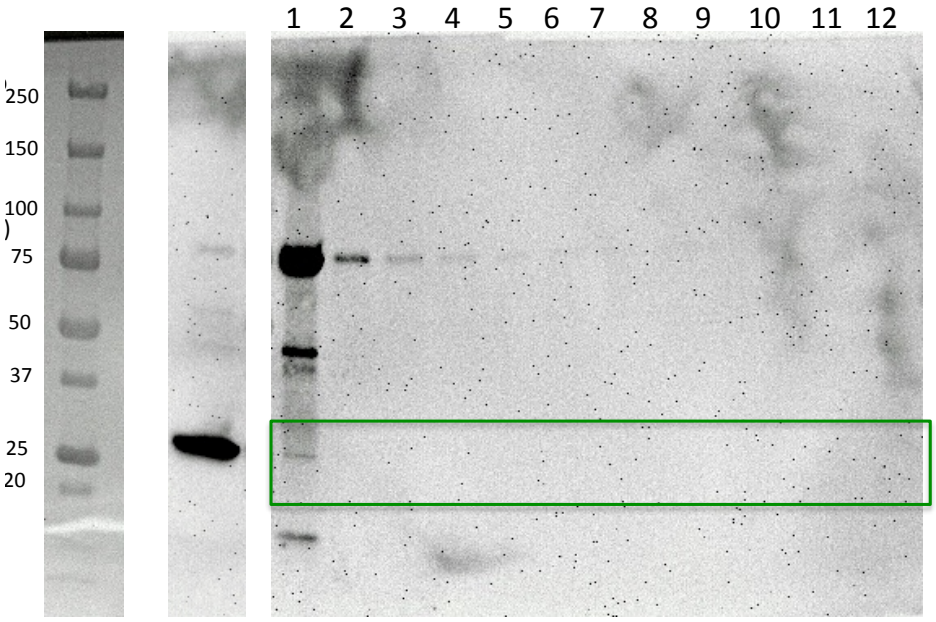

Appendix 6A Figure 6.2: HEK 293 VLP M1 Iodixanol western blot

Appendix 6B: Sf9 VLP NA and M1 Iodixanol Western Blots

The iodixanol western blots for NA, M1 and GP64 for also correlate with the HA blot. In each blot, there are bands in every fraction, but they pool in higher concentrations in the bottom and top fractions, where there are VLPs are potentially free protein. The NA blot was overexposed, which is why there are white spots on the blot. NA has three bands above and below 50 kDa and at 25 kDa; M1 was found at 25 kDa and GP64 around 60 kDa.

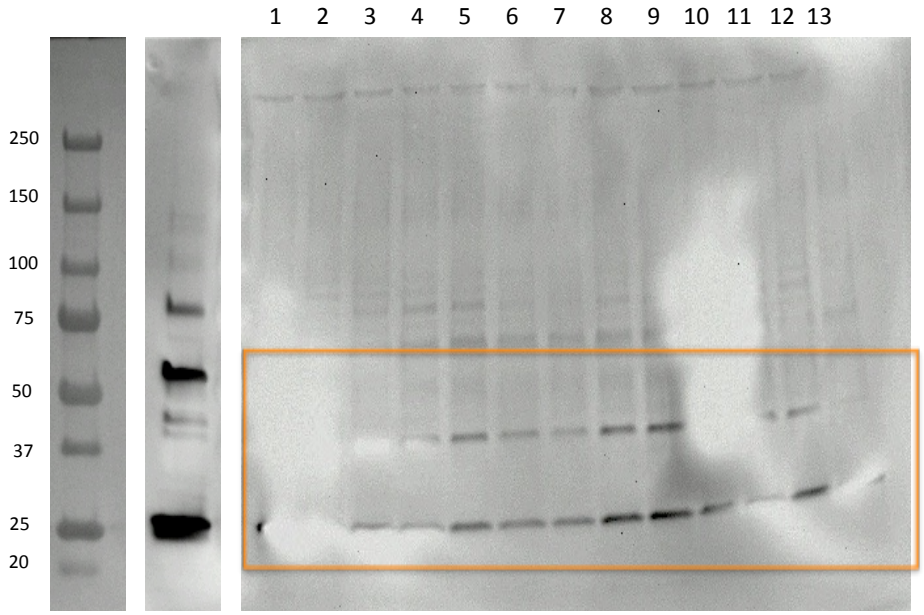

Appendix 6B Figure 6.1: Sf9 VLP NA iodixanol western blot

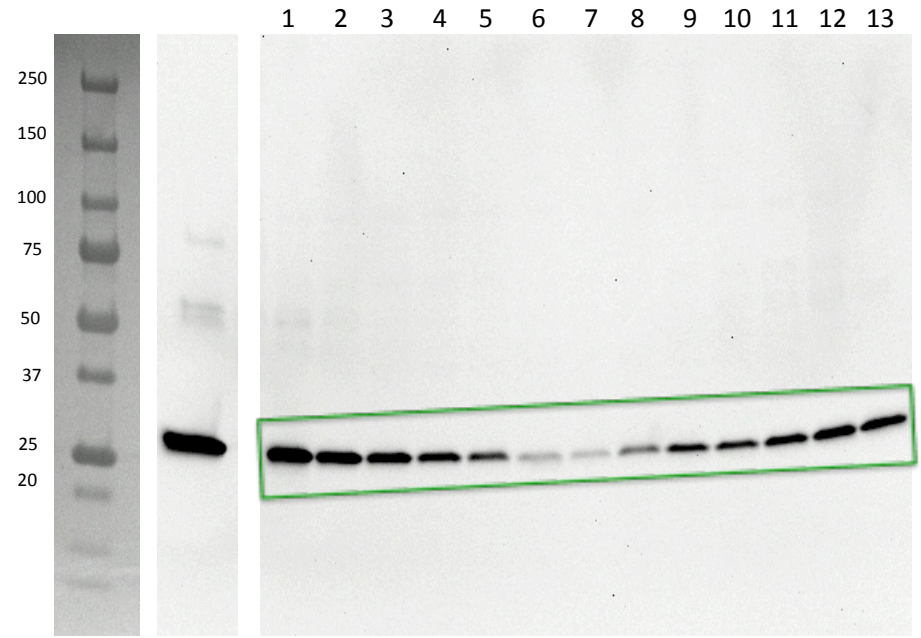

Appendix 6B Figure 6.2: Sf9 VLP M1 iodixanol western blot

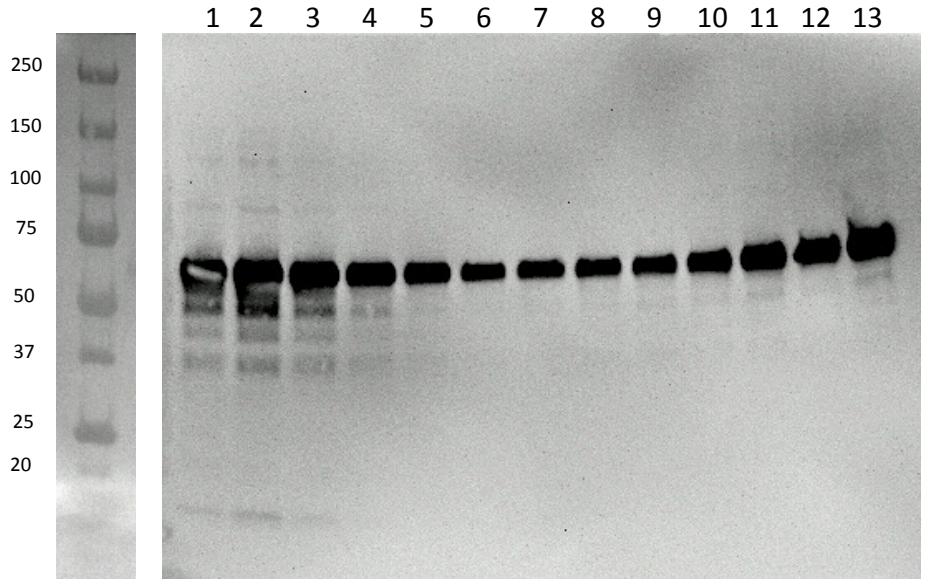

Appendix 6B Figure 6.3: Sf9 VLP GP64 iodixanol western blot

Appendix 7: Sf9 Optimization Western Blot

The best condition was picked on the condition that each protein was found in the supernatant from western blot analysis. The different MOIs used for each baculovirus are outlined in Table 7.1.

Appendix 7 Table 7.1: List of MOIs used for influenza VLP production in Sf9 cells

# on Western Blot (Pellet, Supernatant)	HA	NA	M1	Total
1, 2	0.1	0.1	0.1	0.3
3, 4	0.5	0.5	0.5	1.5
5, 6	1	1	1	3
7, 8	1	0.1	0.1	1.2
9, 10	0.1	0.1	1	1.2
11, 12	0.1	1	0.1	1.2

In Appendix 7 Figure 7.1, the western blot for HA from Sf9 VLP production is show. Lanes 1-6 are from the pellet and supernatant of the first MOI experiment, where each baculovirus was added at the same MOI (Appendix 7 Table 7.1). From this western, it was clear that the majority of the HA protein found was still in the pellet (Lanes 1, 3, 5), so it was decided to try and change the MOIs and see if more influenza proteins were found in the supernatant. Lane 8 from Appendix 7 Figure 7.1 showed a band for HA0 in the supernatant. Additionally, lane 10 from Appendix 7 Figure 7.2 had a band for NA in the supernatant, but not an obvious band for HA0 in that condition. M1 was seen in each supernatant (Appendix 7 Figure 7.3), but in higher quantities in lane 10. From all this data, it was chosen to use an MOI of 1, 0.1 and 1 for HA, NA and M1, respectively, to give the highest chance of influenza proteins in the supernatant, in the form of VLPs.

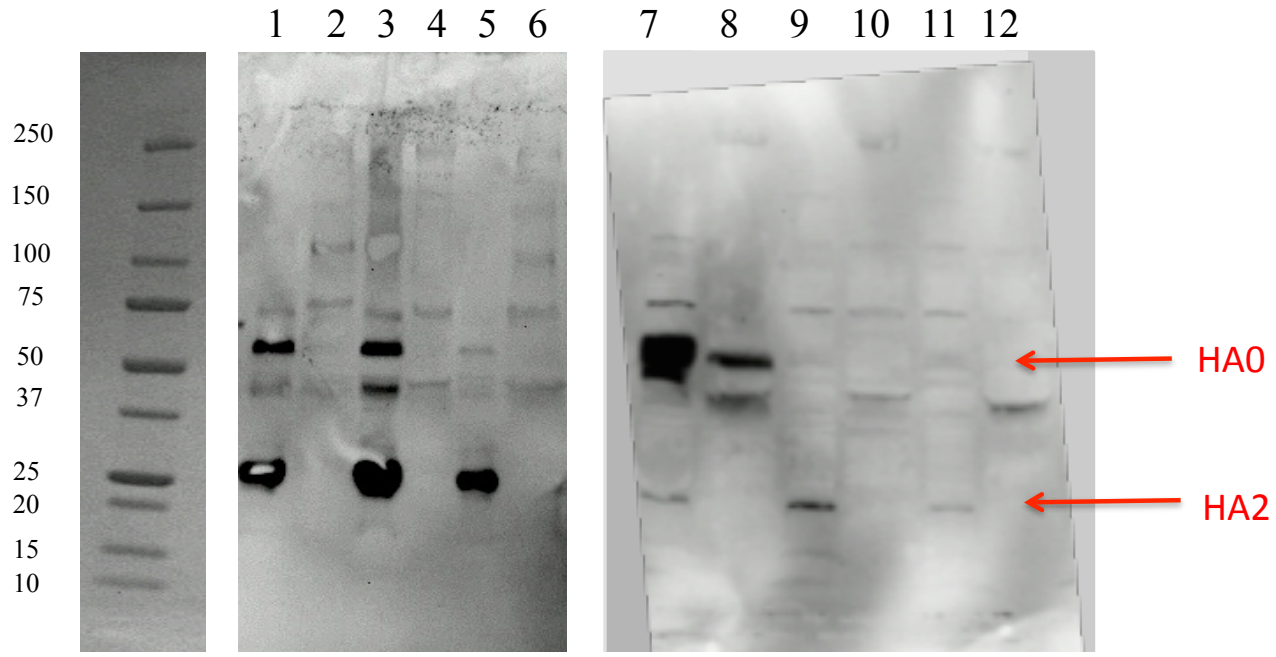

Appendix 7 Figure 7.1: HA western blot of Sf9-VLP productions at different MOIs with NIBSC anti-HA

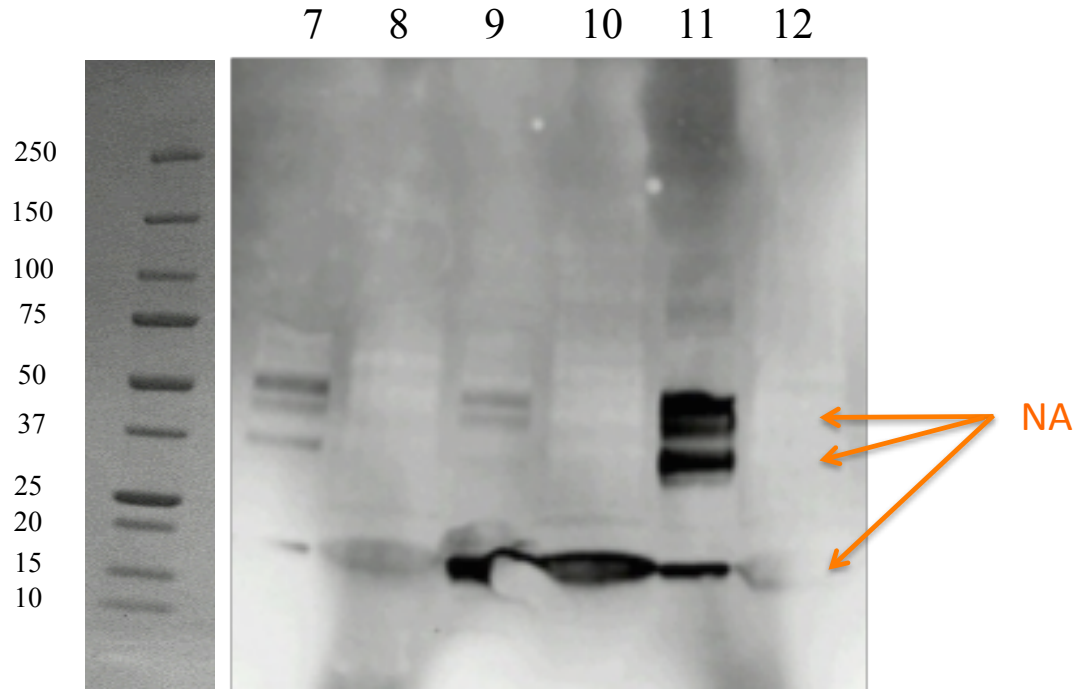

Appendix 7 Figure 7.2: NA western blot of Sf9-VLP productions at different MOIs with NIBSC anti-NA

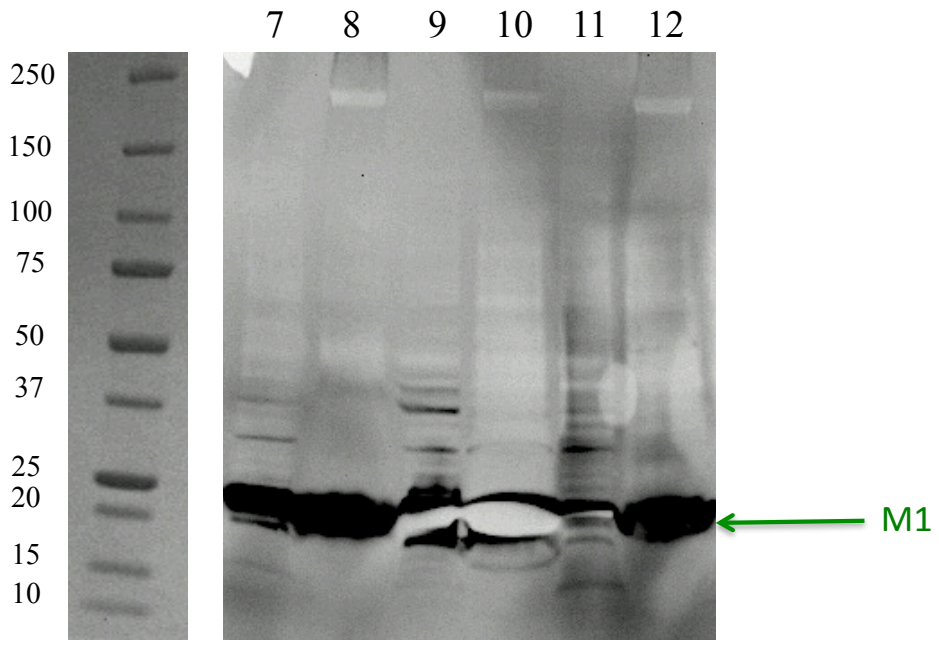

Appendix 7 Figure 7.3: M1 western blot of Sf9-VLP productions at different MOIs with NIBSC anti-NA

Appendix 8: HPLC Method for In-process VLP Analysis

A high-throughput method that is able to analyze crude samples and that can detect and ideally quantify total VLP particles is needed. High Performance Liquid Chromatography (HPLC) has been previously used as a quantification method for total baculovirus particles (Transfiguracion, Mena, Aucoin, & Kamen, 2011) and as a process analytical technology (PAT) tool (Rathore, Yu, Yeboah, & Sharma, 2008). It has the potential to analyze crude material in large quantities, making this method suitable for particle detection/quantification during different stages of process development. There already exists an HPLC based method for HA protein quantification that is currently in use or in development for use as an in-process method (Lorbetskie et al., 2011), but it does not give information on the total amount of particles. The following section outlines the advances made on VLP detection using an HPLC method with an ion exchange monolith column for total influenza particle quantification. The goal for these experiments was to investigate if total VLPs could be detected using an existing in-house total particle influenza quantification method. Considering the difficulties experienced during process optimization (cumbersome protocols, low yields and poor limit of detections for existing influenza quantification techniques), this method could be a valuable tool during process development and could give further insight into the development of an HPLC quantification method.

Appendix 8.1 Monolith Column

A convective interactive media (CIM) Quaternary Amine (QA) monolith column (CIMac™ QA-0.1 Analytical column, BiaSeparations, Austria) was chosen based on its potential to purify large particles, such as viruses (Barut, Podgornik, Urbas, & Al, 2008), to circumvent resin based chromatographic methods, which cannot be used due to virus size (20-750 μm) (Oksanen, Domanska, & Bamford, 2012).

Appendix 8.2 HPLC Method for Influenza Quantification Method

A method was developed in Dr Kamen's group for total particles influenza virus quantification (data not shown) and is still in development The method consisted of loading virus or VLP samples onto the column at a salt concentration of 200mM. At this concentration, it was found that particles are able to bind to the column, but free proteins cannot, allowing them to flow

through. Next, elution occured at three different salt concentrations of 450mM, 650mM and 1M NaCl, and resulted in three separate peaks labeled Peak 1, Peak 2 and Peak 3 (Appendix 8 Figure 8.1). Peak 2 has been identified as infectious influenza particles from TCID50 and western blot measurements of the eluted sample. The peak at 1M is hypothesized to be DNA based on its 260/280 ratio of approximately 2 with UV (Held, 2006). It remains unknown what is eluting in the 450 mM NaCl peak, but we estimate it could be HEK 293 system vesicles or large protein aggregates that were able to bind during the 200mM NaCl loading step. The detection method used was fluorescence at ex290/em335, which is the intrinsic fluorescence of the HA protein tryptophan residues (Ohnishi, 1983), and UV detection at 260 and 280 nm.

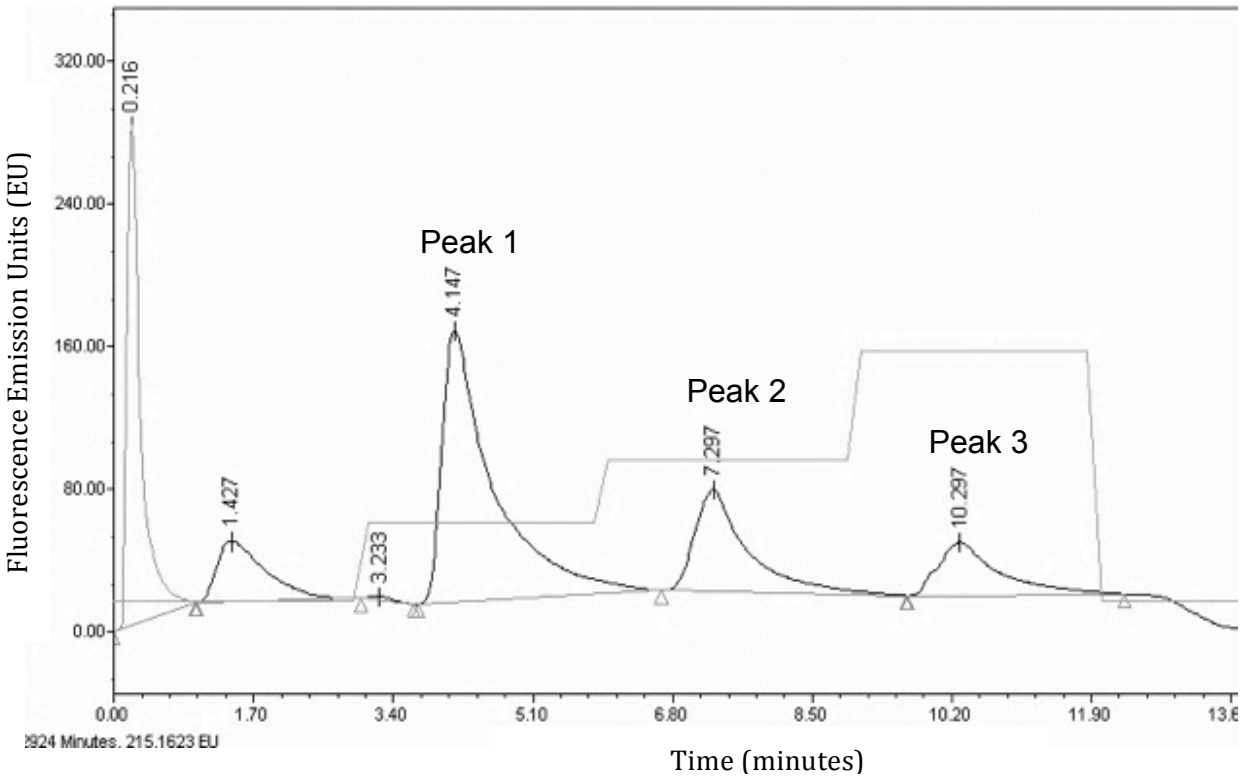

Appendix 8 Figure 8.1: Elution profile for SCC-A/H1N1/Puerto Rico/8/1934

Appendix 8.3 Application to VLPs

Appendix 8.3.1 Detection of HEK 293 VLPs

Crude VLP supernatant, SCC and iodixanol purified VLPs all gave the same profile as influenza virus when using the same method as described above. Appendix 8 Figure 8.2 is a representation of the profiles generally obtained. The peak at 450mM NaCl (Peak 1) had a 260/280 ratio of 0.89, which indicated that this peak contained mainly proteins. The peak at 650mM NaCl (Peak 2), which was the peak identified as infectious influenza virus, had a 260/280 ratio of 1.3-1.5, which indicates that this peak contained mainly proteins with some associated nucleic acid. Finally, the peak at 1M NaCl has a 260/280 ratio of 1.8, indicating it contains mainly nucleic acids. A ratio of 1.3-1.5 is close to the ratio for viruses (Tancevski, Wehinger, Patsch, & Ritsch, 2006), indicating that there was nucleic acid co-eluting with the VLPs. When each peak was collected (3x 150ul sample, crude supernatant), the western blot for HA, NA and M1 was unclear, with many bands present in each peak probably due to protein degradation from TCA precipitation, which was required due to dilution during peak collection. Another possibility for degradation of the VLPs is the high salt concentration present in the elution buffer, as nothing is known to date about influenza VLP stability in high salt concentrations. Nevertheless, we chose to move forward focusing on Peak 2 on the basis that it was identified as infectious influenza virus, making the assumption that Peak 3 is nucleic acids and that Peak 1 could either be protein aggregates, VLPs or vesicles based on their 260/280 ratios.

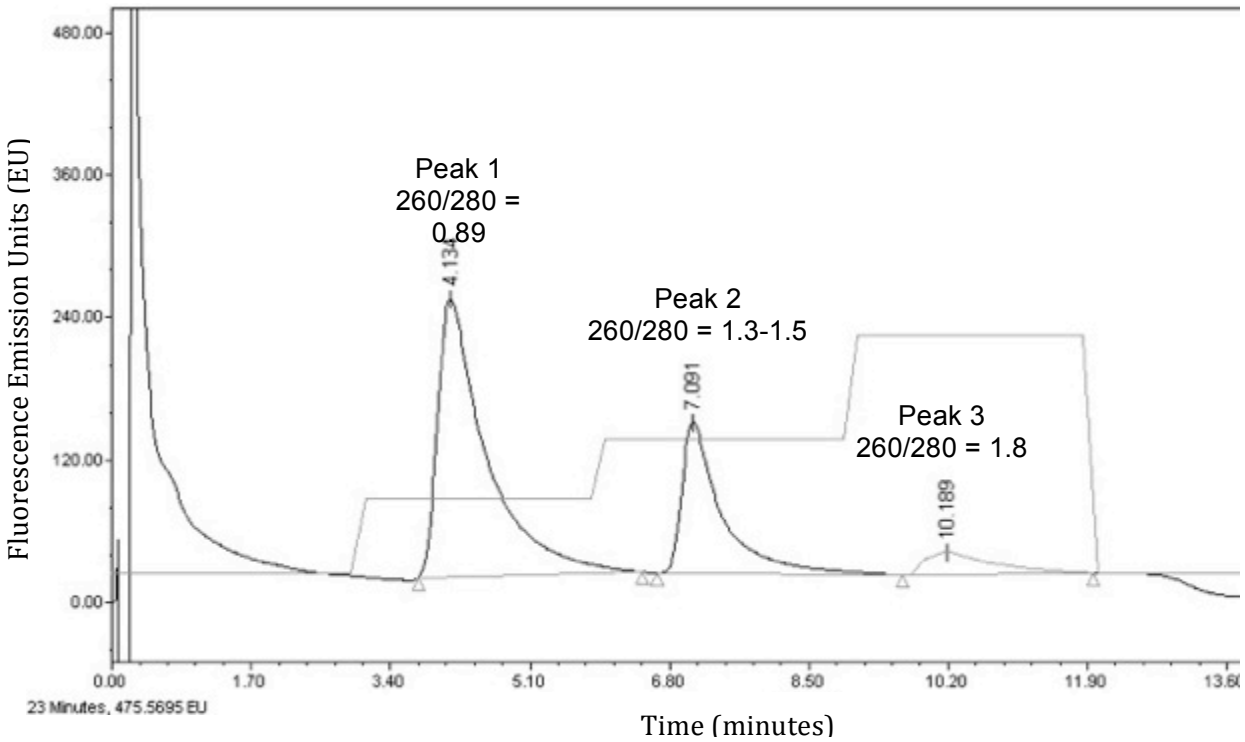

Appendix 8 Figure 8.2: Elution profile for HEK 293 SF 25x concentrated sucrose cushion purified VLP

When comparing the area of Peak 2 from crude supernatants, there was a correlation found between the peak area and the western blot signals from the MOI experiments. Appendix 8 Figure 8.3 shows a histogram of Peak 2 areas for MOIs of 1, 20, 60, 120 and 200 compared to the HA western blot profile for different. In the western blot, MOIs of 60 and 120 had the highest intensity level, suggesting that the greatest amount of HA was produced using these conditions. An MOI of 60 has the largest peak area followed by an MOI of 120 then 200, suggesting that an MOI of 60 produced the greatest amount of VLPs. Paring these two methods allows for selection of the condition that produces the highest amount of VLPs, not just the greatest amount of HA protein. This is important because it cannot be assumed that the condition that produces the greatest amount of HA correlates direction to the greatest amount of VLPs. However, there is one aspect of this result that needs to be mentioned, and that is the peaks for MOIs of 1 and 20. In western blot profile there are very slight bands present for these conditions, but a considerable peak from the HPLC method. This background could be from contaminating vesicles that also contain proteins with the same intrinsic fluorescence as HA, especially since such a low amount of HA was on the western blot. This can be confirmed by applying the control supernatant to the

HPLC column. Considering that intrinsic fluorescence is based on tryptophan, tyrosine and phenylalanine residues, host cell proteins or vesicle proteins could emit a signal if they contain these residues.

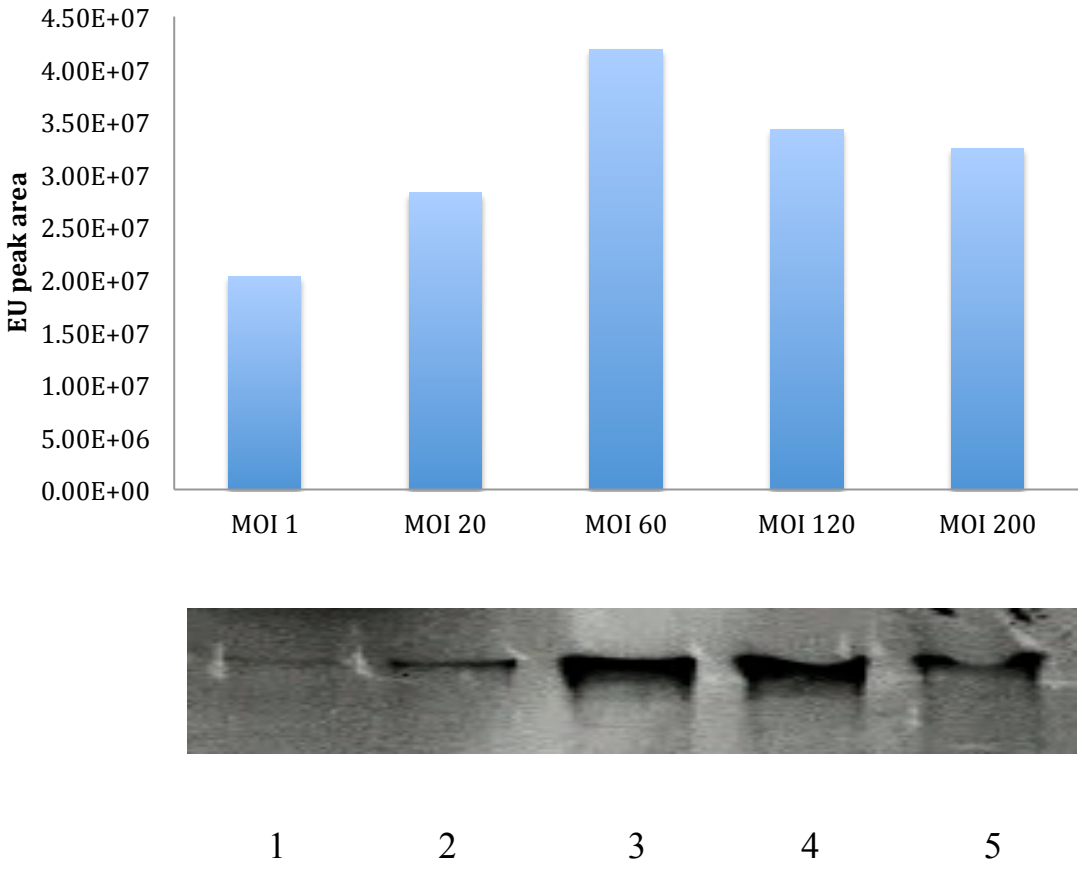

Appendix 8 Figure 8.3: Peak areas of 650mM NaCl elution (Peak 2) at different MOIs for HEK 293 VLP production and their corresponding HA western blot signal.
NIBSC anti-HA anitbodies. Numbers 1-5 corresponds to MOIs of 1-200, respectively.

The final observation found from these experiments was the difference in the peak area between crude supernatant and SCC-VLP samples. Appendix 8 Figure 8.4 illustrates this difference clearly with the supernatant peak area represented with the bar on the left and the sucrose cushion peak area on the right.

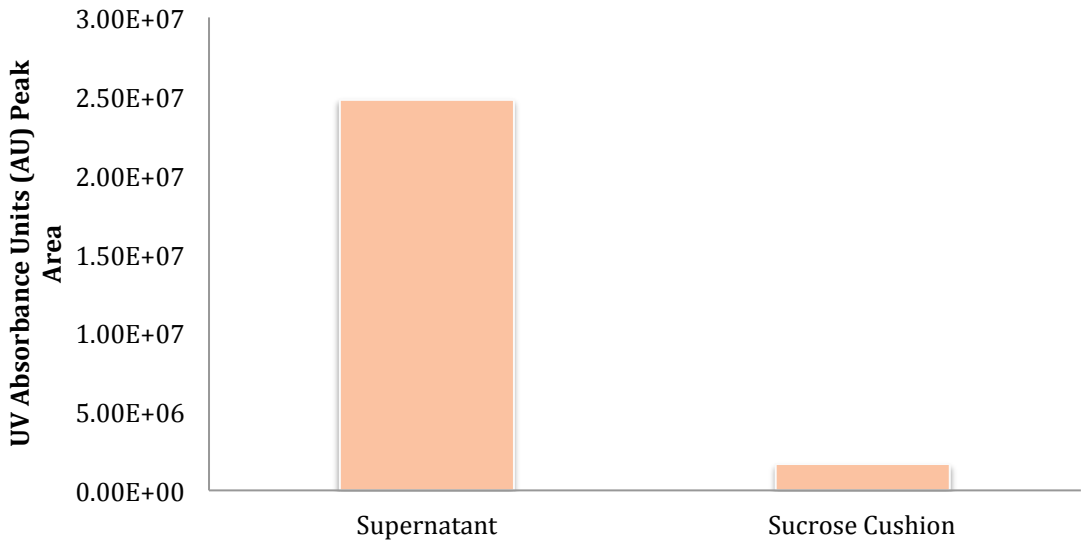

Appendix 8 Figure 8.4: Peak 2 area of crude supernatant and sucrose cushion purified HEK 293 VLPs measured by 290/330

The calculated yield from the sucrose cushion is 6.6%. An explanation for this observation may lie in the NSEM pictures from the sucrose cushion purified VLP samples. Appendix 8 Figure 8.5 shows a zoomed out image of the sucrose cushion VLPs and influenza virus A H1N1/Puerto Rico/8/1934 produced in HEK 293 cells. The VLP sample (A, VLPs labeled with black arrows) has a lot of debris that could be broken VLPs unable to withstand the concentration step, thus leading to the major decrease in peak area in the sucrose cushion sample (debris labeled with white arrows). The influenza virus sample shows much less cell debris than the VLP sample for comparison (Appendix 8 Figure 8.5 B).

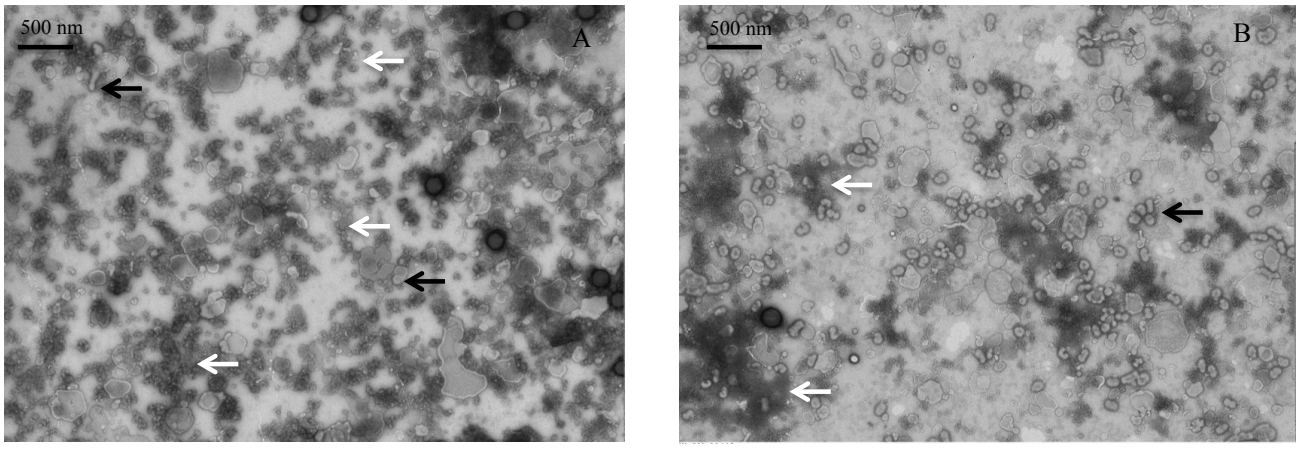

Appendix 8 Figure 8.5: NSEM images of sucrose cushion purified HEK 293 VLPs (A) and influenza virus A/H1N1/Puerto Rico/8/1934 (B).

Appendix 8.3.2 Application to Sf9 VLPs

When Sf9 VLPs were applied on the HPLC with the method developed for influenza virus, a similar profile was obtained as for HEK 293 VLPs. Both crude, sucrose cushion and iodixanol samples were tested. Peak 1 had a 260/280 ratio of 1.3, Peak 2 and Peak 3 both had a ratio of 1.6. A 260/280 ratio of 1.3 is close to that of a virus (Tancevski et al., 2006) and is very close to the ratio found by Transfiguracion et al (Transfiguracion et al., 2011) in their baculovirus quantification protocol using an anion exchange column with elution at 480mM NaCl. Additionally, Gerster *et al*.(2013) found when purifying baculovirus with a CIM QA monolithic column, that the majority of BV eluted at 440mM NaCl, which is very close to the peak found here at 450mM NaCl. It is therefore possible for baculovirus and influenza VLP separation, under the assumption that influenza VLPs should elute in Peak 2 at 650 mM salt and the BV particles at around 450mM NaCl. A 260/280 ratio of 1.6 indicates that nucleic acids were eluting with the VLPs, as was the case for HEK293 VLPs. When crude supernatant and sucrose cushion VLPs were run on the column, there was not such a drastic decrease in peak area like there was observed for the HEK 293 SF system (Appendix 8 Figure 8.6), with a yield of 62%. When comparing the zoomed out image of the NSEM image of Sf9 sucrose cushion VLPs (Appendix 8 Figure 8.7) to those from HEK 293 SF, it is clear there is much less debris present (indicated with white arrows), besides the obvious contamination from baculovirus, potentially indicating that Sf9 VLPs have a greater stability.

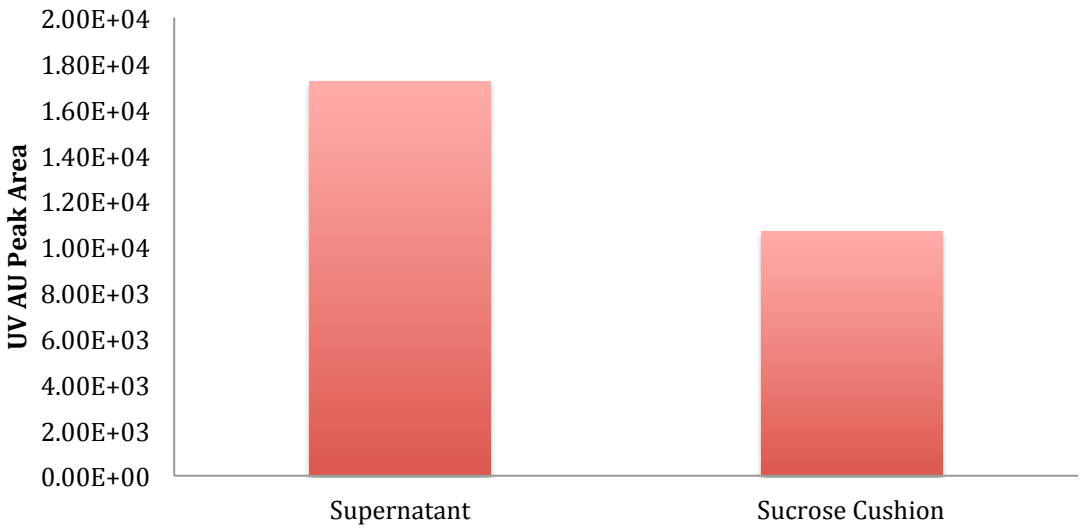

Appendix 8 Figure 8.6: Peak 2 area of crude supernatant vs. sucrose cushion purified Sf9 VLPs measured by UV 280nm.

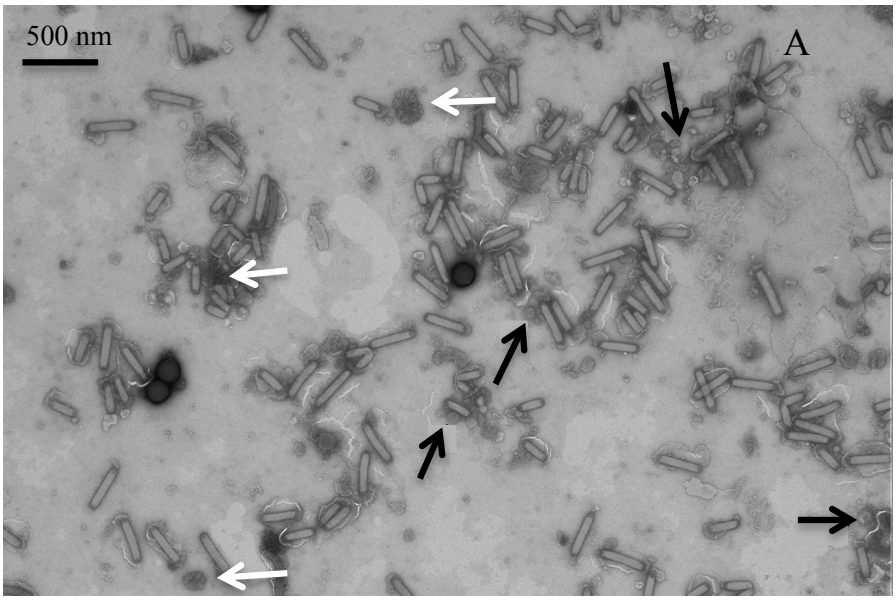

Appendix 8 Figure 8.7: NSEM image zoomed out of sucrose cushion Sf9 VLPs.